

Department of Physiology and Pharmacology “V. Erspamer”
Ph.D. in Clinical-Experimental Neuroscience and Psychiatry
- XXX Cycle -

BACKTRANSLATION OF EEG BIOMARKERS OF ALZHEIMER’S DISEASE FROM PATIENTS TO MOUSE MODELS

Ph.D. thesis by Dott. Susanna Lopez

Coordinator:

Prof. Marco Salvetti

Tutors:

Prof. Cristina Limatola

Prof. Claudio Babiloni

1	<u>PREAMBLE</u>	6
2	<u>ALZHEIMER'S DISEASE: A GLOBAL EPIDEMY</u>	8
2.1	INCIDENCE	8
2.2	STAGES	8
2.2.1	PRECLINICAL ALZHEIMER'S DISEASE	8
2.2.2	MILD COGNITIVE IMPAIRMENT (MCI) DUE TO AD	9
2.2.3	MILD DEMENTIA DUE TO AD	9
2.2.4	MODERATE DEMENTIA DUE TO AD	9
2.2.5	SEVERE DEMENTIA DUE TO AD	10
2.3	AD PATHOLOGY	10
2.4	DIAGNOSTIC AND TOPOGRAPHIC BIOMARKERS FOR AD	13
2.5	MOUSE MODELS OF AD	15
2.5.1	TRANSGENIC MICE WITH OVEREXPRESSION OF APP	16
2.5.2	TRANSGENIC MICE WITH PRESENILIN MUTATION	16
2.5.3	TRANSGENIC MICE WITH TAU MUTATION	17
3	<u>ELECTROENCEPHALOGRAPHIC (EEG) RHYTHMS</u>	18
3.1	ELECTROENCEPHALOGRAPHY	18
3.2	THE EEG RHYTHMS	18
3.3	PARADIGMS OF EEG DATA ACQUISITION	20
3.3.1	SUBJECT'S MENTAL STATE	20
3.3.2	ENVIRONMENTAL CONDITIONS	21
3.3.3	INSTRUCTIONS TO SUBJECTS	21
3.3.4	MONTAGE OF EEG ELECTRODES	21
3.3.5	MONTAGE OF OTHER SENSORS FOR THE QUALITY CONTROL OF EEG RECORDING	22
3.3.6	SETTING OF RSEEG RECORDING PARAMETERS (SAMPLING FREQUENCY, BANDPASS FILTER, AMPLIFICATION, ETC...). 22	
3.4	EEG SOURCE ESTIMATION	23
4	<u>STUDY I: TWO-YEAR LONGITUDINAL MONITORING OF AMNESTIC MILD COGNITIVE IMPAIRMENT PATIENTS WITH PRODROMAL ALZHEIMER'S DISEASE USING TOPOGRAPHICAL BIOMARKERS DERIVED FROM FUNCTIONAL MAGNETIC RESONANCE IMAGING AND ELECTROENCEPHALOGRAPHIC ACTIVITY</u>	25
4.1	INTRODUCTION	25
4.2	MATERIALS AND METHODS	27
4.2.1	PARTICIPANTS, CLINICAL EXAMS, AND NEUROPSYCHOLOGICAL TESTS	27
4.2.2	FUNCTIONAL MRI DATA	28

4.2.3	EEG DATA	28
4.2.4	PATIENTS' CLASSIFICATION IN PRODROMAL AD AND CONTROL AMCI PATIENTS	29
4.2.5	STATISTICAL ANALYSIS	30
4.3	RESULTS	31
4.3.1	PATIENTS' FEATURES	31
4.3.2	RSfMRI CONNECTIVITY MEASURES OF PRODROMAL AD	34
4.3.3	RSEEG AND ERP FUNCTIONAL BIOMARKERS OF PRODROMAL AD	36
4.3.4	CORRELATION OF RSfMRI AND EEG MARKERS WITH ADAS-COG13 SCORE	38
4.4	DISCUSSION	39
4.4.1	FUNCTIONAL BIOMARKERS GROUP EFFECTS	40
4.4.2	FUNCTIONAL BIOMARKERS TIME X GROUP EFFECTS: DIFFERENTIAL PROGRESSION PROFILES	42
4.4.3	WHAT DO RSfMRI AND EEG TOPOGRAPHIC BIOMARKERS TELL US ABOUT PRODROMAL AD?	43

5 STUDY II: ON-GOING ELECTROENCEPHALOGRAPHIC RHYTHMS RELATED TO CORTICAL AROUSAL IN WILD TYPE MICE: THE EFFECT OF AGING

5.1	INTRODUCTION	45
5.2	METHODS	46
5.2.1	ANIMALS	46
5.2.2	PRE-SURGERY PHASE (3 WEEKS)	47
5.2.3	SURGERY	47
5.2.4	QUIET POST-SURGERY PERIOD (1 WEEK)	48
5.2.5	HANDLING POST-SURGERY PERIOD (1 WEEK)	48
5.2.6	EXPERIMENTAL DAY	48
5.2.7	DETERMINATION OF THE BEHAVIORAL MODE OF THE MICE	49
5.2.8	EEG DATA ANALYSIS	50
5.2.9	SPECTRAL ANALYSIS OF THE EEG DATA	50
5.2.10	STATISTICAL ANALYSIS	51
5.3	RESULTS	52
5.3.1	NORMALIZED EEG POWER DURING ACTIVE AND PASSIVE CONDITIONS	52
5.3.2	EFFECT OF AGE ON THE NORMALIZED EEG POWER	53
5.3.3	EFFECT OF SEX ON THE NORMALIZED EEG POWER	54
5.3.4	RELIABILITY OF THE SPECTRAL EEG MARKERS AMONG THE RECORDING CENTERS	56
5.4	DISCUSSION	58
5.4.1	ON-GOING CORTICAL EEG RHYTHMS IN WT MICE DIFFER BETWEEN THE PASSIVE AND ACTIVE CONDITIONS	58
5.4.2	ON-GOING CORTICAL EEG RHYTHMS IN WT MICE DIFFER ACROSS AGING	59
5.4.3	TRANSLATIONAL VALUE OF THE PRESENT RESULTS	59

6 STUDY III: ONGOING ELECTROENCEPHALOGRAPHIC ACTIVITY ASSOCIATED WITH CORTICAL AROUSAL IN TRANSGENIC PDAPP MICE (HAPP V717F)

6.1	INTRODUCTION	61
6.2	METHODS	63
6.2.1	ANIMALS	63
6.2.2	PRE-SURGERY (3 WEEKS)	64
6.2.3	SURGERY	64
6.2.4	QUIET POST-SURGERY PERIOD OF 1 WEEK	66
6.2.5	HANDLING POST-SURGERY PERIOD OF 1 WEEK	66
6.2.6	EXPERIMENTAL DAY	66
6.2.7	DETERMINATION OF THE ANIMAL BEHAVIOR	66
6.2.8	EEG DATA ANALYSIS	67
6.2.9	SPECTRAL EEG DATA ANALYSIS	68
6.2.10	STATISTICAL ANALYSIS	68
6.2.11	CONTROL ANALYSIS	69
6.3	RESULTS	70
6.3.1	ABSOLUTE EEG POWER (DENSITY) DURING PASSIVE AND ACTIVE CONDITIONS IN WT AND PDAPP GROUPS	70
		71
6.3.2	COMPARISON OF THE FREQUENCY AND ABSOLUTE EEG POWER BETWEEN THE WT AND THE PDAPP GROUP	71
6.3.3	CONTROL ANALYSIS	73
6.4	DISCUSSION	75

7 STUDY IV: ONGOING ELECTROENCEPHALOGRAPHIC RHYTHMS RELATED TO CORTICAL AROUSAL IN TRANSGENIC TASTPM MICE **79**

7.1	INTRODUCTION	79
7.2	METHODS	82
7.2.1	ANIMALS	82
7.2.2	PRE-SURGERY (3 WEEKS)	83
7.2.3	SURGERY	83
7.2.4	QUIET POST-SURGERY PERIOD (1 WEEK)	84
7.2.5	HANDLING POST-SURGERY PERIOD (1 WEEK)	84
7.2.6	EXPERIMENTAL DAY	84
7.2.7	DETERMINATION OF THE BEHAVIORAL MODE	85
7.2.8	EEG DATA ANALYSIS	86
7.2.9	SPECTRAL ANALYSIS OF THE EEG DATA	86
7.2.10	STATISTICAL ANALYSIS	87
7.2.11	CONTROL ANALYSIS	88
7.3	RESULTS	88
7.3.1	NORMALIZED EEG POWER DENSITY DURING ACTIVE AND PASSIVE CONDITIONS IN WT AND TASTPM MICE	88
		90
7.3.2	COMPARISON OF THE NORMALIZED EEG POWER BETWEEN WT AND TASTPM MICE	90
7.4	DISCUSSION	92

<u>8</u>	<u>CONCLUSIONS</u>	<u>97</u>
8.1	EEG BIOMARKERS IN AD PATIENTS	97
8.2	EEG BIOMARKERS IN AD MOUSE MODELS	98
<u>9</u>	<u>REFERENCES</u>	<u>100</u>

1 Preamble

The present Ph.D. thesis has been mainly developed on the data of the project with the short name PharmaCog (2010-2015), granted by the European Framework Programme 7 with about 28 millions of Euro (i.e. Innovative Medicine Initiative, IMI, grant agreement n°115009; www.pharmacog.org). This project involved 15 academic institutions, 12 global pharmaceutical companies, and 5 small and medium sized enterprises (SMEs).

The PharmaCog project aimed at improving the pathway of drug discovery in Alzheimer's disease (AD), based on a major interest of pharma companies, namely the validation of electrophysiological, neuroimaging, and blood biomarkers possibly sensitive to the effect of disease-modifying drugs reducing A β 42 in the brain in AD patients at the prodromal stage of amnesic mild cognitive impairment (aMCI). The core concept of the PharmaCog project was that the pathway of drug discovery in AD may be enhanced by (1) the validation of biomarkers derived from blood, EEG, magnetic resonance imaging (MRI), and positron emission tomography (PET) in patients with aMCI due to AD diagnosed by in-vivo measurement of A β 42 and phospho-tau in the brain and (2) the evaluation of the translational value of those human biomarkers in wild type (WT) mice and animal models of AD including transgenic mice with the mutation of PS1 and/or APP (i.e. PDAPP and TASTPM strains). Those genetic factors induce an abnormal accumulation of A β 42 in the brain and related cognitive deficits. The expected results may be (1) the identification of a matrix of biomarkers sensitive to the prodromal AD (aMCI cognitive status) and its progression in patients and (2) the selection of similar biomarkers related to AD neuropathology and cognitive deficits in PDAPP and TASTPM strains. These biomarkers were expected to be very useful in clinical trials testing the efficacy and neurobiological impact of new disease-modifying drugs against prodromal AD.

For the development of this Ph.D. thesis, the access to the experiments and the data of the PharmaCog project was allowed by Prof. Claudio Babiloni, leader of an Italian Unit (University of Foggia in 2010-2012 and Sapienza University of Rome in 2013-2015) of the PharmaCog Consortium and coordinator of study activities relative to biomarkers derived from electroencephalographic (EEG) signals recorded from human subjects and animals in that project. Specifically, Prof. Claudio Babiloni was in charge for the centralized qualification and analysis of EEG data recorded from aMCI patients (Work Package 5, WP5) and transgenic mouse models of AD such as PDAPP and TASTPM strains (WP6). The data of the present Ph.D. thesis mostly derived from the WP5 and WP6.

This document illustrating the Ph.D. thesis is structured in three main Sections:

- An Introductive part illustrating concisely the AD neuropathology, the mouse models of AD used in this thesis, and basic concepts of EEG techniques useful to understand the present study results;
- An Experimental part describing the result of the four research studies led in the framework of this Ph.D. project. Two of these studies were published in international journals registered in ISI/PubMed with impact factor, while the other two are being currently under minor revisions in those journals;
- A Conclusion section.

Preamble

Since the results of the present Ph.D. thesis are based on experiments developed in the framework of the PharmaCog project, the specific contribution of this Ph.D. candidate (Miss Susanna Lopez) may be not immediately detectable. To elucidate it, the following declaration of Prof. Claudio Babiloni is added to this preamble.

Declaration of Prof. Claudio Babiloni

During her Ph.D. course in Clinical/Experimental Neuroscience and Psychiatry (XXX Cycle), Miss Susanna Lopez has developed her Ph.D. project (curriculum in Neurophysiology) with two main scientific issues:

- *Study of electroencephalographic (EEG) progression biomarkers of Alzheimer's Disease (AD) in the prodromal stage of amnesic Mild Cognitive Impairment amnesico (aMCI);*
- *Evaluation of translational value of above-mentioned EEG biomarkers in wild type (WT) mice and in transgenic mouse models with PS1 and/or APP mutation, inducing abnormal accumulation of A β 42 in the brain, resembling those in humans, and cognitive deficits.*

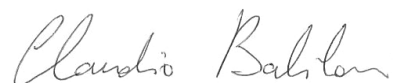
These scientific issues have been addressed under my supervision using EEG data of PharmaCog project (2010-2015), which received funding of about 28 millions of Euro from European Commission in the 7th Framework Programme (i.e. Innovative Medicine Initiative, IMI, grant agreement n°115009; www.pharmacog.org). This project comprised 14 academic institutions, 12 pharma companies and 5 small-middle enterprises (SMEs). In the PharmaCog consortium, my Unit of University of Foggia and University of Rome was in charge for the centralized analysis of EEG data showed in Miss. Lopez's Ph.D. thesis. In this framework, Miss. Lopez has distinguished herself in contributing to my Unit's action. Specifically, in her project she has worked with scientific initiative and maturity in the following activities:

- *Bibliographic review of the literature inherent to Ph.D. project;*
- *Visual, spectral and statistical analysis of EEG data of PharmaCog project of aMCI patients and WT and transgenic mice (PS1 and/or APP mutations);*
- *Participation to teleconference of PharmaCog WP5 and WP6, before and after the end of the project, for the discussion of EEG results for the publications of the scientific papers;*
- *Contribution for the writing of the scientific reports (i.e., Deliverables on the activities in the PharmaCog WP6), poster and scientific articles on the EEG data in the framework of Ph.D. project.*

Miss Susanna Lopez presented posters in two European Conferences receiving a good feedback:

- *European Congress on Clinical Neurophysiology 2015 (October 2015; Brno, Czech Republic)*
- *First Synanet Meeting (January 2017; Lisbon, Portugal)."*

Sincerely,
Prof. Claudio Babiloni



2 Alzheimer's Disease: a global epidemic

2.1 Incidence

Recent statistics taken from Alzheimer's Association report of 2017 show that someone in the world develops dementia every 3 seconds. In 2015 there were an estimated 46.8 million people worldwide living with dementia and this number is believed to be close to 50 million people in 2017. This number will almost double every 20 years, reaching 75 million in 2030 and 131.5 million in 2050 for the progressive ageing going on in most developed country, even though much of the increase will be in developing countries. Already 58% of people with dementia live in low and middle-income countries, but by 2050 this will rise to 68%. The fastest growth in the elderly population is taking place in China, India, and their south Asian and western Pacific neighbours.

Alzheimer's Disease (AD) is a neurodegenerative disease and one of the most common causes of dementia (60-70% of cases). AD was first described in 1906 at a conference in Tübingen, Germany by Alois Alzheimer, as a "peculiar severe disease process of the cerebral cortex" (Alzheimer, 1906), but about 70 years passed before it was recognized as a common cause of dementia and a major cause of death. It is characterized by specific episodic memory disorders at its initial stages but progressively other symptoms appear, such as problems with language, disorientation (including easily getting lost), mood swings, loss of motivation, not managing self-care, and behavioural issues with the final loss of independence in the daily living activities.

An estimated 5.5 million Americans of all ages are living with AD dementia in 2017. This number includes an estimated 5.3 million people age 65 and older and approximately 200,000 individuals under age 65 who have younger-onset AD, though there is greater uncertainty about the younger-onset estimate. One in 10 people aged 65 and older (10 percent) has AD dementia. The percentage of people with AD dementia increases with age: 3 percent of people age 65-74, 17 percent of people age 75-84, and 32 percent of people age 85 and older have AD dementia. Of people who have AD dementia, 82 percent are age 75 or older.

Of note, these statistics are extrapolated from prevalence studies in which all the subjects enrolled received a diagnosis of dementia. Outside from the research applications, only half of those who would meet the diagnostic criteria for AD and other dementias are diagnosed with dementia by a physician (Boustani et al., 2003, Bradford et al., 2009, Kotagal et al, 2015). Thus, as AD dementia is underdiagnosed and underreported, a large portion of patients with AD may not know they have it.

2.2 Stages

Several studies (Sperling et al., 2011; Albert et al., 2011; McKhann et al., 2011) established that AD is a pathology beginning years before the clear manifestation of clinical symptoms and the onset of dementia. Five stages in AD pathogenesis could be recognized according to Mayo Clinic classification:

2.2.1 Preclinical Alzheimer's disease

Introductory part

AD begins long before any symptoms become apparent. This stage is called preclinical AD. Symptoms during this stage won't be noticed, nor by the patients nor by people around him. This stage of AD can last for years, possibly even decades. Although any changes happen, imaging technologies can identify deposits of A β . The ability to identify these early deposits may be especially important in the future as new treatments are developed for Alzheimer's disease. Additional biomarkers indicating an increased risk of disease have been identified for AD. These biomarkers can be used to support the diagnosis of AD typically, after symptoms are evident. There are also genetic tests indicating a higher risk of AD, particularly early-onset AD. As with newer imaging techniques, biomarkers and genetic tests will become more important as new treatments for Alzheimer's disease are developed.

2.2.2 Mild cognitive impairment (MCI) due to AD

People with mild cognitive impairment have mild changes in their memory and thinking ability. These changes aren't significant enough to affect work or relationships yet. People with MCI may have memory lapses when it comes to information that is usually easily remembered, such as conversations, recent events or appointments. Furthermore, they may also have trouble judging the amount of time needed for a task, or they may have difficulty correctly judging the number or sequence of steps needed to complete a task. The ability to make sound decisions can become harder for people with MCI. Not everyone with MCI will develop AD. The same procedures used to identify preclinical Alzheimer's disease can help determine whether MCI is due to AD or something else.

2.2.3 Mild dementia due to AD

AD is often diagnosed in the mild dementia stage, when it becomes clear to family and doctors that a person is having significant trouble with memory and thinking that impacts daily functioning.

In the mild Alzheimer's stage, people may experience:

- *Memory loss for recent events.* Individuals may have an especially hard time remembering newly learned information and ask the same question over and over.
- *Difficulty with problem-solving, complex tasks and sound judgments.* Planning a family event or balancing a checkbook may become overwhelming. Many people experience lapses in judgment, such as when making financial decisions.
- *Changes in personality.* People may become subdued or withdrawn — especially in socially challenging situations — or show uncharacteristic irritability or anger. Reduced motivation to complete tasks also is common.
- *Difficulty organizing and expressing thoughts.* Finding the right words to describe objects or clearly express ideas becomes increasingly challenging.
- *Getting lost or misplacing belongings.* Individuals have increasing trouble finding their way around, even in familiar places. It's also common to lose or misplace things, including valuable items.

2.2.4 Moderate dementia due to AD

During the moderate stage of AD, people grow more confused and forgetful and begin to need more help with daily activities and self-care.

People with moderate AD may:

- *Show increasingly poor judgment and deepening confusion.* Individuals lose track of where they are, the day of the week or the season. They may confuse family members or close friends with one another,

Introductory part

or mistake strangers for family. They may wander, possibly in search of surroundings that feel more familiar. These difficulties make it unsafe to leave those in the moderate Alzheimer's stage on their own.

- *Experience even greater memory loss.* People may forget details of their personal history, such as their address or phone number, or where they attended school. They repeat favorite stories or make up stories to fill gaps in memory.
- *Need help with some daily activities.* Assistance may be required with choosing proper clothing for the occasion or the weather and with bathing, grooming, using the bathroom and other self-care. Some individuals occasionally lose control of their bladder or bowel movements.
- *Undergo significant changes in personality and behavior.* It's not unusual for people with moderate Alzheimer's disease to develop unfounded suspicions — for example, to become convinced that friends, family or professional caregivers are stealing from them or that a spouse is having an affair. Others may see or hear things that aren't there. Individuals often grow restless or agitated, especially late in the day. Some people may have outbursts of aggressive physical behavior.

2.2.5 *Severe dementia due to AD*

In the severe (late) stage of AD, mental function continues to decline, and the disease has a growing impact on movement and physical capabilities.

In severe AD, people generally:

- *Lose the ability to communicate coherently.* An individual can no longer converse or speak coherently, although he or she may occasionally say words or phrases.
- *Require daily assistance with personal care.* This includes total assistance with eating, dressing, using the bathroom and all other daily self-care tasks.
- *Experience a decline in physical abilities.* A person may become unable to walk without assistance, then unable to sit or hold up his or her head without support. Muscles may become rigid and reflexes abnormal. Eventually, a person loses the ability to swallow and to control bladder and bowel functions.

2.3 AD pathology

The earliest and most severe degeneration that could be observed at autopsy in AD patients is usually found in the medial temporal lobe (entorhinal/perirhinal cortex and hippocampus), lateral temporal cortex, and nucleus basalis of Meynert.

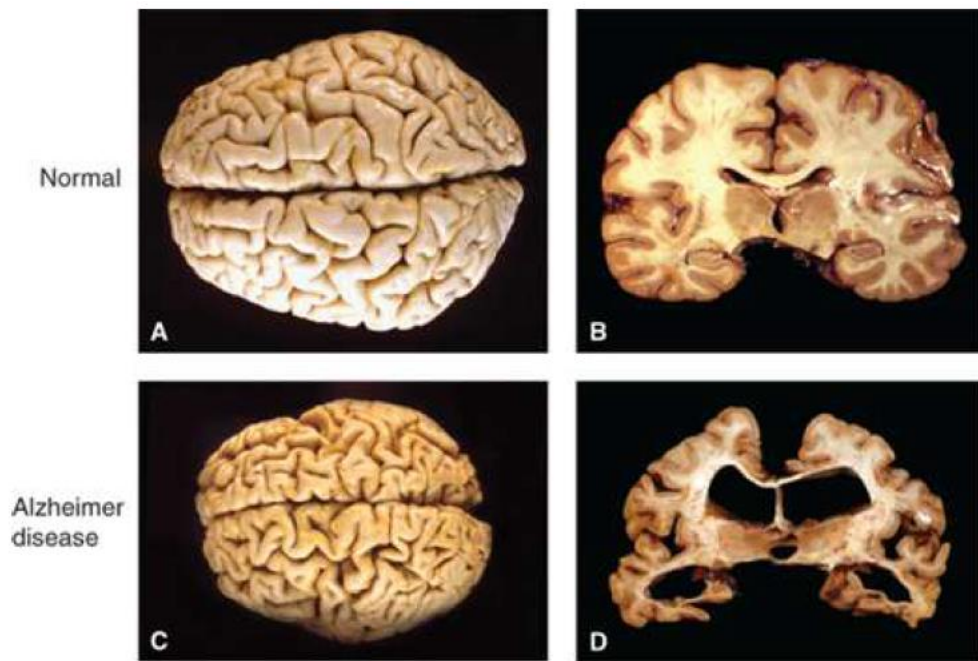


Figure 1. Differences between normal and AD brains.

At the microscopic level, neuritic plaques and neurofibrillary tangles (NFTs) could be observed. They may appear also in normal ageing but are specifically linked with AD pathology. Increasing evidence suggest that cellular dysfunction is caused by soluble amyloid species called oligomers, which are toxic. Further amyloid polymerization and fibril formation lead to neuritic plaques, formed by an amyloid central core, proteoglycans, ApoE4, and other proteins. A β is a protein formed by 39 to 41 aminoacids derived from the Amyloid Precursor Protein (APP), a large transmembrane protein, which is cleaved from α and γ -secretases. The normal functional role of A β is still not clear, while APP is known to have neurotrophic and neuroprotective properties. The amyloid core is surrounded by a halo composed by dystrophic and tau-immunoreactive neurites and activated microglia. NFTs are formed by silver-staining neuronal cytoplasmic fibrils composed by abnormally hyperphosphorylated tau protein (appearing as paired helical filaments). Tau binds to and stabilize microtubules, supporting axonal transport of several molecules (organelles, neurotransmitters, ...). When phosphorylated, tau protein cannot bind microtubules and tends to invade the neural cytoplasm, compromising the functions of distal dendrites.

At biochemical level, AD is associated with a decrease at the cortical level of several proteins and neurotransmitter, especially acetylcholine, its synthetic enzyme choline acetyltransferase, and nicotinic cholinergic receptors. The most important effect is that reduced acetylcholine induces degeneration of cholinergic neurons. Indeed, a typical feature of the AD is the deficit in the brain cholinergic neurotransmission, which has been related to cognitive, neuropsychiatric, and functional deficits in AD patients (Cummings and Back, 1998). As the human cerebral cortex does not contain local cholinergic neurons, the acetylcholine deficiencies are attributed typically to a dysfunction of the ascending cholinergic innervations from the basal nucleus of Meynert in the basal forebrain to the cerebral cortex (Arendt et al., 2015). This

Introductory part

nucleus includes approximately 80% of the cholinergic neurons in the brain and is severely atrophic in the advanced stages of the AD (Arendt et al., 2015).

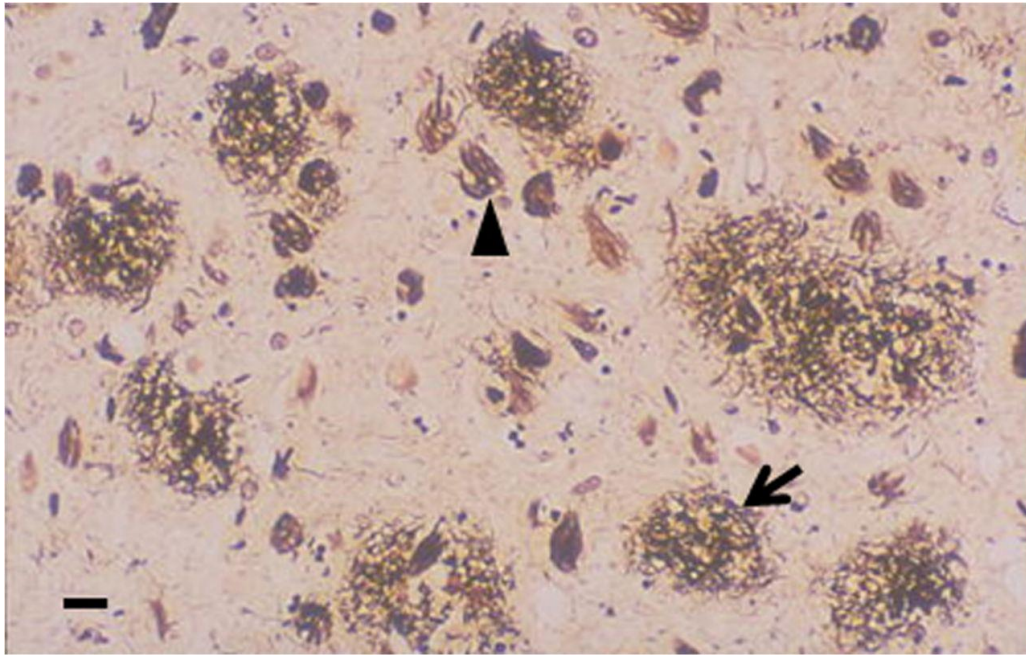


Figure 2. Histopathology of AD senile plaques (arrow) and neurofibrillary tangles (arrowhead) are detected by silver staining of a section of brain cortex (scale bar, 10 μ M, Allsop and Mayes, 2014)

APP is catabolized by α , β , and γ -secretases. As a first step, APP is cleaved by α and β secretases producing non-toxic molecules; after the cleavage by γ secretases on the β secretases product could lead to toxic ($A\beta_{42}$) or non-toxic ($A\beta_{40}$) peptide. The cleavage by α -secretases produces non-toxic P3 peptide. The accumulation of toxic $A\beta_{42}$ is a key initial step for cellular damage in AD. Thus, therapies have focussed on reducing this accumulation by inhibiting the activity of β and γ -secretases, or by promoting α secretases, or clearing $A\beta_{42}$ with specific antibodies. Figure 3 schematically illustrates the action mechanism of β and γ -secretase enzyme.

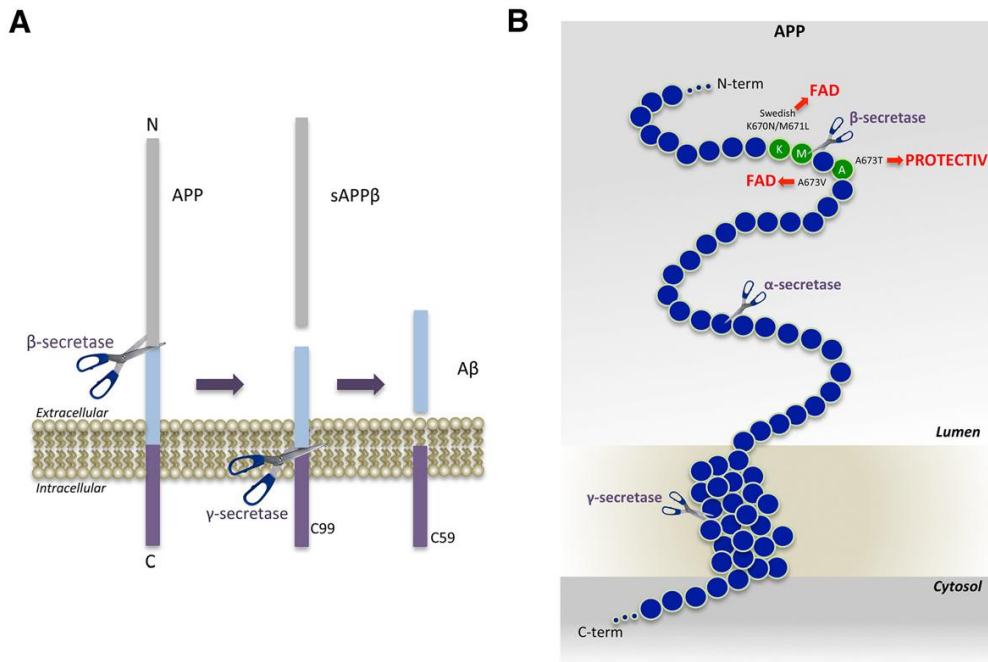


Figure 3. APP processing and A β generation and mutations that affect β -secretase cleavage. A. APP is a Type-I membrane protein that is sequentially cleaved by two aspartic proteases to generate A β . First, the β -secretase enzyme cuts APP (1) to create the N-terminus of A β . Second, C99 is cleaved by the γ -secretase enzyme (2) to generate the C-terminus of A β . A β is then released into the lumen of the endosome and secreted into the extracellular medium. An intracellular domain, C59, is also produced. B. The amino acids in and around the A β domain of APP are represented as blue circles. Amino acids that affect β -secretase processing of APP in humans are green circles, within which the wild-type residue is identified by the single-letter amino acid code. The K670N/M671L (Swedish) and A673V mutations cause FAD (Familial AD) by increasing β -secretase cleavage and A β production, while the A673T mutation protects against AD by doing the opposite. All three mutations occur at or within one amino acid of the β -secretase cleavage site. Scissors indicate cleavage sites of the various secretases (Vassar, 2014).

In 1% of patients, AD is a familial disorder resulting from the mutation in one of three functionally related membrane proteins: APP, presenilin 1 (PS1) and presenilin 2 (PS2). Onset of the disease typically happens between 30 and 60 years old. Down syndrome (trisomy 21) patients develop AD early too, with a mean onset age of 50 years old, which is thought to be related with an extra copy of APP gene, located on chromosome 21. Although the cause of sporadic AD is still unknown, the gene defects in familial AD support possible roles for both APP (neurotrophic properties) and presenilins (involved in APP metabolism).

2.4 Diagnostic and Topographic biomarkers for AD

AD has traditionally been defined as a type of dementia, a notion brought into existence with the publication of criteria from the National Institute of Neurological and Communicative Disorders and Stroke–Alzheimer’s Disease and Related Disorders Association (NINCDS– ADRDA) in 1984 (McKhann et al., 1984). These criteria showed two major critical points, i.e. (i) the clinical diagnosis of AD could only be designated as “probable” while the patient was alive and could not be made definitively until AD pathology had been confirmed post mortem; and (ii) the clinical diagnosis of AD could be assigned only when the disease had advanced to the point of causing significant functional disability and met the threshold criterion of dementia. The absence at that time of clinical criteria for the other dementias and the lack of biomarkers resulted in a low

Introductory part

specificity in differentiation of AD from other dementias (Varma et al., 1999). In 2007, the International Working Group (IWG) for New Research Criteria for the Diagnosis of AD provided a new conceptual framework that moved AD from a clinicopathological to a clinicobiological entity (Dubois and Albert, 2004). These 2007 IWG criteria proposed that AD could be recognised in vivo and independently of dementia, in the presence of two requisite features. The first was a core clinical phenotypic criterion that required evidence of a specific episodic memory profile characterised by a low free recall that is not normalised by cueing.⁵ The second criterion was the presence of biomarker evidence consistent with and supportive of AD on: (1) structural MRI; (2) molecular neuroimaging with PET (F-2-fluoro-2-deoxy-D-glucose PET, FDG PET, or C-labelled Pittsburgh compound B PET, PiB PET); or (3) CSF analysis of amyloid β (A β) or tau protein (total tau, T-tau, and phosphorylated tau, P-tau) concentrations. The most innovative aspect of the 2007 criteria was the first introduction of biomarkers into the core diagnostic framework.

Another revision of diagnostic guidelines was published in 2014 proposing that pathophysiological biomarkers of AD pathology and downstream topographical markers of AD should be reconceptualised, whereby biomarkers of AD pathology are restricted to those indicating the specific presence of tau pathology (CSF or PET tau) and amyloid pathology (CSF or PET amyloid) These biomarkers have the necessary specificity for a diagnosis of AD at any point on the disease continuum.

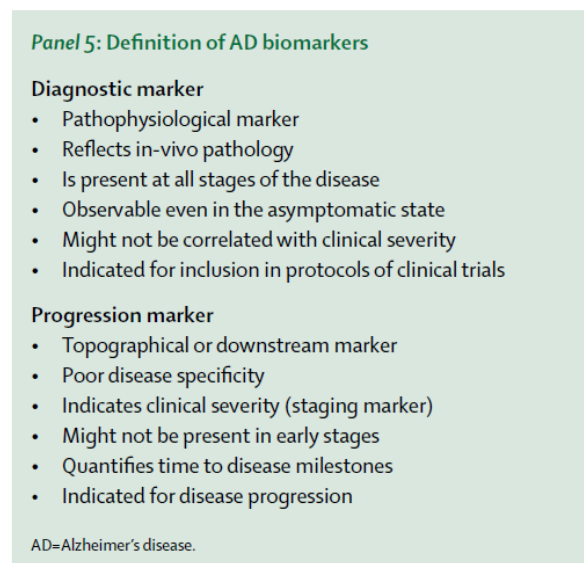


Figure 4. Definition of AD biomarkers (Dubois et al., 2014)

Downstream topographical markers of brain regional structural and metabolic changes have insufficient pathological specificity and but can be used to measure disease progression, as able to reflect topographical evidence of brain damage (regional atrophy or hypometabolism). They include particularly hippocampal atrophy assessed by MRI, cortical hypometabolism measured by FDG PET, and the subsequent cognitive and behavioural changes lack pathological specificity for AD, and they might be particularly valuable for detection and quantification of disease progression. These changes might be good markers to monitor time to disease milestones—eg, dementia onset—or for determination of disease stages.

Introductory part

A further update of international guidelines consists in the clear distinction between AD and AD pathologic changes (Jack et al., 2018). The prototypical multidomain amnesic dementia phenotype used to define probable AD, as defined by McKhann et al., (1984) does not “rule in” AD pathologic change (which implies change from normal) at autopsy (Nelson et al., 2011, Serrano-Pozo et al., 2014, Barnes et al., 2015) and the absence of the syndrome does not “rule out” AD pathologic change. Thus, the multidomain amnesic dementia phenotype is not specific; it can be the product of other diseases as well as AD (Serrano-Pozo et al., 2014). Nonamnesic clinical presentations, that is, language, visuospatial, and executive disorders, may also be due to AD (Rabinovici et al., 2008, Dubois et al., 2010, Murray et al., 2011). In addition, AD neuropathologic changes are often present without signs or symptoms, especially in older persons. An individual with biomarker evidence of A β deposition alone (abnormal amyloid PET scan or low CSF A β 42 or A β 42/A β 40 ratio) with a normal pathologic tau biomarker would be assigned the label “Alzheimer’s pathologic change”. The term “Alzheimer’s disease” would be applied if biomarker evidence of both A β and pathologic tau was present.

Unfortunately, none of the mentioned CSF, MRI, and PET markers allows a clear-cut diagnosis or prediction of all clinical presentations of AD. Furthermore, they cannot be serially used along years for the evaluation of AD individuals before and after pharmacological and non-pharmacological interventions. Indeed, these biomarkers are invasive (e.g., lumbar puncture for CSF sampling; the injection of radioactive tracers in PET procedures) and/or expensive (e.g., PET, MRI) for serial recordings. Therefore, there is a quest for new cost-effective, largely available, and non-invasive biomarkers of AD to be used in serial recordings and suitable for application to elderly subjects with some cognitive impairment (i.e., not requiring the subject’s collaboration or prolonged states of complete immobilization).

Electroencephalographic (EEG) markers potentially fit the ideal features mentioned above. Its recording is non-invasive and cost-effective. The high temporal resolution of EEG signals (e.g., milliseconds) is ideal for investigating emerging features of brain physiology, namely awake brain rhythms. In the condition of resting state eyes-closed, human brain produces dominant oscillations at about 8–13 Hz, the so-called alpha rhythms (Babiloni et al., 2010, 2011, 2013, 2016). Cognitive processes such as attention, perceptual binding, and working memory are typically related to a reduction in power of resting state alpha and beta (14–30 Hz) rhythms and to an increase in power of delta (1–4 Hz), theta (4–7 Hz), and gamma (30–70 Hz) rhythms (Babiloni et al., 2010, 2011, 2013, 2016). Markers of resting state EEG rhythms may probe the neurophysiological “reserve” in patients with dementing disorders; defined as the residual ability of the brain to ensure (1) the synchronization of neural activity at different spatial scales and frequencies from small cellular populations to large regions and (2) the coordination of this synchronization across subcortical and cortical neural networks (Babiloni et al., 2016).

2.5 Mouse models of AD

Animal models are crucial for translational research. They offer the possibility of applying pharmacological intervention *in vivo* to study pharmacodynamic/pharmacokinetics properties, to evaluate drugs’ safety and

Introductory part

adverse effects and to assess its efficacy. The more the model can reproduce human system physiological functions and behaviour, the better is the model.

Several mouse models of AD have been developed, as this disease is characterized by well-recognized pathological hallmarks, consisting of senile plaques and NFTs, and features, including neuronal and synaptic loss, dystrophic neurites, reactive astrocytes, and activated microglia. Transgenic mice may be generated by introducing a genetic modification on top of the existing genetic makeup or by modifying selectively the homologous gene of interest in its normal chromosomal position (gene targeting; Elder et al., 2010).

2.5.1 Transgenic mice with overexpression of APP

Based on amyloid hypothesis (Hardy and Selkoe, 2002), attempts were made to overexpress wildtype APP in transgenic mice by pronuclear injection. Although a variety of promoters were tried, none of these efforts produced anything that resembled an amyloid plaque or any other recognizable AD-type pathology. The introduction of FAD (familial AD) mutations in APP had greater outcome: Games et al. (1995) reported the first successful application of this approach using a platelet derived growth factor- β (PDGF) promoter to drive a human APP transgene that contained an FAD associated mutation (V717F) in the so-called PDAPP mouse. These models were characterized by mutations only at the γ -secretase cleavage site, exhibiting age-dependent amyloid deposition in the brain along with thioflavin-S-positive plaques, including compact plaques with dense cores that were highly reminiscent of those seen in human AD. Dystrophic neurites, reactive astrocytes, and activated microglia were all found near plaques. The process was age-related, in that plaque deposition was minimal at 6 months of age but clear by 9 months, increasing dramatically by 12 to 15 months (Reilly et al., 2003). PDAPP mice were subsequently shown to develop age-related learning defects (Chen et al., 2000) and synapse loss (Dodart et al., 2000).

Hsiao et al., (1996) overexpressed a human APP transgene containing the Swedish FAD mutation (K670N/M671L), affecting the β -secretase cleavage site. These mice, termed Tg2576 mice, expressed human APP at levels more than 5-fold above the levels of the endogenous mouse APP, and A β 40 and A β 42 levels increased with age. Like PDAPP mice, Tg2576 mice exhibited age-dependent amyloid deposition, which resulted in thioflavin-S-positive plaques like those found in AD, along with gliosis and dystrophic neurites. Plaque amyloid was first clearly seen by 11 to 13 months, eventually becoming widespread in cortical and limbic structures. Water maze learning, a test of spatial memory in mice, was normal in 3-month-old animals but impaired in 9- to 10-month-old mice. The Tg2576 mouse line has been made widely available and has been the most widely studied transgenic AD model.

2.5.2 Transgenic mice with Presenilin mutation

Mutations in Presenilin 1 (PS1, associated with a locus on chromosome 14) are the most commonly recognized causes of early-onset FAD, and to date more than 160 mutations in PS1 linked to FAD have been discovered (Elder et al., 2010). Mutations in a related gene on chromosome 1 were soon linked to FAD as well (Ertekin-

Introductory part

Taner, 2007) and called Presenilin 2 (PS2). Singly transgenic PS1 or PS2 mice do not develop plaques, expressing increased A β 42 levels with no effect on A β 40 although when crossed with plaque-forming APP lines, the presenilin FAD mutations cause earlier and more extensive plaque formation.

TASTPM mice (Howlett et al., 2004, 2008) were produced by a double mutation in APP KM670/671NL (Swedish) and PS1 M146V. These models are characterized by amyloidosis beginning at 3-4 months in the cerebral cortex, with mature plaques forming by 6-8 months, and eventually severe A β plaque deposition by 10 months (Howlett et al., 2004, 2008). TASTPM mice show both age-related neuropathology and early and progressive cognitive impairment, thus reproducing features of the pathophysiological and clinical presentation of familial AD (Howlett et al., 2004, 2008).

2.5.3 Transgenic mice with tau mutation

Mouse models of AD neurofibrillary pathology have mostly relied on expressing transgenic human tau with mutations that cause frontotemporal dementia, even though tau mutations do not cause AD, and thus it is unclear that the mechanisms induced by tau mutations are involved in AD pathophysiology.

TAPP mice were hAPP/tau double transgenic mice produced by crossing the Tg2576 line of human APP transgenic mice and the JNPL3 line expressing P301L human tau (Lewis et al., 2001). A β deposition in TAPP mice is similar to the Tg2576 line, but tau pathology is more severe than the JNPL3 line, indicating that A β can accelerate the tau pathology (Bolmont et al., 2001, Götz et al., 2007, Lewis et al., 2001).

3xTg line was produced combining mutant APP (hAPP Swedish mutation), PS1 (M146V mutation), and tau (P301L mutation) transgenes. These models develop extracellular A β plaques before tangle pathology, as in human AD (Oddo et al., 2003). However, the A β and tau pathologies in 3xTg mice appear to develop independently, without a causal link, since tau pathology was unaffected by crossing with BACE-deficient mice to eliminate A β production (Winton et al., 2011).

3 Electroencephalographic (EEG) rhythms

3.1 Electroencephalography

Electroencephalography (EEG) is the technique aiming at recording the electrical activity produced by brain cells. The first recording of the electric field of the human brain was made by the German psychiatrist Hans Berger in 1924 in Jena. He gave this recording the name electroencephalogram. This technique is typically a non-invasive invasive method to record the electrical activity of the brain along the scalp. On the contrary, stereoelectroencephalography records the electrical activity in deep structures of the brain. EEG measures voltage dynamical changes resulting from ionic current within the neurons of the brain (Niedermeyer and Lopes da Silva, 2004). In clinical contexts, EEG typically refers to the recording of the brain's spontaneous electrical activity from multiple electrodes placed on the scalp over a period.

The electric potential generated by an individual neuron is far too small to be picked up by electroencephalography (Nunez et al., 1981). Therefore, the activity captured by EEG is always produced by summation of the synchronous activity of thousands or millions of neurons with similar spatial orientation. If spatial orientation is different, cells' ionic currents are not aligned and do not create enough electrical voltage to be detected. Pyramidal neurons of the cortex are thought to produce the most EEG signal because they are well-aligned and fire together. Because voltage fields fall off with the square of distance, activity from deep sources is more difficult to detect than currents near the skull (Klein and Thorne, 2006). Synchronization refers to a process wherein some linear and/or nonlinear oscillatory components of a system adjust a given property of their activity over time showing a collective behavior (Boccaletti et al., 2002). In the context of EEG rhythms, features of the “synchronization” class reflect the temporal dynamics of the synchronized activity in local cortical neural populations, showing a collective oscillatory behavior at a macroscopic spatial scale of a few centimeters. Distributed populations of those neurons in the cerebral cortex are considered as the main source of EEG rhythms recorded by scalp electrodes in both resting and task conditions. Peculiar frequency ranges and spatial distributions are associated with different states of brain functioning (e.g., waking and the various sleep stages). These oscillations represent synchronized activity over a network of neurons.

The EEG is typically described in terms of rhythmic activity, divided into bands by frequency, and transient. These frequency bands are mostly a matter of nomenclature, but these designations arose because rhythmic activity within a certain frequency range was noted to have a certain distribution over the scalp or a certain biological significance.

3.2 The EEG rhythms

Most of the cerebral signal observed in the scalp EEG falls in the range of 1–20 Hz (activity below or above this range is likely to be artifactual, under standard clinical recording techniques). Waveforms constituting

Introductory part

EEG signals are subdivided into frequency bands known as delta, theta, alpha, beta, and gamma as commonly defined in clinical practice (Figure 5).

- Delta is the frequency range up to 4 Hz. It tends to be the highest in amplitude and the slowest waves. It is seen normally in adults in slow wave sleep. It is also seen normally in babies. It may occur focally with subcortical lesions and in general distribution with diffuse lesions, metabolic encephalopathy hydrocephalus or deep midline lesions. It is usually most prominent frontally in adults (e.g. FIRDA - Frontal Intermittent Rhythmic Delta) and posteriorly in children (e.g. OIRDA - Occipital Intermittent Rhythmic Delta).
- Theta is the frequency range from 4 Hz to 7 Hz. Theta is seen normally in young children. It may be seen in drowsiness or arousal in older children and adults; it can also be seen in meditation. Excess theta for age represents abnormal activity. It is considered as a focal disturbance in focal sub-cortical lesions; it can be seen in generalized distribution in diffuse disorder or metabolic encephalopathy or deep midline disorders or some instances of hydrocephalus. On the contrary this range has been associated with reports of relaxed, meditative, and creative states.
- Alpha is the frequency range from 7 Hz to 13 Hz. Hans Berger named the first rhythmic EEG activity he saw as the "alpha wave". This was the "posterior basic rhythm" (also called the "posterior dominant rhythm" or the "posterior alpha rhythm"), seen in the posterior regions of the head on both sides, higher in amplitude on the dominant side. It emerges with closing of the eyes and with relaxation and attenuates with eye opening or mental exertion. The posterior basic rhythm is actually slower than 8 Hz in young children (therefore technically in the theta range).
- Beta is the frequency range from 14 Hz to about 30 Hz. It is seen usually on both sides in symmetrical distribution and is most evident frontally. Beta activity is closely linked to motor behavior and is generally attenuated during active movements. Low amplitude beta with multiple and varying frequencies is often associated with active, busy or anxious thinking and active concentration. Rhythmic beta with a dominant set of frequencies is associated with various pathologies and drug effects, especially benzodiazepines. It may be absent or reduced in areas of cortical damage. It is the dominant rhythm in patients who are alert or anxious or who have their eyes open.
- Gamma is the frequency range approximately 30–100 Hz. Gamma rhythms are thought to represent binding of different populations of neurons together into a network for the purpose of carrying out a certain cognitive or motor function.

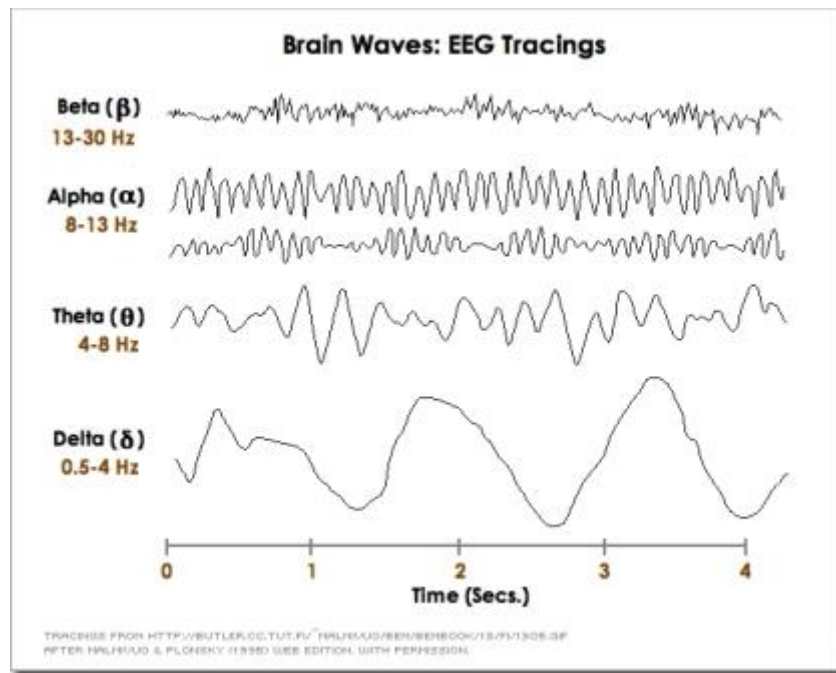


Figure 5. Normal adult brain waves (they are referred to 1 s of duration): delta (< 4 Hz), theta (4-7 Hz), alpha (8-13 Hz), beta (14-30 Hz), and gamma (30-100 Hz).

3.3 Paradigms of EEG data acquisition

Several guidelines (Jobert et al., 2012) have been produced to provide indications to allow reproducibility of EEG experiments, thus data acquired from a subject could be compared over time with data from the same subject or from other subjects.

3.3.1 Subject's mental state

For clinical research, some important conditions should be considered. Firstly, a few days prior to the recording of rsEEG rhythms, subjects should be instructed to have regular sleep on the night before that recording. Subjects should also be instructed not to use psychoactive substances and medications (i.e., foods and drinks including nicotine, caffeine, alcohol, and other stimulants in any form in the morning of the experiment). In the same line, benzodiazepines, antidepressant, and/or antihypertensive drugs (when typically used by subjects) may have to be withdrawn for about 24h before the recording if the drug effects may interfere with interpretation of rsEEG rhythms.

Secondly, the preferred time for the recording of rsEEG rhythms is the morning. At that time, it is expected that the subject is not tired or sleepy and has had only a satisfying light breakfast.

Thirdly, a brief interview of the subjects should confirm if the above conditions are adequately met in the morning of the EEG recording. Ideally, the subjects' quality of sleep during the night preceding the recording should not be different from usual. In the case of conditions incompatible with a recording of good quality, the event should be postponed to another date.

Introductory part

3.3.2 Environmental conditions

Ideal environment is achieved through the careful control of general conditions during the recording and specific instructions given to the subject, i.e. room lighting, acoustic noise, comfortability of armchair or bed during for the subjects, wall painting.

3.3.3 Instructions to subjects

Subject should be instructed clearly according to the peculiar experimental protocol adopted. Several paradigms and following analyses could be applied:

- Recording and processing of EEG at rest (resting state is defined as a mental state of quite vigilance) or during sleep stages;
- Recording and processing of EEG during mental tasks, sensory stimulation or motor acts;
- Recording and processing of EEG event-related, i.e. the short activation immediately following a specific task.

3.3.4 Montage of EEG electrodes

In conventional scalp EEG, the recording is obtained by placing electrodes on the scalp with a conductive gel or paste, usually after the preparation of the area by exercising a gentle abrasion to reduce impedance due to dead skin cells. Many systems typically use single-use electrodes, each with its own individual wire. Some systems use caps or nets into which electrodes are embedded; this is particularly common when high-density arrays of electrodes are needed (64 electrodes or higher).

The 10–20 system or International 10–20 system is an internationally recognized method to standardize the location of scalp electrodes for EEG clinical acquisition or experiment. In this way, reproducibility is ensured, and data acquired from a subject could be compared over time with data from the same subject or from other subjects. This system is based on the relationship between the location of an electrode and the underlying area of cerebral cortex. The "10" and "20" refer to the fact that the actual distances between adjacent electrodes are either 10% or 20% of the total front–back or right–left distance of the skull. Each site has a letter to identify the lobe and a number to identify the hemisphere location. The letters F, T, C, P and O stand for frontal, temporal, central, parietal, and occipital lobes, respectively. The "C" letter is used only for identification purposes because there exists no central lobe; a "z" (zero) refers to electrodes placed on the midline. Even numbers (2, 4, 6, 8) refer to electrode positions on the right hemisphere, whereas odd numbers (1, 3, 5, 7) refer to those on the left hemisphere. In addition, the letter codes A, Pg and Fp identify the earlobes, nasopharyngeal and frontal polar sites respectively. Two anatomical landmarks are used for the essential positioning of the EEG electrodes: first, the nasion which is the distinctly depressed area between the eyes, just above the bridge of the nose; second, the inion, which is the lowest point of the skull from the back of the head and is normally indicated by a prominent bump (Figure 6).

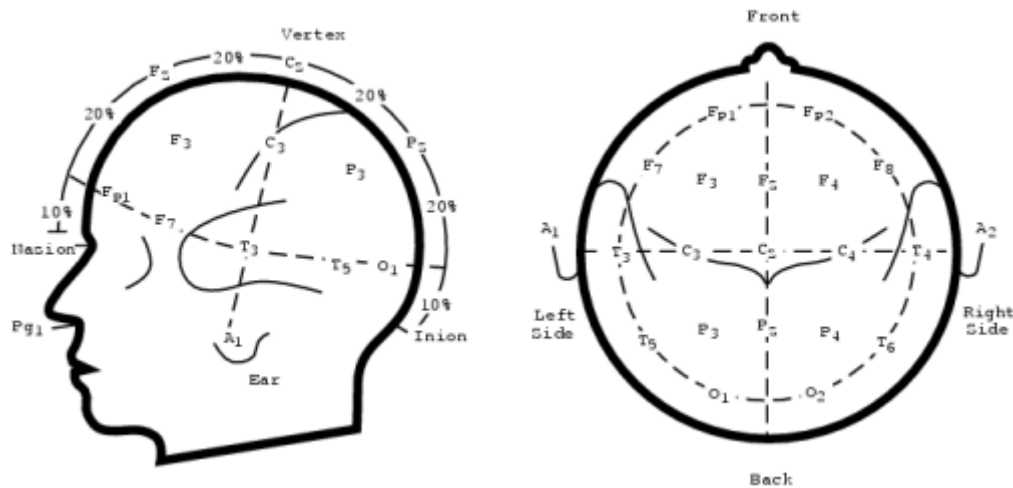


Figure 6. Diagram of the international 10/20 system. Each electrode is assigned a nomenclature with a letter and a number. The letters indicate the areas of the scalp: F (Frontal), C (Central), T (Temporal), P (Parietal) and O (Occipital); numbers are odd for the left side and even for the right side.

3.3.5 Montage of other sensors for the quality control of EEG recording

To control of eye movements (i.e., saccades) or blinking in clinical routine and research applications, vertical and horizontal electro-oculographic (EOG) potentials should be recorded from bipolar electrode pairs placed around the dominant eye. For specific clinical research purposes, other EOG montages as well as infrared or optical eye tracking can be used.

To control of the subject's arousal, vital signs, and behavior, other electrodes can be mounted. These electrodes typically allow the recording of electrocardiographic (EKG) activity from Einthoven's derivations (e.g., left vs. right wrist), skin conductance (previously "galvanic resistance") from one or two hands, electromyographic (EMG) activity from neck or other relevant sites to monitor the subject's behavior, and respiration from a sensor belt. Of note, EKG (e.g., heart rate variability), EMG, and skin galvanic resistance can provide independent measurements of the general level of brain arousal to be related to dominant posterior rsEEG rhythms supposed to reflect that arousal (Barry et al., 2011).

3.3.6 Setting of rsEEG recording parameters (sampling frequency, bandpass filter, amplification, etc...).

Standard setting when the interest of scalp rsEEG recordings is focused on frequency under 50 Hz includes a minimum sampling rate of 250^2 samples per second (Hz) and 12/14-bit resolution per sample with a resolution down to 0.5 μ V. Indeed, analog filters of devices used for the recordings of rsEEG rhythms should be available with settings down to a cut-off frequency of 0.1 Hz for the high-passband filter and at least 60-70 Hz for the low-passband filter where the frequency sampling is set at 256 Hz, considering a minimum factor of 4 between the sampling frequency and the anti-aliasing filter to avoid aliasing. Analog 50 or 60 Hz notch-reject filter or high-pass filter set at 1 or 2 Hz should be set only when off-line digital filters are not available.

Introductory part

In devices used for the recording of scalp rsEEG rhythms in both clinical routine and research applications, the amplified signal for each electrode should be matched to reduce electrode-to-electrode variability to a maximum of 1% after computer-adjusted gains based on calibration pulses and bio-calibration comparisons. An even better agreement would be preferable. Calibration of devices used for recording and analysis of scalp EEG rhythms should carefully cover the whole extent of equipment used, from the electrode input box through the data processing and onto the final display.

3.4 EEG source estimation

Source estimation consists in localizing the different activated functional networks implicated in a given mental task or state. Positron emission topography (PET) and functional magnetic resonance imaging (fMRI) are not the most suitable for addressing the question of when during the mental task the different modules become active due to their low temporal resolution (> 1 s). In addition, they are not suitable to readily discriminate between sequential versus parallel activation, feedforward versus feedback processes, or how information is ‘bound’ together to form unified percepts (Michel et al., 2004). Electro- and magnetoencephalography (EEG, MEG) offer this possibility by measuring the electrical activity of neuronal cell assemblies on a submillisecond time scale. Unfortunately, these techniques face the problem that the signals measured on the scalp surface do not directly indicate the location of the active neurons in the brain due to the ambiguity of the underlying static electromagnetic inverse problem (Helmholtz, 1853).

From the distribution of electric potential on the scalp recorded by EEG, the aim is that of estimating the location and strengths of the current sources that generate the measured data. This problem of source localization is an ill-posed inverse problem. There are an infinite number of solutions that explain the measured data equally well because silent sources (i.e., sources that generate no measurable EEG signals) exist, and these can always be added to a solution without affecting the data fit. Because of this nonuniqueness, a priori information is needed to constrain the space of feasible solutions. Nonuniqueness is handled by making assumptions about the nature of the sources (e.g., number of sources, anatomical and neurophysiological constraints, prior probability density functions, norms, smoothness, correlation, covariance models, sparsity, diversity measures, spatial extent constraints, etc.). Thus, the accuracy and validity of the estimates depend to some extent on the biological correctness of the assumptions and priors adopted in our models. Therefore, priors should not only be informed by neurophysiology domain knowledge but should also be flexible and adaptive to data sets.

Several problems affect the source estimation with EEG data:

- *Number of electrodes:* the influence of the number of electrodes on source localization precision is not linear, thus it is not true that higher number of electrodes means better localization;
- *Volume conduction:* it is possible that the EEG signal recorded in a specific site on the scalp is due to the activity of a source localized not immediately under the recording site;

Introductory part

- *Common feeding*: the correlated EEG signals recorded in two specific sites may be due to the activity of a third common source and does not mean that also the source activities are dependent and thus functionally connected.

4 Study I: Two-year longitudinal monitoring of amnesic mild cognitive impairment patients with prodromal Alzheimer's disease using topographical biomarkers derived from functional magnetic resonance imaging and electroencephalographic activity

4.1 Introduction

The International Working Group has recently made a useful distinction between diagnostic and topographical biomarkers of Alzheimer's disease (AD) for research applications in patients with amnesic mild cognitive impairment (aMCI) due to the prodromal manifestation of the pathology (Dubois et al., 2014). Diagnostic biomarkers were defined as those measuring *in-vivo* intrinsic pathophysiological variables characterizing neurobiologically AD, namely amyloid deposition and neurofibrillary tangles in the brain. They are expected to be present at all stages of the disease, are observable even in the preclinical asymptomatic state, are not necessarily correlated with disease severity, and are indicated for inclusion of AD patients in clinical trial protocols. Diagnostic biomarkers include low doses of A β 42 and high doses of total tau (T-tau) or phospho tau (P-tau) in cerebrospinal fluid (CSF) or evidence of significant amyloid deposition and tau aggregation in the brain in maps of positron emission tomography (PET) (Agosta et al., 2012).

In contrast, topographic or progression biomarkers may not be specific of AD neuropathology or absent in early disease stages, but they can be very useful to monitor the progression of the disease in the brain and may be related to the kind and severity of cognitive deficits (Dubois et al., 2014). Progression markers include hippocampal atrophy or cortical thickness, assessed by structural MRI, and cortical hypometabolism in posterior cingulate, parietal, temporal, and hippocampal regions, measured by FDG-PET (Dubois et al., 2014). Of note, these topographic biomarkers are limited in the sense that they do not directly measure brain amyloid deposition and neurofibrillary tangles in AD patients, so they cannot be used as primary neuropathological endpoints in the evaluation of AD-modifying agents.

Promising candidates as topographic markers of AD are those reflecting functional aspects of brain neurotransmission and connectivity, as human cognition is the result of collective and coordinated behavior of brain networks. In this line, functional MRI accompanying resting state condition (rsfMRI) allows the computation of intrinsic hemodynamic low-frequency (< 1 Hz) statistical correlations of blood oxygenation level dependent (BOLD) signals between brain regions as a marker of brain functional connectivity (Biswal et al., 1995, Fox et al., 2005). The default mode network (DMN), which includes posterior and anterior cingulate areas, angular gyri, occipital, and parietotemporal regions, is a particularly relevant network to actively maintain resting state condition in low vigilance and self-awareness (Raichle, 2015). Several studies have shown a significant reduction of DMN brain connectivity in groups of patients with aMCI and AD dementia compared with control seniors with intact cognition (Agosta et al., 2014, Damoiseaux, 2012, Damoiseaux et

Experimental part

al., 2012, Teipel et al., 2016, Zhang et al., 2010, Zhou et al., 2017). As topographic biomarker of progression, these fMRI biomarkers pointed to a reduction of brain functional connectivity in DMN in aMCI and AD patients with dementia at about 1-year follow up (Damoiseaux, 2012, Damoiseaux et al., 2012, Binnewijzend et al., 2012, Dennis and Thompson, 2014). Other candidate topographic biomarkers of AD derive from electroencephalographic (EEG) techniques, which are noninvasive, cost-effective, and can be repeated several times along disease progression without learning effects affecting paradigms using tasks. When compared to fMRI and FDG-PET, EEG techniques have a modest spatial resolution of some centimeters but a very high temporal resolution (milliseconds); that temporal resolution is ideal to investigate brain rhythms during resting state condition (i.e. resting state EEG, rsEEG) and quick brain dynamics in response to cognitive-motor events challenging attention and short episodic memory (i.e., event-related potentials, ERPs). Derived rsEEG/ERP biomarkers may reflect synchronization and connectivity between large populations of cortical pyramidal neurons in resting state conditions or during cognitive tasks [Babiloni et al., 2016]. Previous studies have shown that compared to control seniors, patients with aMCI and dementia due to AD were characterized by increased rsEEG power density at delta (< 4 Hz) and theta (4-7 Hz) frequency bands in widespread cortical regions as well as decreased rsEEG power density at alpha (8-13 Hz) and beta (14-30 Hz) frequency bands in central and posterior cortical regions (Agosta et al., 2012, Babiloni et al., 2016, Babiloni et al., 2006, Babiloni et al., 2007, Babiloni et al., 2014, Babiloni et al., 2013, Babiloni et al., 2013, Babiloni et al., 2011, Huang et al., 2000, Jelic et al., 2000, Koenig et al., 2005). Furthermore, these patients were also characterized by latency increase and amplitude decrease in late positive parietal ERPs (i.e., P3b) peaking at about 300-400 ms from the onset of a rare (20-30% of probability to occur in a sequence with frequent auditory stimuli to be ignored) auditory or visual stimulus triggering hand motor responses or mental stimulus counting (Jervis et al., 2010, Papaliagkas et al., 2008, Papaliagkas et al., 2010, Papaliagkas et al., 2011, Polich and Corey-Bloom, 2005, Tsolaki et al., 2017). As topographic biomarkers of progression, these EEG/ERP readouts pointed to increased abnormalities in delta/alpha rhythms and P3b peak in aMCI and AD patients with dementia at about 1-year follow up (Babiloni et al., 2014, 2013, Papaliagkas et al., 2008, 2011). These effects were typically discussed in relationship to death of cortical neurons, axonal pathology, and cholinergic neurotransmission deficits (Babiloni et al., 2013, Babiloni et al., 2015, 2016, 2006, 2009, Czigler et al., 2008, Jelles et al., 2008 Jeong, 2004).

The mentioned findings motivate the evaluation of rsfMRI and rsEEG/P3b as topographic biomarkers sensitive to prodromal (MCI) and dementia stages of AD. This process needs to overcome the following methodological limitations of typical multi-centric longitudinal studies: (1) retrospective nature, (2) the use of few recording sessions over time (mostly a baseline and a 1-year follow up) subjected to the confounding effect of disease onset and trajectories in aMCI patients, (3) the lack of a careful characterization of aMCI due to AD as cognitive profile (only one test of episodic memory) and positivity to standard diagnostic biomarkers of AD, and (4) the absence of a control group of aMCI patients not due to AD with expected different disease evolution over time. The European, prospective, multi-centric study entitled “PharmaCog - E-ADNI” (<http://www.pharmacog.org>) addressed such limitations. In the PharmaCog study, 147 aMCI patients were

Experimental part

screened as APOE genotyping and AD diagnostic markers of CSF and followed longitudinally with clinical, neuropsychological, MRI, rsEEG/ERP, and blood markers for 24 months. The aMCI patients were separated into two sub-groups, namely those “positive” (i.e. prodromal AD) and “negative” to CSF diagnostic markers of AD (i.e. statistical thresholds for A β 42/P-tau ratio based on APOE ϵ 4 carrier status, Marizzoni et al., 2017). Preparatory PharmaCog studies described the successful multisite MRI harmonization efforts (Albi et al., 2017, Jovicich et al., 2013, 2014 2016, Marchitelli et al., 2016, Marizzoni et al., 2015) and the characterization of the “positive” and “negative” aMCI subjects as neuropsychological, MRI (i.e., hippocampal atrophy, morphometry, and diffusion), and rsEEG/ERP at the baseline stage (Agosta et al., 2014, Galluzzi et al., 2016, Nathan et al., 2017).

This article is part of a Mini Forum on PharmaCog matrix of biomarkers of prodromal AD in patients with aMCI, which is based on four papers published in Journal of Alzheimer’s disease. The specific aim of this article is to evaluate longitudinal functional topographical biomarkers derived from rsfMRI and rsEEG/ERP data in a population of aMCI enrolled in the PharmaCog project and test if these markers can differentiate the group of the “positive” aMCI patients with prodromal AD from the “negative” aMCI subgroup during a time window of 24 months with 5 serial recordings 6 months apart. A linear mixed model adjusted by nuisance covariates was used to investigate those functional biomarkers in terms of Group (“positive” vs “negative” differences regardless of time), Time (temporal effects regardless of Group effects), and Time x Group fixed effects (differential progression between the two subgroups). In the experimental design, the observation time (i.e., 24 months) was expected to account for possible different disease stages in the “positive” and “negative” aMCI patients, while the “negative” aMCI patients were used as a control subgroup. This allowed dissociating, at least in part, cognitive impairment and functional biomarker differences between prodromal and non-prodromal AD in the aMCI subgroups. For sample homogeneity, the statistical design included aMCI data only until conversion to dementia.

4.2 Materials and Methods

4.2.1 Participants, clinical exams, and neuropsychological tests

Participants’ demographics, clinical, and neuropsychological data have been described in recent PharmaCog studies (Marizzoni et al., 2015, 2017, Galluzzi et al., 2016). Briefly, 147 aMCI patients were enrolled in 13 European memory clinics of the Innovative Medicine Initiative (IMI) PharmaCog project (<http://www.pharmacog.org>). Follow-up examinations were performed every 6 months for at least 2 years or until patient progressed to clinical dementia. The main inclusion/exclusion criteria were (1) age between 55 and 90 years; (2) complaints of memory loss by the patient, confirmed by a family relative; (3) Mini-Mental State Examination (MMSE) score of 24 and higher; (4) overall Clinical Dementia Rating score of 0.5; (5) score on the logical memory test lower than 1 standard deviation from the age-adjusted mean; (6) 15-item Geriatric

Experimental part

Depression Scale score of 5 or lower; and (7) absence of significant other neurologic, systemic or psychiatric illness.

4.2.2 Functional MRI data

The multi-site 3T rsfMRI acquisition and analysis protocols have been described in recent studies from the PharmaCog project, also demonstrating high test-retest reproducibility across the Consortium with the use of harmonized MRI acquisition protocols (Jovicich et al., 2013, 2016). Briefly, 13 European clinical sites equipped with 3.0T scanners used a harmonized MRI acquisition protocol that included structural 3D T1 images (Jovicich et al., 2013) and resting state echo-planar imaging (EPI) sessions using manufacturer-provided sequence (Jovicich et al., 2016). This resulted in a sample of 882 rsfMRI datasets (147 subjects, 6 sessions per subject).

Standard brain data preprocessing was performed using SPM8 (<http://www.fil.ion.ucl.ac.uk/spm>) running under Matlab R2012a (The MathWorks, Inc., Natick MA, USA) and code developed in-house (Jovicich et al., 2016). The main focus of the analysis of rsfMRI data was the functional connectivity within the nodes of DMN, which is expected to be reduced in the early stages of AD (Agosta et al., 2014, Damoiseaux, 2012, Damoiseaux et al., 2012, Binnewijzend et al., 2012, Dennis and Thompson, 2014). In this line, DMN nodes of interest for this study were the following: medial prefrontal cortex (MFC), bilateral precuneus and posterior cingulate cortex (PCC), and inferior left and right parietal cortex (LPC and RPC, respectively). We also included the left attention frontal-parietal (LFP) network given its potential role in memory cognitive reserve (Agosta et al., 2014, Franzmeier et al., 2017). The anatomical characteristics of the DMN and LFP regions and the data analysis procedure are reported in previous methodological study of the Consortium (Jovicich et al., 2016). In brief, Group Independent component analysis (ICA) was performed using 10 spatial components on the concatenated data from each MRI site followed by back-reconstruction (Calhoun et al., 2001) to derive the single session DMN and attention LFP network from each subject (Jovicich et al., 2016). DMN regions-of-interest (ROIs) for functional connectivity measurements were obtained by thresholding at $z > 4$ the aggregate DMN site component (Jovicich et al., 2016). For each participant and session, this analysis yielded the average connectivity z-score within the whole DMN, LFP, and also considering separately each one of the separate nodes within the DMN (PCC, LPC, RPC, and MFC, Jovicich et al., 2016). These z-scores were used as functional connectivity measures and were the rsfMRI dependent variables in the statistical analyses.

The statistical analyses considered also two MRI-related nuisance regressors for each session, the white matter temporal signal-to-noise ratio (tSNR), given its high variability across sites mostly driven by hardware differences (Jovicich et al., 2016), and the median head movement.

4.2.3 EEG data

Experimental part

Recordings of rsEEG (eyes-closed and -open; N = 126) and auditory “oddball” ERPs (N = 125) were performed by commercial digital EEG systems in the Clinical Units of the PharmaCog Consortium (see more details in Galluzzi et al., 2016). A minimum of 19 scalp electrodes was positioned according to the international 10–20 montage system and referenced to linked earlobes or cephalic reference according to the constraints of the local EEG systems. Ground electrode was placed over the scalp, according to the local standard of the Clinical Units. To monitor eye movements and blinking, bipolar vertical and horizontal electrooculograms (EOGs; 0.3–70 Hz bandpass) were simultaneously recorded. Furthermore, a standard electrocardiographic (EKG) channel was also recorded by a monopolar V6 derivation to remove possible EKG artifacts from EEG data. All electrophysiological data were digitized in continuous recording mode (from 128 to 1000 Hz sampling rate according to the constraints of the local EEG systems). To minimize drowsiness and sleep onset, the duration of the rsEEG recordings was established subject-by-subject from at least 3 minutes to a maximum 5 minutes for each condition (i.e., eyes closed, eyes open).

The rsEEG and ERP data were segmented and analyzed offline in consecutive 2-s and 3-s epochs, respectively. Artifactual epochs were identified using a computerized home-made automatic software procedure (Moretti et al., 2003), confirmed by two EEG experts (CDP, RL), and then eliminated. Artefact-free rsEEG epochs recorded during eyes open condition were used to control the expected reactivity of alpha rhythms as a sign of good quality of rsEEG recordings. Artifact-free rsEEG epochs recorded during eyes open condition were used as an input for the analysis of EEG power density spectrum and cortical source estimation. Concerning ERPs, artifact-free ERP epochs related to frequent and rare stimuli were averaged separately to form individual ERPs for those two classes of auditory stimuli. The latency of the posterior P3b peak following rare stimuli was measured at the Pz electrode and used as a latency reference for further analysis. Based on that latency peak, voltage amplitude was measured at all scalp electrodes in both ERPs related to rare stimuli and those related to frequent stimuli. For ERP source estimation, individual P3b peak potential distribution was computed according to a standard procedure as the subtraction of P3b peak voltage for the rare stimuli minus the potential distribution for the frequent stimuli at the same latency.

Official exact low-resolution brain electromagnetic tomography (eLORETA) freeware (Pascual-Marqui, 2007) was used for the estimation of cortical sources of the rsEEG and P3b peak data in a standard brain atlas (Pascual-Marqui, 2007). The following rsEEG/P3b peak markers were estimated: (1) activity of global and regional (i.e. frontal, central, parietal, occipital, temporal, and limbic lobes as defined in the eLORETA brain atlas, Pascual-Marqui, 2007) normalized cortical (eLORETA) sources of rsEEG rhythms for delta (2–4 Hz), theta (4–7 Hz), alpha 1 (8–10.5 Hz), delta/alpha 1, and theta/alpha 1 bands, as indexes of cortical neural synchronization; and (2) activity of cortical sources of posterior parietal (i.e., Brodmann areas 5, 7, 39, and 40) and posterior cingulate (Brodmann areas 31 and 23) regions generating P3b peak voltage, as an index of cortical neural synchronization related to attention and short-term auditory episodic memory.

4.2.4 Patients' classification in prodromal AD and control aMCI patients

Experimental part

As mentioned in the Introduction section, the aMCI patients were classified into two subgroups named “positive” (i.e., prodromal AD) and “negative” aMCI based on the results of a Mixture Linear Model with the p sets at < 0.05 (Marizzoni et al., 2017). This Model determined the existence of one or more Gaussian populations of aMCI subjects based on the frequency distributions of CSF A β 42/P-tau levels in the baseline recordings. According to this Model, the aMCI patients were denoted as “positive” aMCI (i.e., prodromal AD) with CSF A β 42/P-tau levels lower than 15.2 for APOE ϵ 4 carriers and 8.9 for APOE ϵ 4 non-carriers. The remaining aMCI patients were denoted as “negative” aMCI.

4.2.5 Statistical analysis

Statistical analyses were performed using SPSS software for descriptive statistics and R software (A language and environment for statistical computing, version 3.4.1) for the computation of Mixture and Linear Mixed Models. Characteristics of the aMCI participants at the baseline recordings were assessed by parametric t-tests (or corresponding non-parametric Mann-Whitney) for continuous Gaussian (or non-Gaussian) distributed variables ($p < 0.05$) and by Chi-square tests for categorical data ($p < 0.05$).

Linear Mixed Models (R-package lme4) were used as statistical tests as they allow the use of individual longitudinal data sets even when some recording sessions are missing in the series (e.g., for technical failures or patients' problems). Specifically, two different types of Linear Mixed Models were used with all available values of the rsfMRI, rsEEG/P3b peak, and clinical variables in the whole aMCI cohort. In the Models, the fixed effect Group included the two subgroups of “positive” and “negative” aMCI patients, while the fixed effect Time included the values of rsfMRI, rsEEG/P3b peak, and ADAScog13 for baseline recordings and follow-ups at 6, 12, 18, and 24 months. The aMCI patients eventually progressing to dementia were no more called for subsequent follow ups in order to have a relatively homogeneous sample of data relative to aMCI condition. Random intercept and random slope across the variables were used as random effects in the Models to account for individual differences in the biomarkers and ADAScog13 values at baseline as well as for individual changes of those variables across all aMCI patients over follow-ups. All Models were adjusted for age, sex, and education. The output of the Linear Mixed Models was presented in terms of standardized η^2 coefficient, corresponding P-value and, for the interaction factor only, effect size (pseudo h^2) calculated as ratio of explained variability of interaction effect on total variability of each model.

The first Linear Mixed Models of rsfMRI and EEG biomarkers were conducted with Time, Group, and Time X Group interaction as fixed effects. The rsfMRI biomarkers were adjusted also for median head motion and white matter tSNR. The main interest was focused on functional biomarkers (i.e. rsfMRI, rsEEG/P3b peak) associated with the Group effects (regardless of Time), Time effects (regardless of Group), and the Time X Group interaction (the differential progression of the positive aMCI subgroup relative to the negative aMCI subgroup). Specifically, the Group effect showed functional biomarkers distinguishing the two subgroups of aMCI patients regardless the Time effect, while the Group X Time interaction unveiled those biomarkers characterizing the disease progression over-time in the “positive” aMCI subgroup (i.e., prodromal AD).

Experimental part

The second Linear Mixed Models of rsfMRI and EEG biomarkers tested if those functional biomarkers (independent variable) and Time effects predicted cognitive decline over time in the aMCI subgroups as revealed by ADAS-cog13 scores (dependent variable).

4.3 Results

4.3.1 Patients' features

Diagnostic markers of CSF and APOE genotypes were available in 144 out of 147 aMCI patients of the PharmaCog/E-ADNI cohort, thus the final data analyses were performed in 144 patients. The main demographic and clinical characteristics of these 144 aMCI patients are reported in Table 1. All of them underwent rsfMRI acquisitions, while a slightly smaller group underwent to rsEEG/ERP recordings (N = 126 patients). The main demographic and clinical characteristics of them are reported in Table 2. In both Tables, as mentioned above, the aMCI patients were aggregated in subgroups based on the baseline A β 42, phospho tau (P-tau), and total tau (T-tau) values in the CSF as a function of APOE genotype [49]. Compared with the aMCI patients “negative” to CSF A β 42/P-tau ratio, the “positive” aMCI patients (i.e., prodromal AD) did not differ in age, gender, and education ($p > 0.05$) but showed worse global cognitive performance ($p < 0.05$). MMSE score took into account that difference in the statistical analyses.

Table 3 reports the number of aMCI patients who converted to AD or other non-AD pathologies during the study. The “negative” aMCI patient group did not present conversions to dementia due to AD within 24 months but presented 2-3% of conversions to dementia due to non-AD pathologies at 12-month follow up and 4-5% at 24-month follow up. In contrast, the “positive” aMCI patients (i.e., prodromal AD) showed 11% of conversion to dementia due to AD at 12-month follow up, 27-29% at 24-month-follow up, and no conversion to dementia due to non-AD pathologies within 24 months.

	“Negative” aMCI (N = 63)	“Positive” aMCI (N = 81)	P value ^a
Age, mean (Standard Deviation, SD)	68.3 (8.4)	69.8 (6.3)	.2
Sex, F/M, No.	36/27	46/35	1
Education, mean (SD)	10.0 (4.3)	11.1 (4.4)	.1
APOEϵ4 carriers, No. (%)	3 (5)	63 (78)	<.001
MMSE score, mean (SD)	27.1 (1.8)	26.2 (1.8)	.006

Experimental part

ADAS-cog13, mean (SD)^{b,c}	19.1 (5.9)	21.6 (8.1)	.052
CSF biomarkers, mean (SD, pg/ml)			
Aβ42	949 (244)	495 (132)	<.001
P-Tau	47 (15)	84 (38)	<.001
T-tau	301 (149)	614 (394)	<.001

Table 1: Clinical and socio-demographic features of amnesic mild cognitive impairment (aMCI) patients receiving resting state functional magnetic resonance imaging recordings (rsfMRI) in the present study. Patients were stratified into cerebrospinal (CSF) Aβ42/P-tau “positive” and “negative” according to APOE4-specific cut-offs for carriers and non-carriers of APOE4 genotyping. See Methods section for more details.

^a Assessed by ANOVA (for continuous Gaussian distributed variables) or Kruskal-Wallis with Dunn correction (for continuous non-Gaussian distributed variables) and Chi-square tests (for categorical variables).

^b Range 0-85, with 0 as the best score.

^c Information was missing for 1 patient.

Abbreviations: Legend: MMSE, mini mental state evaluation; SD, standard deviation; ADAS-cog13, Alzheimer Disease Assessment Scale-Cognitive Subscale, version 13; Aβ42, β-amyloid; APOE, apolipoprotein E; CSF, cerebrospinal fluid; P-tau, tau phosphorylated at threonine 181; T-tau, total tau; SD, standard deviation.

	“Negative” aMCI (N = 54)	“Positive” aMCI (N = 72)	P value ^a
Age, mean (Standard Deviation, SD)	68.5 (8.5)	69.9 (6.0)	.2
Sex, F/M, No.	30/24	42/30	0.8
Education, mean (SD)	9.9 (4.1)	11.0 (4.5)	.2
APOEε4 carriers, No. (%)	3.7%	77.8%	<.001
MMSE, mean (SD)	26.3 (2.2)	25.2 (2.2)	.01
ADAS-cog13, mean (SD) ^b	20.2 (6.8)	23.1 (7.7)	.04
CSF biomarkers, mean (SD, pg/ml)			
Aβ42	932 (253)	500 (132)	<.001

Experimental part

P-Tau	47 (15)	84 (36)	<.001
T-tau	297 (151)	600 (316)	<.001

Table 2: Clinical and socio-demographic features of aMCI patients undergone to resting state electroencephalographic (rsEEG) and event-related potential (ERP) recordings in the present study. These patients, a subgroup of those described in Table 1, were stratified into CSF A β 42/P-tau “positive” and “negative” according to APOE4-specific cut-offs for carriers and non-carriers of APOE4 genotyping. See Methods section for more details.

^a Assessed by ANOVA (for continuous Gaussian distributed variables) or Kruskal-Wallis with Dunn correction (for continuous non-Gaussian distributed variables) and Chi-square tests (for categorical variables).

^b Range 0-85, with 0 as the best score.

Abbreviations: ADAS-cog13, Alzheimer Disease Assessment Scale-Cognitive Subscale, version 13; A β 42, β -amyloid; APOE, Apolipoprotein E; CSF, cerebrospinal fluid; P-tau, tau phosphorylated at threonine 181; T-tau, total tau; SD, standard deviation.

aMCI patients with rsfMRI recordings

	CSF A β 42/P-tau “negative” aMCI group	CSF A β 42/P-tau “positive” aMCI group
N	63	81
Converted in AD (12 months)	0.0% (N=0)	11.1% (N=9)
Converted in AD (24 months)	0.0% (N=0)	27.2% (N=22)
Converted in other dementias (12 months)	3.2% (N=2)	0.0% (N=0)
Converted in other dementias (24 months)	4.8% (N=3)	0.0% (N=0)

aMCI patients with rsEEG/ERP recordings

	CSF A β 42/P-tau “negative” aMCI group	CSF A β 42/P-tau “positive” aMCI group
N	54	72
Converted in AD (12 months)	0.0% (N=0)	11.1% (N=8)
Converted in AD (24 months)	0.0% (N=0)	29.2% (N=21)
Converted in other dementias (12 months)	1.9% (N=1)	0.0% (N=0)
Converted in other dementias (24 months)	3.7% (N=2)	0.0% (N=0)

Experimental part

Table 3: Number of patients who converted from aMCI to dementia due to AD and other pathologies. These patients were stratified into CSF A β 42/P-tau “positive” and “negative” according to APOE4-specific cut-offs for carriers and non-carriers of APOE4 genotyping. See Methods section for more details.

4.3.2 rsfMRI connectivity measures of prodromal AD

Table 4 reports the results of a Linear Mixed Model showing the variance explained in rsfMRI connectivity measures (population described in Table 3) by the fixed effects of Group (“positive” vs. “negative” group differences regardless of time), Time (temporal differences regardless of group), and Time X Group interaction (differential progression across groups) in aMCI patients over the observation time (24 months, 5 recording session 6 months apart).

Concerning Group and Time, rsfMRI functional connectivity in both the DMN and PCC showed significant effects ($p < 0.05$). Specifically, Time effects in DMN and PCC showed a global reduction of functional connectivity over time regardless of Group (DMN: P-value = 0.01, Std β = -0.1; PCC: P-value = 0.05, Std β = -0.09). Furthermore, both DMN and PCC functional connectivity measures also exhibited a significant Group effect pointing to reduced functional connectivity in the “positive” aMCI subgroup (i.e., prodromal AD) compared with the “negative” aMCI subgroup (DMN: P-value = 0.01, Std β = -0.2; PCC: P-value = 0.001, Std β = -0.3). Figure 7 (upper diagrams) illustrates these Group and Time effects of functional connectivity in PCC. The plot displays the mean modeled connectivity in the two subgroups of aMCI patients over the 5 recording sessions. The profile of DMN changes is very similar (results not shown). As it can be seen in Figure 7 for PCC, the functional connectivity decay in the time interval of the study is similar in both subgroups, which is consistent with the finding of no significant Time X Group interactions in DMN and PCC.

Interestingly, only functional connectivity in the LPC node showed a significant Time X Group interaction, indicating an increase of connectivity over time in the “positive” (i.e. prodromal AD) relative to the “negative” aMCI subgroup (P-value = 0.01, Std β = 0.2). Figure 8 (upper diagram) illustrates the mean values of rsfMRI connectivity in LPC in the “positive” (i.e., prodromal AD) and “negative” aMCI subgroups over the 5 recording sessions.

The attention LFP network showed no Group effect or Group X Time interaction ($p > 0.05$). Indeed, the only significant finding was a Time effect indicating a lower functional connectivity over time in the LFP network in both “positive” and “negative” aMCI subgroups (P-value = 0.01, Std β = -0.1).

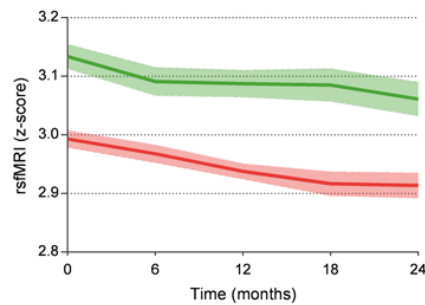
rsfMRI connectivity measure	Group		Time		Time X Group	
	Std β	P-value	Std β	P-value	Std β	P-value
PCC	-0.3	0.001	-0.09	0.04	-0.05	0.5

Experimental part

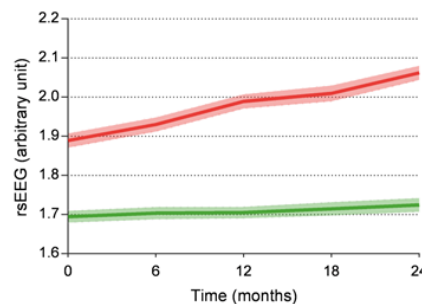
LPC	0.2	0.08	-0.06	0.100	0.2	0.01
DMN	-0.2	0.01	-0.1	0.01	0.01	0.9
LFP	-0.002	1	-0.1	0.01	0.03	0.8

Table 4. Resting state fMRI nodes showing significant functional connectivity effects explained by a Linear Mixed Model of longitudinal changes (baseline, 6, 12, 18, 24 months follow ups) in aMCI patients stratified into two groups (“positive” as prodromal AD and “negative” as a control group). The model included Group ($A\beta_{42}/P$ -tau ratio), Time, and Time X Group interaction as main predictors of interest adjusted by age, sex, baseline MMSE score, temporal signal-to-noise ratio, and mean fractional head displacement as nuisance variables. Significant (P -value < 0.05) fixed effects are emphasized in bold. Abbreviations: DMN, default mode network (all nodes); PCC, posterior cingulate cortex; LPC, inferior left parietal cortex; LFP, left attention frontal-parietal network; Std β , standardized β coefficient of Linear Mixed Model.

Functional rsfMRI connectivity in posterior cingulate cortex



Cortical global delta sources of rsEEG rhythms



Cortical parietal sources of auditory oddball P3b peak

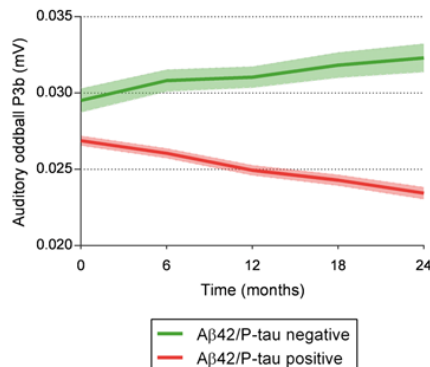


Figure 7. Longitudinal profile of functional topographical biomarkers showing significant Group effects regardless of time (p -value < 0.05). Patients were stratified in two amnesic mild cognitive impairment (aMCI) subgroups: $A\beta_{42}/P$ -tau “positive” (red) as prodromal AD as an experimental subgroup and $A\beta_{42}/P$ -tau “negative” (green) as a control subgroup. Mean (\pm standard error of the mean, SEM) model values are shown from 5 recording sessions starting at time zero (baseline) and 6-, 12-, 18, and 24-month follow-ups. Top: resting state functional magnetic resonance imaging (rsfMRI) functional connectivity measures in the precuneus and posterior cingulate cortex (PCC) of the DMN. Of note, functional rsfMRI connectivity in both PCC and global default mode network (DMN; not shown) gave a similar pattern of significant Group effects (connectivity reduction in “positive” group regardless of time) and Time effects (functional decay in Time regardless of Group, p -value < 0.05). Middle: Mean (\pm standard error of the

Experimental part

mean, SEM) values of global cortical sources of resting state electroencephalographic (rsEEG) rhythms at delta frequency band (< 4 Hz). Bottom: mean (\pm SEM) values of parietal cortical sources of auditory “oddball” event-related potentials (ERPs) peaking at about 400 ms (P3b peak) post-stimulus following rare minus frequent stimuli in those groups.

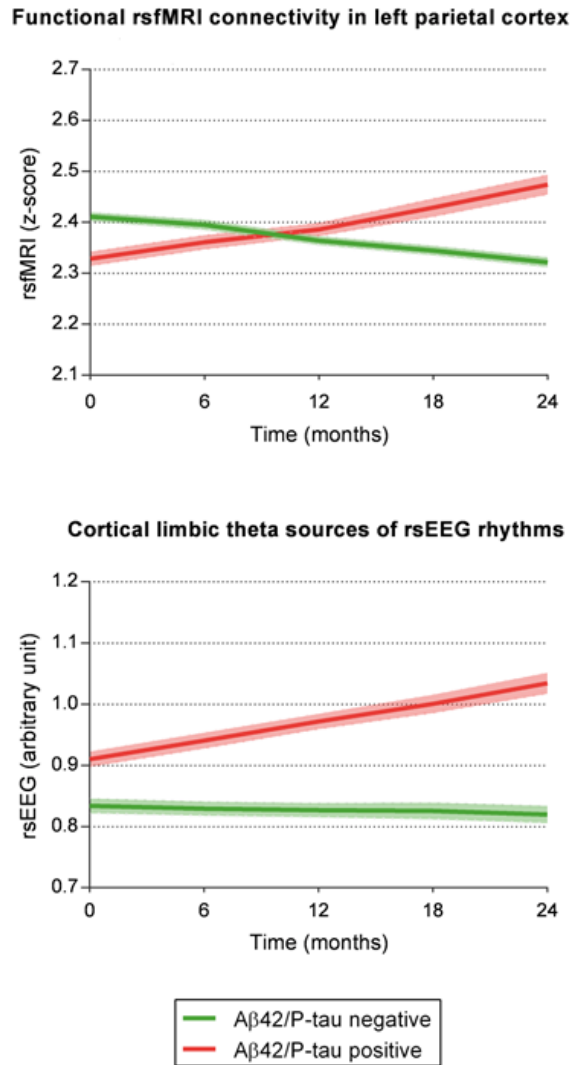


Figure 8. Longitudinal profile of functional topographical biomarkers showing significant Time x Group effects (p -value < 0.05). Patients were stratified in two aMCI groups: Aβ42/P-tau “positive” (red) as prodromal AD and Aβ42/P-tau “negative” (green) as a control group. Mean (\pm standard error of the mean, SEM) model values are shown from 5 recording session starting at time zero (baseline) and 6-, 12-, 18, and 24-month follow-ups. Time x Group effects show differential progression in the two groups. Top: rsfMRI functional connectivity measures in the left parietal cortex (LPC) of the DMN, showing a progression towards increased connectivity in the “positive” aMCI subgroup relative to the “negative” aMCI subgroup. Bottom: Mean (\pm SEM) values of cortical limbic sources of rsEEG rhythms at theta frequency band (4-8 Hz), showing an increase in cortical neural synchronization in the “positive” (i.e., prodromal AD) subgroup relative to the “negative” aMCI control subgroup.

4.3.3 RsEEG and ERP functional biomarkers of prodromal AD

Table 5 reports the results of a Linear Mixed Model showing the variance explained in rsEEG and ERP measures (i.e. functional biomarkers) by the fixed effects of Group (“positive” vs. “negative” aMCI subgroups as defined by CSF Aβ42/P-tau ratio), Time, and Time X Group interaction in aMCI patients over the

Experimental part

observation time (24 months, 5 recording sessions 6 months apart). The main interest was focused on the significant Group and Time X Group interaction effects ($p < 0.05$).

Concerning the significant Group effect, 13 rsEEG biomarkers showed higher cortical source activation in the “positive” (i.e., prodromal AD) over the “negative” aMCI subgroup ($p < 0.05$) for frequency bands and ratios (e.g. delta, theta, delta/alpha1, and theta/alpha1) typically associated with abnormally high values in AD patients. The strongest statistical effects were found on global cortical sources of delta rsEEG rhythms (P-value = 0.005, Std β = 0.3) and limbic cortical sources of theta rsEEG rhythms (P-value = 0.004, Std β = 0.3). In the same line, two auditory “oddball” ERP biomarkers also pointed to significant Group effects (e.g., P3b peak as difference between ERPs associated with rare minus frequent stimuli). Compared to the “negative” aMCI subgroup, the “positive” aMCI subgroup (i.e. prodromal AD) pointed to lower cortical source activation of P3b peak in posterior parietal (P-value = 0.005, Std β = -0.3) and posterior cingulate (P-value = 0.004, Std β = -0.2) regions. Figure 1 (lower diagrams) illustrates the mean values of global cortical sources of delta rsEEG rhythms and cortical source activation of P3b peak in posterior parietal regions in the two subgroups of aMCI patients over the 5 recording sessions.

Concerning the Time X Group interaction (differential progression between “positive” and “negative” subgroups of aMCI patients), only limbic sources of theta rsEEG rhythms showed a significant effect (P-value = 0.046, Std β = 0.1). Results pointed to a *differential* increase of activation in limbic sources of theta rhythms over time in the “positive” (i.e., prodromal AD) compared to the “negative” aMCI subgroup ($p < 0.05$). Figure 2 (bottom) depicts the mean (\pm SEM) values of those sources in the two subgroups of aMCI patients over the 5 recording sessions.

rsEEG/ERP measures	Group		Time		Time X Group	
	Std β	P-value	Std β	P-value	Std β	P-value
Central delta rsEEG	0.2	0.014	-0.0	0.5	0.1	0.2
Temporal delta rsEEG	0.2	0.044	0.0	0.6	0.0	0.5
Limbic delta rsEEG	0.2	0.031	0.0	0.3	0.1	0.5
Global delta rsEEG	0.3	0.005	0.0	1.0	0.1	0.1
Limbic	0.3	0.004	-0.0	0.6	0.1	0.046

Experimental part

theta rsEEG						
Global	0.2	0.020	-0.0	0.6	0.1	0.1
theta rsEEG						
Parietal	0.2	0.038	-0.1	0.2	0.1	0.2
delta/alpha1 rsEEG						
Frontal	0.2	0.045	0.0	0.9	0.1	0.5
theta/alpha1 rsEEG						
Central	0.3	0.009	-0.0	0.6	0.1	0.1
theta/alpha1 rsEEG						
Occipital theta/alpha1 rsEEG	0.2	0.049	-0.1	0.1	0.1	0.1
Temporal theta/alpha1 rsEEG	0.2	0.016	-0.0	0.3	0.1	0.1
Limbic	0.3	0.010	-0.0	0.8	0.1	0.1
theta/alpha1 rsEEG						
Global	0.2	0.013	-0.0	0.4	0.1	0.1
theta/alpha1 rsEEG						
Parietal	-0.3	0.005	0.0	0.5	-0.2	0.1
P3b peak						
Posterior cingulate	-0.2	0.017	0.0	0.6	-0.2	0.1
P3b peak						

Table 5: Resting state EEG and auditory oddball ERP measures showing significant cortical neural synchronization effects explained by a Linear Mixed Model of longitudinal changes (baseline, 6, 12, 18, 24 months follow ups) in aMCI patients stratified into two groups (“positive” as prodromal AD and “negative” as a control group). ERP component of interest was the P3b peak as difference between ERPs peaking about 400 ms post-stimulus associated with rare minus frequent stimuli. The model included Group ($A\beta_{42}/P\text{-tau}$ ratio), Time, and Time X Group interaction as main predictors of interest adjusted by age, sex and baseline MMSE score as nuisance variables. Significant ($P\text{-value} < 0.05$) fixed effects are emphasized in bold. Abbreviation: Std β , standardized β coefficient of the Linear Mixed Model.

4.3.4 Correlation of rsfMRI and EEG markers with ADAS-cog13 score

Linear Mixed Models were also used to test the correlation of rsfMRI and rsEEG/ERP functional biomarkers with ADAS-cog13 scores in the whole aMCI group (all CSF $A\beta_{42}/P\text{-tau}$ “positive” and “negative” aMCI patients) and only “positive” aMCI patients (i.e., prodromal AD). As expected, regardless the kind of the functional biomarkers, the Time effect explained an increase of ADAS-cog13 scores (i.e., sign of reduced cognitive performance) in the whole group of aMCI patients over the observation time ($p < 0.001$).

Experimental part

For rsfMRI biomarkers, the increase of ADAS-cog13 score was significantly correlated with a reduction of functional connectivity measured in DMN ($p < 0.003$, whole aMCI group; $p < 0.002$, CSF A β 42/P-tau “positive” aMCI subgroup), PCC ($p < 0.004$, whole aMCI group; $p < 0.003$, CSF A β 42/P-tau “positive” aMCI subgroup), and LFP network ($p < 0.032$, CSF A β 42/P-tau “positive” aMCI subgroup).

For rsEEG-ERP biomarkers, the increase of ADAS-cog13 score was significantly correlated with an increased activation of occipital sources of theta/alpha 1 rsEEG rhythms in the “positive” aMCI subgroup (i.e., prodromal AD; $p = 0.041$), these rhythms being typically augmented in magnitude in AD patients.

As a control analysis, Linear Mixed Models were used for the study of the correlation between rsEEG/ERP functional biomarkers and ADAScog13 score in all aMCI patients without the random intercept and random slope as random effects. The Linear Mixed Models were adjusted for age, sex, and education. Results showed that many rsEEG (e.g. central delta, limbic delta, global delta, limbic theta, global theta, frontal theta/alpha 1, central theta/alpha 1, temporal theta/alpha 1, limbic theta/alpha 1, and occipital theta/alpha 1) and ERP (e.g. parietal and posterior cingulate cortex) functional biomarkers pointed to a significant correlation with ADAS-cog13 score measured over the 5 recording sessions ($p < 0.001$). This control finding remarks the substantial impact of the use of random intercept and random slope as random effects in the present Linear Mixed Models. Therefore, the results of the present study are true under the assumption that the factors Group and Time are the fixed effects (independent variables of the statistical design) and the random intercept and random slope of the variables as random effects.

4.4 Discussion

Functional topographic biomarkers are of interest because they may reflect early interactions between neuropathological alterations specific to prodromal AD (e.g. extracellular accumulation of A β 1-42 and intracellular aggregation of P-tau in the brain) and the neurophysiological mechanisms of functional brain connectivity and cortical synchronization as measured by rsfMRI and EEG biomarkers, respectively. In the present longitudinal PharmaCog study, we evaluated rsfMRI and rsEEG/ERP functional topographic biomarkers to differentiate a “positive” aMCI (prodromal AD) subgroup relative to a “negative” aMCI subgroup over 24 months.

The two aMCI subgroups were defined according to a standard diagnostic marker of AD in CSF samples (A β 42/P-tau ratio; Dubois et al., 2014), based on the results of a Linear Mixture Model (Marizzoni et al., 2017). As expected, a substantial percentage of the “positive” aMCI patients (i.e., prodromal AD) of the present study showed APOE ϵ 4 carriers (63%) in line with previous large studies in AD patients (Geifman et al., 2017). Furthermore, those patients showed a standard annual conversion rate to AD dementia of about 15%, compatible with the use of 1 SD as a threshold of memory deficits in the present inclusion criteria (Amieva et al., 2004). As another confirmation of the different nature of aMCI condition in the two subgroups of aMCI patients, none of the “negative” aMCI patients converted to AD dementia within 24 months.

Experimental part

In the present study, functional rsfMRI and EEG topographic biomarkers of prodromal AD were tested by Linear Mixed Models of Group, Time, and Time X Group effects adjusted for nuisance covariates such as age, sex, and education. The models accounted for confounding effects of different disease stages among aMCI patients by using random intercept and slope across the variables of interest and subjects. In what follows, we discuss the main effects of Group (“positive” vs “negative” aMCI subgroup differences regardless of Time) and Time X Group (differential progression profiles across subgroups) on the functional biomarkers evaluated.

4.4.1 Functional biomarkers Group effects

The Linear Mixed Models showed a fixed effect of Group (“positive” versus “negative” aMCI subgroups) on both rsfMRI and EEG (i.e., rsEEG and auditory “oddball” ERPs) topographic biomarkers regardless of Time effects. From a general neurophysiological point of view, this finding suggests that the prodromal AD group can be differentiated from the non-prodromal aMCI group by intrinsic functional connectivity and cortical neural synchronization differences (i.e., at rest), as well as by synchronization differences during the oddball task.

Concerning rsfMRI topographic biomarkers, functional connectivity within the DMN, especially within the PCC, was significantly lower in the “positive” (i.e., prodromal AD) than in the “negative” aMCI subgroup regardless of Time effects, while no group difference was observed in the attention LFP network. This finding complements and extends to the prodromal AD condition a large body of previous rsfMRI evidence of cross-sectional studies pointing to a selective disruption of functional connectivity in DMN regions as possible early functional consequences of amyloid-neurodegenerative cascade on cortical systems underpinning resting state condition and low vigilance in AD patients relative to cognitively intact controls (Agosta et al., 2014, Zhang et al., 2010, Gili et al., 2011, Lau et al., 2016 Petrella et al., 2011, Song et al., 2013); for review see Zhou et al., 2017). As a novelty, the present finding showed a selective disruption of functional connectivity within DMN regions (no difference at an attention frontoparietal network) using a longitudinal study design with several serial recording sessions and a relatively large sample of aMCI patients suffering from prodromal AD (N = 81) compared with control aMCI patients not due to AD. Such a control group made the present finding on prodromal AD independent of patients’ cognitive grade (i.e. all patients suffered from an aMCI condition), while the longitudinal design with variable intercepts as random effects minimized the confound of patients’ disease stage in the comparison of the two aMCI subgroups. The present finding has also the robustness of international multicentric studies using harmonized and qualified MRI scanners (Jovicich et al., 2016).

On the whole, the design of the present study overcomes the methodological limitations of typical cross-sectional studies comparing biomarkers in cognitively intact subjects and AD patients. Furthermore, it overcomes the methodological limitations of longitudinal studies just based on one follow up (typically after 1 year). On the other hand, some of the methodological limitations of this study have been previously discussed (Jovicich et al., 2016). In particular, the harmonization of the rsfMRI acquisitions across the 3T Consortium

Experimental part

resulted in a common acquisition rate of $TR = 2.7$ s for full brain coverage. Full brain sub-second acquisition protocols [54] are possible with simultaneous multi-slice selection techniques, which are becoming more widely available as product sequences in clinical scanners and maybe preferable in future studies. The use of higher temporal resolution protocols may improve not only the sensitivity and specificity of rsfMRI connectivity estimates but also enable the exploration of advanced markers of cortical network dynamics (de Pasquale et al., 2017, Preibisch et al., 2015, Wig, 2017).

The rsfMRI and rsEEG recordings of this study were not recorded simultaneously, yet the results from both modalities refer to a very similar patients' psychophysiological condition as induced by instructions to the patients. In both recordings, aMCI patients were invited to keep eyes closed, stay relaxed, not to sleep, and not focus attention on environmental stimuli or specific internal mental contents (i.e., the so-called "wondering" mental state). In this resting state condition, the mentioned Linear Mixed Models showed a fixed effect of Group ("positive" and "negative" aMCI) on several rsEEG biomarkers. Compared with the "negative" aMCI subgroup, the "positive" (i.e., prodromal AD) aMCI subgroup exhibited lower posterior (parietal, occipital, temporal and limbic) source activity of the low-frequency alpha band (8-10.5 Hz) while widespread delta (< 4 Hz) and theta (4-8 Hz) source activity was higher. These results specify in source space and prodromal AD condition a bulk of previous rsEEG evidence showing that AD patients with dementia are characterized by high power in widespread delta and theta rhythms, as well as low power in posterior alpha and/or beta (13-20 Hz) rhythms (Babiloni et al., 2006, Huang et al., 2000, Jelicet al., 2000, Jeong, 2004, Dierks et al., 2000, 1993, Ponomareva et al., 2003). In temporal areas, delta power is also abnormally high in AD patients with dementia in relation to regional hypometabolism and memory deficits (Valladares-Neto et al., 1995). Furthermore, a short-term cholinergic regimen with Acetylcholinesterase inhibitors partially normalizes theta (Brassen and Adler, 2003), alpha (Onofrj et al., 2003), and delta (Reeves et al., 2002) rhythms. In the same line, long-term administration of the drug regimen shows beneficial effects on theta and alpha/theta band ratio, especially over the frontal areas (Kogan et al., 2001, Rodriguez et al., 2002). Here the Linear Mixed Models also showed a fixed effect of Group ("positive" and "negative" aMCI) on P3b peak of an auditory "oddball" paradigm, namely a typical cognitive task in which patients receive a sequence of frequent (80% of probability) and rare (20%) stimuli with the request to respond with a hand movement or silent counting only to the rare ones (see Rossini et al., 2007 for a review). In this paradigm, ignoring frequent stimuli and reacting to rare stimuli involves attention and short-term episodic memory. Compared with the "negative" aMCI subgroup, the "positive" (i.e., prodromal AD) aMCI subgroup pointed to lower parietal and posterior cingulate source activities. These findings extend to spatial source localization previous evidence showing that P3b peak amplitude at scalp posterior electrodes was smaller in AD patients than control seniors, as a possible dynamic neural underpinning of abnormal attention and short-term episodic memory information processes. However, these findings did not replicate in the two aMCI subgroups previous slowing of P3b peak latency in aMCI and AD patients with dementia compared with elderly control subjects, even across various "oddball" task difficulties and stimulus modalities (Polich and Corey-Bloom, 2005, Golob et al., 2007, Polich and Comerchero, 2003). Those effects were previously discussed as related to AD pathology for visual and

Experimental part

olfactory modalities (Morgan and Murphy, 2002, Polich and Pitzer, 1999). In contrast, the present findings would suggest that P3b peak latency may preferably reflect physiological aging (van Dinteren et al., 2014) and general deterioration of cognitive performance across pathological aging rather than specific processes of prodromal AD.

4.4.2 Functional biomarkers Time x Group effects: differential progression profiles

Here the Linear Mixed Models showed a significant interaction between Time (5 recording sessions 6 months apart) and Group (“positive” and “negative” aMCI) on both rsfMRI and rsEEG biomarkers. This interaction suggests that in an aMCI group, differential progression profiles between prodromal and non-prodromal AD may be captured by intrinsic functional connectivity (e.g., rsfMRI biomarkers) and cortical neural synchronization (e.g., rsEEG biomarkers).

Concerning rsfMRI biomarkers, we found that the sensitivity to disease progression in aMCI patients varies across cortical networks. Specifically, we found that functional connectivity in the whole DMN, PCC, and LFP were sensitive to short-term longitudinal decay both in the “positive” prodromal AD and the “negative” (control) aMCI patients. But these networks showed no significant differences in the progression of the connectivity profiles. Instead, functional connectivity in LPC exhibited significant differential effects, with increased functional connectivity over time faster in the “positive” (i.e., prodromal AD) relative to the “negative” aMCI subgroup. Again, this finding stressed the selective feature of this disruption of functional connectivity within DMN regions as compared to the lack of effects in the attention frontoparietal network.

Our longitudinal rsfMRI findings are in good agreement with previous evidence showing both cortical network impairment (connectivity reduction) and compensation (connectivity increase) effects in the DMN in aMCI subjects relative to control seniors, despite gray matter atrophy (Damoiseaux, 2012), Qi et al., 2010, Serra et al., 2016, Bai et al., 2011). Here we extend those results by confirming similar effects in prodromal AD relative to control aMCI subgroup. Further, the present findings showed a maximum sensitivity of rsfMRI LPC functional connectivity at 2-year follow up, generally consistent with previous longitudinal rsfMRI studies considering baseline and 2-3 years follow-up evaluations in groups of patients with AD dementia and aMCI (Damoiseaux, 2012, Damoiseaux et al., 2012, Binnewijzend et al., 2012, Bai et al., 2011), the latter sometimes diagnosed only on clinical basis. Interestingly, the present lateralization in the left LPC of the effects of longitudinal disease progression in prodromal AD extends recent findings of a longitudinal rsfMRI study with two measurements 2 years apart in a small population of aMCI patients (Serra et al., 2016). Such previous study exhibited sensitivity of functional connectivity between left precuneus and other DMN nodes in accounting for the greater progression of aMCI patients in the group of converters to dementia (N=14) than that of non-converters (N=17, Serra et al., 2016). Another recent longitudinal rsfMRI study (baseline and 35 months follow up) in aMCI patients evaluated genotype-by-diagnosis interaction effects (Agosta et al., 2014, Ye et al., 2017). Using seed-based rsfMRI analyses on the hippocampus, the Authors detected functional cortical connectivity reductions in APOEε4 carriers and functional cortical connectivity increases in non-

Experimental part

carriers. In the light of those findings, the present results should not be interpreted as an indication that rsfMRI functional biomarkers of prodromal AD are limited to DMN nodes. It is reasonable that functional connectivity within the episodic memory brain networks including prefrontal, entorhinal regions, and hippocampus may represent another sensitive dimension in prodromal AD.

Concerning rsEEG biomarkers, the “positive” (i.e., prodromal AD) aMCI subgroup was characterized by increasing limbic source activity of theta rhythms over time. The effect was evident across the serial recordings and robust effects were evident for the progression of prodromal AD in periods of about 12 months. Taking into account the relatively low spatial resolution of the EEG techniques used in the present study (i.e. they cannot disentangle the various limbic regions of cortical midline and medial temporal lobe), this finding suggests a limbic localization of prodromal AD processes affecting the generation of abnormal rsEEG rhythms during the disease progression in aMCI patients. This topographical suggestion is in line with the well-known localization of initial AD physiopathological processes in entorhinal regions, medial temporal lobe, and midline regions of DMN. Furthermore, it provides a neuroanatomical framework to previous rsEEG evidence showing that AD patients with dementia are characterized by high power in widespread scalp regions of delta and theta rhythms, as well as low power in posterior alpha and/or beta (13-20 Hz) rhythms (Babiloni et al., 2013, 2014, Jelic et al., 2000, Coben et al., 1985, Soininen et al., 1989)

4.4.3 What do rsfMRI and EEG topographic biomarkers tell us about prodromal AD?

The rsfMRI findings of the present study support the general view that at least for two years, prodromal AD is associated with a partial functional cortical disconnection within DMN nodes in the resting state condition. It can be speculated that this functional disconnection might induce an abnormal elaboration of information about self-body milieu and autobiographical memory, thus affecting the sense of self-awareness and continuity of self across time (Agosta et al., 2014, Bai et al., 2011). This speculation is based on the well-known concept that midline cortical nodes of DMN such as PCC and MPF contribute to the integration of the general functions related to the sense of self-awareness (Northoff and Bermpohl, 2004, Northoff et al., 2006). In this line of reasoning, PCC might represent information concerning individual’s own self-beliefs and first-person perspective in adults (Ochsner et al., 2005). Furthermore, structural maturation of the neural connectivity between PCC and MPF in the adolescence accompanies the development of self-related and social-cognitive functions (Supekar et al., 2010). Moreover, previous evidence has shown that posterior parietal regions of DMN might contribute to the formation of self-related cognitive representation as a convergence zone binding cortical neural populations involved in the memorization of intermodal details of episodic events concerning the self (Shimamura, 2011). Patients with lesions in those parietal regions manifest difficulties in re-experiencing a past autobiographic event when request by experimenters (Berryhill, 2012). This speculation encourages the inclusion of cognitive tests probing the richness of the autobiographic memories and self-awareness in prodromal AD patients over time and the analysis with Linear Mixed Models of the correlation between rsfMRI topographic biomarkers of DMN and the performance to those tests.

Experimental part

The rsEEG findings of the present study enlightened neurophysiological mechanisms characterizing prodromal AD patients compared to control aMCI patients. Based on those findings and prior knowledge on the role of thalamocortical loops in the generation of rsEEG rhythms in humans, it can be speculated that in quiet wakefulness, the abnormal delta and theta source activity in prodromal AD is due to an abnormal interaction between thalamic and cortical pyramidal neural populations, associated with a loss of functional connectivity and a sort of functional isolation of parietal, temporal, and occipital cortical modules (Klimesch, 1999, Pfurtscheller and Lopes da Silva, 1999, Steriade and Llinas, 1988). It can be also speculated that the alteration of this neurophysiological mechanism is responsible for the reduced parietal and posterior cingulate source activity of auditory “oddball” P3b peak in prodromal AD patients enrolled in the present study. Indeed, P3b peak is mostly an expression of cognitive event-related oscillatory response of thalamocortical circuits oscillating at delta and theta frequencies. In this line, previous studies have shown that delta event-related impulse oscillations in response to visual and auditory “oddball” stimuli were attenuated in amplitude in AD patients with dementia compared with control seniors (see for a review Yener and Basar, 2013). In AD patients with dementia, an abnormal thalamocortical interaction might be due to a cortical blood hypoperfusion and synaptic dysfunction (Valladares-Neto et al., 1995, Rae-Grant, 1987, Brenner et al., 1986, Stigsby et al., 1981, Kwa et al., 1993, Niedermeyer, 1997, Passero et al., 1995, Rodriguez et al., 1999, Steriade, 1994). Another cause of such an abnormal thalamocortical interaction might be an impairment of the cortical gray matter especially in the posterior regions (Babiloni et al., 2013, 2015, Killiany et al., 1993, Fernandez et al., 2003, Delli Pizzi et al., 2014, 2015, 2016, Graff-Radford et al., 2016, Sarro et al., 2016), as well as a lesion in the brain white matter connecting cerebral cortex (Agosta et al., 2012, 2014).

Another interesting finding of the present study is the characterization of prodromal AD patients by widespread alpha sources. A tentative neurophysiological explanation of that finding can be based on the insightful research in cats and mice of the group by Dr. Crunelli at Cardiff University. Based on their research, it can be speculated that the reduction of alpha sources in prodromal AD patients over aMCI control patients might denote a progressive alteration in the interplay of glutamatergic and cholinergic neurons, thalamocortical high-threshold, GABAergic interneurons, thalamocortical relay-mode, and cortical pyramidal neurons that constitute the complex network regulating the cortical arousal and vigilance in quiet wakefulness in mammals (Hughes and Crunelli, 2005, Lorincz et al., 2008, 2009). In physiological conditions, this network produces cycles of excitation and inhibition in thalamic and cortical neurons that might frame perceptual events in discrete snapshots of approximately 70–100 ms during vigilance (Hughes and Crunelli, 2005, Lorincz et al., 2008, 2009).

5 Study II: On-going electroencephalographic rhythms related to cortical arousal in wild type mice: the effect of aging

5.1 Introduction

Alzheimer's disease (AD) is the most prevalent progressive neurodegenerative disorder across aging (Braak and Braak, 1995; Bastos Leite et al., 2004; Glodzik-Sobanska et al., 2005). Recent guidelines propose a diagnostic algorithm using physiopathological and topographical biomarkers of AD (Dubois et al., 2014). The physiopathological markers would be mandatory to confirm the diagnosis of dementia of AD type. These physiopathological biomarkers include A β -42 and tau in the cerebrospinal fluid (CSF) or map them in the brain by ligand positron emission tomography (PET; Förstl and Kurz, 1999). Topographic markers are suggested to track the disease progression. These topographic markers included maps of brain hypometabolism obtained by fluorodeoxyglucose (FDG)-PET and maps of brain atrophy or abnormal structural connectivity obtained by magnetic resonance imaging (MRI).

Unfortunately, these PET and MRI methodologies are not easily translated into preclinical research using mouse models of AD for fundamental and applied research (i.e. drug discovery). For this reason, other kinds of biomarkers are being developed. Among them, a promising biomarker is derived from on-going electroencephalographic (EEG) rhythms (Schroeter et al., 2009; Babiloni et al., 2013). These rhythms are an emerging feature of the mammalian brain. They are mainly generated by the synaptic currents associated with the synchronization or desynchronization of the activity of many cortical pyramidal neurons, due to cortical and sub-cortical signals (Pfurtscheller and Lopes da Silva, 1999). Two main conditions are typically used to probe these neurophysiological synchronization and desynchronization mechanisms in a clinical setting. In a “passive” behavioral condition, the subject remains in relaxed wakefulness (resting state) with eyes closed for few minutes. This mode is contrasted with a more “active” behavioral condition in which the subject remains in relaxed wakefulness with eyes open for few minutes (monitoring the surrounding environment). In the resting state eyes-closed condition, EEG rhythms show the highest power (density) at about 8 and 12 Hz in posterior cortical areas, the so-called dominant alpha rhythms (Pfurtscheller and Lopes da Silva, 1999). The higher the alpha power, the lower the cortical arousal, the lower the vigilance. After eyes opening, alpha rhythms exhibit a power reduction (i.e. desynchronization) as a reflection of increased cortical arousal related to higher vigilance (Pfurtscheller and Lopes da Silva, 1999).

EEG power exhibited a different reactivity to eyes opening in normal elderly subjects (Nold) compared with AD subjects. It has been repeatedly reported a lower reduction (reactivity) of the posterior alpha power in AD and MCI patients than in Nold subjects (Stam et al., 1996; Stevens and Kircher, 1998; van der Hiele et al., 2007; Jeong, 2004; Babiloni et al., 2010). This poor reactivity of alpha power predicted a deterioration of higher functions in subjects with cognitive decline (van der Hiele et al., 2008). These results were confirmed

Experimental part

by the analysis of magnetoencephalographic rhythms in the same resting state conditions (Berendse et al., 2000; Kurimoto et al., 2008).

Can these EEG topographic markers be translated to preclinical AD research in rodents? A logical premise for the back-translation of EEG topographic markers from human to rodents is the existence of common neurophysiological mechanisms. Active brain state was associated with high cholinergic activity and hippocampal theta (6-9 Hz) rhythms both in humans and rodents (Moruzzi and Magoun, 1949; Vanderwolf, 1969; Buzsáki et al., 2003; Zhang et al., 2010). In both species, alertness was associated with enhanced power of low-voltage fast frequencies in EEG rhythms (i.e. beta rhythms spanning about 14–30 Hz), whereas non-rapid eye movement (REM) sleep and drowsiness were characterised by the enhanced power of high-voltage slow frequencies in EEG rhythms (i.e. delta and theta rhythms spanning about 1-7 Hz; Marshall and Born, 2002; Vyazovskiy et al., 2005). Anxiety has been shown to increase the power of low-voltage high frequencies in the resting-state EEG rhythms in both humans and rodents (Sviderskaia et al., 2001; Oathes et al., 2008). Finally, cholinergic and monoaminergic drugs caused similar effects on spontaneous ongoing EEG rhythms in humans and rodents (Dimpfel et al., 1992; Coenen and Van Luijtelaar, 2003; Dimpfel, 2005).

A limitation of the mentioned EEG studies in rodent models is that across prolonged EEG recordings, spontaneous ongoing EEG rhythms included several behavioral states of the animals. These studies are characterized by the continuous EEG recording for long periods (several days), including active mode (i.e. gross movements, exploratory movements or locomotor activity), awake passive mode (immobility or small movements of trunk, head, and forelimbs), sleep, and instinctual activity (i.e. drinking, eating, mating etc.). Extended EEG recording of this experimental procedure (i.e. tens of hours) presents another disadvantage. It is quite different with respect to the EEG recording in the typical clinical setting in humans. In that setting, EEG recording lasts few minutes in humans in a relaxed wakefulness. This limitation was dealt with in the IMI PharmaCog project, a European academia-industry partnership (Innovative Medicine Initiative, <http://www.imi.europa.eu/content/pharma-cog>). As a solution to this problem, we identified two convenient and translational conditions of EEG recordings for mice. The “Passive” condition was defined as a mode of relaxed wakefulness with no or minimal animal movements in the cage (no sleep). Whereas, the “active” condition was defined as a mode characterized by spontaneous exploratory movements in the cage. In principle, this methodology is cost-effective and time-saving. If validated, it will imply relatively short EEG recordings for few hours to collect few minutes of artifact-free data for any animal behavioral condition of interest. In the present exploratory study, standard EEG recordings and two behavioral conditions were used to test the hypothesis that on-going EEG rhythms reflect changes in cortical arousal and vigilance in freely behaving mice and are sensitive to aging stages.

5.2 Methods

5.2.1 Animals

Experimental part

Eighty-five (19 female; range of age: 4.5-24 months) WT (C57BL6) mice were used in the present study. WT mice were subdivided in three groups: young (N=25; age: 4.5-6 months), middle-aged (N=37; 19 female; age: 12-15 months), and old (N= 23; age: 20-24 months) mice. The data were collected from 1 Belgian center (Janssen Research and Development, Pharmaceutical Companies of J&J), 1 Danish center (H. Lundbeck A/S), and 2 Italian centers (Mario Negri Institute for Pharmacological Research of Milan, MNI; University of Verona, UNIVR). Table 6 reports the amount, age and sex of the WT mice for each center. Procedures involving mice and their care were conducted in line with the institutions' guidelines that were in strict conformity with national and international laws and policies (EEC Council Directive 86/609, OJ L 358, 1, 12 December, 1987; U.S. National Research Council, 1996, Guide for the Care and Use of Laboratory Animals). The respect of these guidelines was carefully controlled by the members of the IMI PharmaCog project, devoted to ethics of research.

Center	N	Sex (F/M)	Age
Janssen	12	5F/7M	12 months
Lundbeck	34	14F/20M	4.5, 15, 24 months
MNI	23	23M	6, 12, 14, 24 months
UNIVR	16	16M	5, 12, 20 months

Table 6. Features of the C57 mice (for the sake of simplicity, wild type, WT) for the following electroencephalographic (EEG) recording centers: Janssen Research and Development (Belgium), H. Lundbeck A/S (Denmark), Mario Negri Institute (Italy), and University of Verona (UNIVR, Italy). Legend: F= female; M= male.

5.2.2 Pre-Surgery phase (3 weeks)

For 3 weeks prior to surgery mice were acclimated to the respective institution for habituation of light switched on-off. Mice were housed at a constant temperature (18-22°C) and relative humidity (55-65%). They were maintained in a standard 12-h light/dark cycle (light hemi-cycle typically spanning from 6:00 a.m. to 6:00 p.m.) with free access to food and water. Gentle handling for about 5-10 minutes a day was applied to reduce the general stress. Such stress was evaluated continuously along all the duration of the experiments by veterinary experts of each center. These experts evaluated standard behavioral and physiological indices such as animal muscle relaxation, abnormal respiration, grooming and hair coat (piloerection or greasy, possibly reflecting reduced grooming), motor postures (hunching or cowering in the corner of the cage, lying on one's side, lack of movement with loss of muscle tone), absence of alertness or quiescence (inattention to ongoing stimuli), changes in body weight, preservation of regular drinking and eating activities, presence of vomit, and intense or frequent vocalizations.

5.2.3 Surgery

The mice were anaesthetized (i.e. inhalation of isoflurane 5% or Equithesin; 1% pentobarbital+4% chloral hydrate, 3.5 ml/kg), and treated with the systemic analgesics and antibiotics (surgical care according to local guidelines). Stainless steel or nichrome-insulated monopolar depth electrodes were used for

Experimental part

electrophysiological recordings. A reference electrode was placed in the cerebellum. A ground electrode was put in the left temporal bone. EEG electrodes were implanted in the frontal and parietal cortex. These electrodes were wired with a multi-pin socket. Alternatively, wireless transmitters were used. The animals were placed inside the cage and connected to a recording apparatus either through a swivel allowing animals to move freely or through a wireless device. Table 7 reports stereotaxic coordinates in a standard brain atlas for the electrode implantation (The Mouse Brain coordinates by Franklin and Paxinos, 1997).

Electrode	Stereotaxic coordinates
Reference	AP:-6, ML:+2
Ground	AP:-2, ML:+2.5
Frontal	AP:+2.8, ML:-0.5
Parietal	AP:-2, ML:+2

Table 7. Stereotaxic coordinates for the implantation of EEG electrodes in the mouse brain according to a standard atlas (The Mouse Brain coordinates by Franklin and Paxinos, 1997).

5.2.4 Quiet Post-surgery period (1 week)

After the surgery, the animals were single-housed for a continuous period of at least two weeks until the experimental day, at the same temperature and humidity conditions. The period of two weeks elapsing between the surgery and experimental day was selected by the veterinary and ethology experts of each preclinical recording center preliminarily to the beginning of the present study. The experts also evaluated whether animals showed unnatural behavior, abnormal anxiety or stress, and symptoms of illness (by the means of the standard behavioral and physiological indices adopted by each center) during the two weeks elapsing between the surgery and experimental day. Typical cage size of the single-house was 45 cm [length] × 24 cm [width] × 20 cm [height]. Light intensity was 90–110 lx in the room, 60 lx in the cage during the light period, and less than 1 lx during the dark period. The mice were treated with the systemic analgesics and antibiotics, during a standard post-surgical period of one week. The week immediately after the surgery, animals underwent a period of recovery with no handling treatment nor EEG recordings.

5.2.5 Handling post-surgery period (1 week)

In the week after the quiet post-surgery period, the mice received no EEG recordings. Gentle handling for about 5-10 minutes a day was applied to reduce the general stress induced by the housing and experimenters. Such stress was controlled by the evaluation of the animal muscle relaxation and standard behavioral indices of stress in freely behaving mice. Furthermore, the animals were gently plugged and unplugged several times (for wired systems only) to familiarize with the procedure of EEG recording and reduce the global stress.

5.2.6 Experimental day

Experimental part

Experiments were performed during both the dark and light phases. During the EEG recording period, the mice received no handling treatment. EEG recordings started after the second hour of the beginning of the light (dark) period. Recording sampling frequency was at least 250 Hz with anti-aliasing bandpass analog filters (Janssen: 250 Hz, Lundbeck: 1000 Hz, MNI: 1600 Hz, UNIVR: 500 Hz; 0.16 Hz-100 Hz passband filter). No notch filter was used.

Table 8 summarizes the time flow of the treatments and procedures adopted in the experimental sessions. Days are referred to the surgical event.

TIME FLOW OF THE TREATMENTS AND PROCEDURE BEFORE AND AFTER THE SURGERY		
Period	Days	Treatments and Procedures
<i>Pre-surgery</i>	-21 to -1	<ul style="list-style-type: none"> ✓ Habituation to light switched on-off ✓ Gentle handling for about 5-10 minutes a day
<i>Surgery</i>	0	<ul style="list-style-type: none"> ✓ Anesthetic procedure ✓ Therapy with systemic analgesics and antibiotics ✓ Electrode placement
<i>Quiet post-surgery</i>	+1 to +7	<ul style="list-style-type: none"> ✓ Therapy with systemic analgesics and antibiotics ✓ No gentle handling ✓ No EEG experiment
<i>Post-surgery</i>	+8 to +14	<ul style="list-style-type: none"> ✓ Facilitating the adaptation by plugging and unplugging several times the animal ✓ Gentle handling for about 5-10 minutes a day ✓ No EEG experiment
<i>Experimental day</i>	from +15	<ul style="list-style-type: none"> ✓ No gentle handling ✓ EEG recording

Table 8. Time flow of the experimental procedures (including EEG recordings) before and after the surgery.

5.2.7 Determination of the behavioral mode of the mice

An important step of the data analysis procedure was the classification of the behavioral mode of the animal during the EEG recordings in terms of the mentioned passive condition and active condition. Specifically, two experimenters of the recording center used visual inspection (i.e. video of the animal), instrumental markers of the movement (actigraphy etc.), and/or EMG activity to classify recording epochs lasting 10 s into behavioral classes. The discrepancy between the two raters was less than 5% of the total classified epochs in a control test with two raters (A.F. and S.L.). The recording epochs with different behavioral classification from the two raters were not considered in the subsequent spectral and statistical analyses. Of note, the low value of the discrepancy between the two raters was because the procedure for the behavioral classification was accurately established before the beginning of the experimental phase within the PharmaCog Consortium. The behavioral classes were:

Experimental part

- (1) Active condition. Each epoch of the active condition showed overt exploratory movements for most of the period. These movements were characterized by ample displacements of the trunk, head, and/or forelimbs. They should not be confounded with movements associated with instinctual activities (*vide infra*).
- (2) Passive condition. Each epoch of the passive condition showed a substantial immobility of the animals for most of the period (no sleep). This condition could include small movements of the trunk, head, and/or forelimbs. Noteworthy, the experimenter did not consider the epochs in which animals stayed continuously immobile for 20 s or more as a passive condition. This was to avoid the risk of “passive condition” being misclassified during a period in which the animal was sleeping.
- (3) Sleep state. Each epoch of the sleep state showed immobility of the animals for the whole period (no sleep). Furthermore, the epoch should be part of longer periods of immobility lasting several minutes with signs of muscle relaxation. As mentioned above, a particular attention was devoted to avoiding the misclassification of the passive condition and sleep state.
- (4) State of instinctual activities: Each epoch of the state of instinctual activities showed movements such as cleaning, drinking, eating, mating, etc. for most of the period. As mentioned above, a particular attention was devoted to avoiding the misclassification of this state and active condition.
- (5) Undefined: Each epoch classified as undefined showed a mix of the other behavioral classes or lack of clarity about the behavioral situation of the animal.

Noteworthy, the experiment did not use EEG data to classify the epochs to avoid circular logic. Based on the analysis of the behavioral states, the first 5 minutes of artifact-free EEG epochs classified as active condition were selected for the EEG data analysis. The same procedure of selection was followed by the epochs of the passive condition. The final data analysis was performed on the EEG epochs of the dark phase of the wake-sleep cycle in which the distinction between the passive condition and sleep state was more reliable than in the light phase was. The advantage of this option was not surprising as mice are nocturnal animals and showed few drowsiness or sleep periods in the dark phase.

5.2.8 EEG data analysis

The behavioral epochs of the active and passive state were segmented off-line in consecutive epochs lasting 2 s each. The 2-s EEG epochs with muscular, EEG, electrocardiographic (EKG), instrumental or other artifacts were detected by two independent experimenters of the center for the centralized EEG data analysis and were discarded. As previously mentioned, EEG data were recorded by a monopolar montage with two exploring electrodes implanted in the frontal and parietal cortex and a reference electrode placed in the cerebellum. To reduce the head volume conductor effects, we re-referenced the EEG data to a frontoparietal bipolar channel. To this aim, we subtracted the EEG signal recorded at the parietal electrode from that recorded at the frontal electrode. The subsequent spectral analysis was performed on EEG epochs re-referenced to that frontoparietal bipolar montage.

5.2.9 Spectral analysis of the EEG data

Experimental part

The artifact-free EEG epochs of the active and passive state were used as an input for the analysis of EEG power (density). This analysis was performed by a standard (Matlab; MathWorks, Natick, Massachusetts USA) FFT algorithm using Welch technique and Hanning windowing function with 1-Hz frequency resolution. A normalization of the results of FFT analysis was obtained by computing the ratio between EEG power at each frequency bin with the EEG power value averaged across all frequency bins (0-100 Hz). After this normalization, the EEG power lost the original physical dimension and was represented by an arbitrary unit scale. According to this scale, the value of “1” was equal to the power value averaged across all frequency bins. The following EEG frequency bands were selected for the statistical comparisons: 1-2 Hz, 2-4 Hz, 4-6 Hz, 6-8 Hz, 8-10 Hz, 10-12 Hz, 12-20 Hz, and 20-30 Hz. These narrow bands were selected to avoid any a priori assumption on the composition of EEG frequency bands in mice. In the same line, sharing of a frequency bin by two contiguous frequency bands is a widely accepted procedure to avoid any assumption about the physiological distinction of two contiguous ones.

5.2.10 Statistical analysis

Two sessions of statistical analysis were performed by Statistical® 10.0 package to test the primary hypotheses of the present study. The first session tested whether the WT mice as a whole group showed differences in EEG power between active and passive conditions, thus reflecting changes in cortical arousal and vigilance. To test this hypothesis, an analysis of variance (ANOVA) used the normalized EEG power as a dependent variable. The ANOVA factors were Condition (passive, active) and Band (1-2 Hz, 2-4 Hz, 4-6 Hz, 6-8 Hz, 8-10 Hz, 10-12 Hz, 12-20 Hz, and 20-30 Hz). The center recording the EEG activity was used as a covariate. The hypothesis would be confirmed by the following two statistical results: (1) a statistical main effect of the factor Condition or a statistical interaction effect between the factors Condition and Band ($p < 0.05$); (2) a post hoc test indicating statistically significant differences in the normalized EEG power between the active and the passive condition (Duncan test, $p < 0.05$, two-tailed).

The second session examined whether the WT mouse groups showed differences in EEG power, thus reflecting changes due to the effect of aging. To test this hypothesis, we computed the difference in the normalized EEG power between the active and the passive condition (active minus passive). An ANOVA used this difference as a dependent variable. The ANOVA factors were Group (young, middle-aged, old; independent variable) and Band (1-2 Hz, 2-4 Hz, 4-6 Hz, 6-8 Hz, 8-10 Hz, 10-12 Hz, 12-20 Hz, and 20-30 Hz). The center recording the EEG activity was used as a covariate. The hypothesis would be confirmed by the following two statistical results: (1) a statistical main effect of the factor Group or a statistical interaction effect between the factors Group and Band ($p < 0.05$); (2) a post hoc test indicating statistically significant differences in the normalized EEG power (active minus passive) in the old group with respect to the others (Duncan test, $p < 0.05$, two-tailed). In this statistical session, only male mice were considered ($N=66$; 25 young, 18 middle-aged, 23 old), to avoid the confounding effects of the sex.

The following other two sessions of statistical analysis tested (secondary) control hypotheses.

Experimental part

A third statistical session tested the effect of sex on the above spectral EEG marker. In this statistical session, the variable age was paired including only 37 middle-aged mice (i.e. 19 females and 18 males). Indeed, this age group had a sufficient number of mice to perform the statistical comparison of interest. To test this hypothesis, an ANOVA used the difference of the normalized EEG power (active minus passive) as a dependent variable. The ANOVA factors were Group (female, male; independent variable) and Band (1-2 Hz, 2-4 Hz, 4-6 Hz, 6-8 Hz, 8-10 Hz, 10-12 Hz, 12-20 Hz, and 20-30 Hz). The center recording the EEG activity was used as a covariate. The hypothesis would be confirmed by the following two statistical results: (1) a statistical main effect of the factor Group or a statistical interaction effect between the factors Group and Band ($p < 0.05$); (2) a post hoc test indicating statistically significant differences in the normalized EEG power (active minus passive) in the female group with respect to the male group (Duncan test, $p < 0.05$, two-tailed).

A fourth statistical session tested the sensitivity of the above spectral EEG marker to the passive and active conditions in the four recording centers separately (i.e. Janssen, Lundbeck, MNI, and UNIVR). To test this hypothesis, four ANOVAs (one for any recording center) used the normalized EEG power as a dependent variable. The ANOVA factors were Condition (passive, active) and Band (1-2 Hz, 2-4 Hz, 4-6 Hz, 6-8 Hz, 8-10 Hz, 10-12 Hz, 12-20 Hz, and 20-30 Hz). For any ANOVA, the hypothesis would be confirmed by the following two statistical results: (1) a statistical main effect of the factor Condition or a statistical interaction effect between the factors Condition and Band ($p < 0.05$); (2) a post hoc test indicating statistically significant differences in the normalized EEG power between the active and the passive condition (Duncan test, $p < 0.05$, two-tailed).

5.3 Results

5.3.1 Normalized EEG power during active and passive conditions

Figure 9 (top) shows the grand average ($N=85$) of the normalized EEG power spectra for the active and passive conditions in all WT mice as a whole group. These spectra showed an EEG power peak at 2-4 Hz (i.e. delta range) that was higher in the passive condition compared to the active one. Furthermore, there was another EEG power peak at 6-8 Hz (i.e. theta range) that was higher in the active condition compared to the passive one. In the figure, the difference in the EEG power between the active and passive conditions (i.e. active minus passive) is also reported. It is observed a negative peak of the EEG power difference at 2-4 Hz, reflecting the maximum EEG power peak in the passive condition. Furthermore, there was a positive peak of the EEG power difference at 6-8 Hz, reflecting the maximum EEG power peak in the active condition.

Figure 9 (bottom) reports the individual values of the normalized EEG power for all WT mice. The values refer to the two behavioral conditions (i.e. active, passive) and eight frequency bands (i.e. 1-2 Hz, 2-4 Hz, 4-6 Hz, 6-8 Hz, 8-10 Hz, 10-12 Hz, 12-20 Hz, and 20-30 Hz). The distributions of these individual values showed no remarkable outliers. Figure 1 (bottom) also illustrates the results of a statistically significant ANOVA interaction ($F(7, 581)=13.39$, $p=0.0001$) between the factors Condition (passive, active) and Band

Experimental part

(1-2 Hz, 2-4 Hz, 4-6 Hz, 6-8 Hz, 8-10 Hz, 10-12 Hz, 12-20 Hz, and 20-30 Hz). All WT mice were considered as a whole group. Duncan planned post hoc testing showed that the EEG power was significantly higher in the passive compared to the active condition at 1-2 Hz ($p=0.000004$), 2-4 Hz ($p=0.000005$), and 4-6 Hz ($p=0.000005$). In contrast, this power was significantly higher in the active compared to the passive condition at 6-8 Hz ($p=0.00001$) and 8-10 Hz ($p=0.000004$). The present results showed statistically significant differences in the EEG power between the passive and active conditions in the WT mice as a whole group ($p<0.05$).

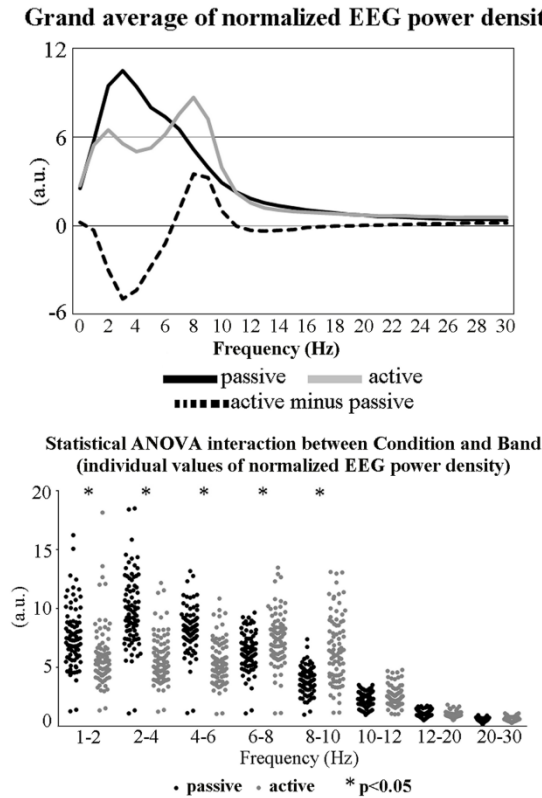


Figure 9. (Top): Grand average of the normalized electroencephalographic (EEG) power density spectra relative to a bipolar cortical frontoparietal channel in 85 C57 adult mice (for the sake of simplicity wild type, WT). The EEG power density spectra range between 0 and 30 Hz. The EEG recordings were performed in a passive (i.e. awake quiet wakefulness with immobility or small movements) or active (i.e. exploratory movements) condition. These recordings refer to the dark phase of the wake-sleep cycle (i.e. the phase of animal activity). In the figure, the difference in the EEG power density between the active and passive conditions (active minus passive) is also reported. (Bottom): Individual values of the normalized EEG power density for all WT mice for the two conditions (active, passive) and the eight frequency bands (1-2 Hz, 2-4 Hz, 4-6 Hz, 6-8 Hz, 8-10 Hz, 10-12 Hz, 12-20 Hz, and 20-30 Hz). A statistically significant ANOVA interaction ($F(7, 581)=13.39$, $p=0.0001$) between the factors Condition (passive, active) and Band (1-2 Hz, 2-4 Hz, 4-6 Hz, 6-8 Hz, 8-10 Hz, 10-12 Hz, 12-20 Hz, and 20-30 Hz) was found. The asterisks indicate the EEG frequency bands at which the normalized EEG power density presented statistically significant differences between the passive and active conditions (Duncan post hoc testing, $p<0.05$).

5.3.2 Effect of age on the normalized EEG power

Figure 10 (top) shows the grand average of the difference of the normalized EEG power spectra between the active and passive conditions (i.e. active minus passive) in the three mouse groups classified based on the age (i.e. the young, middle-aged, and old ones). Of note, the group of the old mice exhibited a dominant negative peak of the EEG power difference at 1-2 Hz.

Experimental part

Figure 10 (bottom) shows the mean values (\pm SE) of the difference in the normalized EEG power between the active and passive conditions (i.e. active minus passive) illustrating a statistically significant ANOVA interaction ($F(14, 434)=2.034, p=0.014$) between the factors Group (young, middle-aged, old) and Band (1-2 Hz, 2-4 Hz, 4-6 Hz, 6-8 Hz, 8-10 Hz, 10-12 Hz, 12-20 Hz, and 20-30 Hz). Duncan planned post hoc testing unveiled the specific statistical differences among the groups of male mice. Compared to the young and middle-aged mice, the old mice were characterized by a dominant EEG power difference (i.e. active minus passive) at 1-2 Hz in the low-frequency delta band ($p<0.05$). Also, the old mice showed a dominant EEG power difference at 6-8 Hz ($p<0.05$), while the other groups displayed this effect at 8-10 Hz ($p>0.05$).

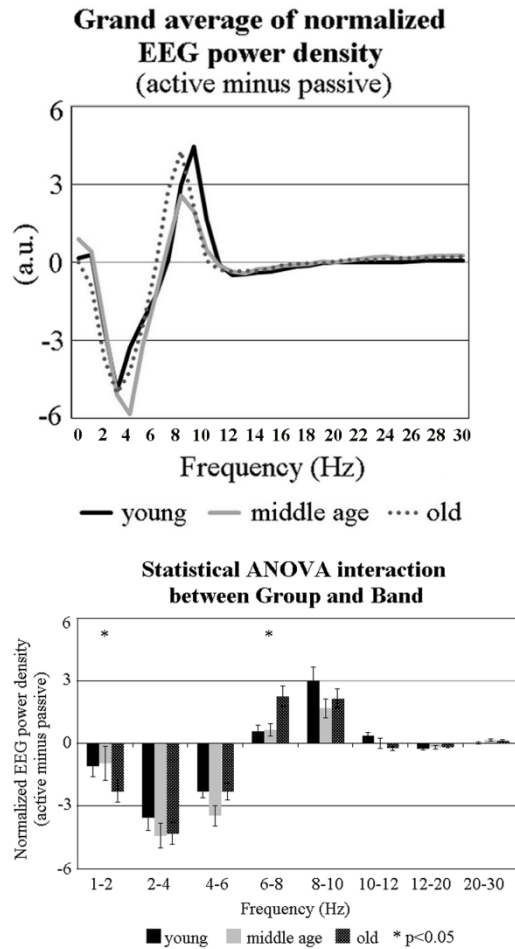


Figure 10. (Top): Grand average of the difference of the normalized EEG power density spectra between the active and passive conditions (active minus passive) obtained averaging the spectral values in the young ($N=25$), middle-aged ($N=18$), and old ($N=23$) male WT mice considered separately. The normalized EEG power density (active minus passive) refers to the frequency range between 0 and 30 Hz. (Bottom): Mean values (\pm SE) of the difference of the normalized EEG power density between the active and passive conditions (active minus passive) illustrating a statistically significant ANOVA interaction ($F(14, 434)=2.034, p=0.014$) between the factors Group (young, middle-aged, and old) and Band (1-2 Hz, 2-4 Hz, 4-6 Hz, 6-8 Hz, 8-10 Hz, 10-12 Hz, 12-20 Hz, and 20-30 Hz). The asterisks indicate the EEG frequency bands at which this difference of the normalized EEG power density presented statistically significant differences between the old mice compared to the young and middle-aged male mice (Duncan post hoc testing, $p<0.05$).

5.3.3 Effect of sex on the normalized EEG power

Figure 11 (top) shows the grand average of the difference in the normalized EEG power spectra between the active and passive conditions (i.e. active minus passive) in a sub-group of female mice and in a sub-group of

Experimental part

male mice. Compared to the male mice, the female mice exhibited the greatest negative values of the EEG power difference in the delta range (i.e. 1-2 Hz). Also, these female mice showed the greatest positive values of the EEG power difference in the theta and alpha range (i.e. 8-10 Hz).

Figure 11 (bottom) illustrates the mean values (\pm SE) of the difference in the normalized EEG power between the active and passive conditions (i.e. active minus passive) illustrating a statistically significant ANOVA interaction ($F(7, 238)=2.386$, $p=0.022$) between the factors Group (male, female) and Band (1-2 Hz, 2-4 Hz, 4-6 Hz, 6-8 Hz, 8-10 Hz, 10-12 Hz, 12-20 Hz, and 20-30 Hz). Duncan planned post hoc testing unveiled the specific statistical differences among these mouse groups. Compared to the male mice, the female mice showed a dominant EEG power difference (i.e. active minus passive) at 1-2 Hz in the low-frequency delta band ($p=0.02$). Compared to the male mice, the female mice also showed a dominant EEG power difference at 8-10 Hz ($p=0.002$). These results suggest a general greater EEG reactivity in the female mice compared to the male mice in both passive and active conditions.

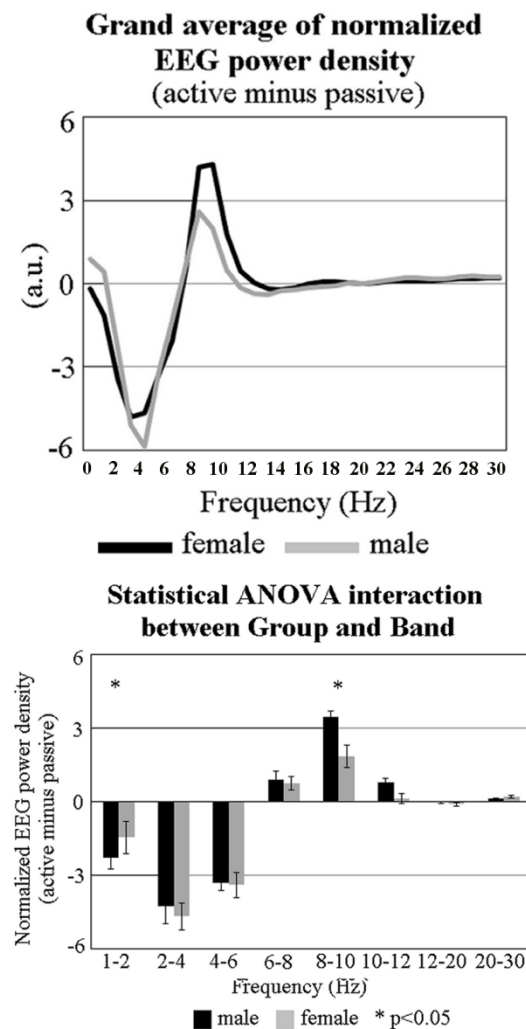


Figure 11. (Top): Grand average of the difference of the normalized EEG power density spectra between the active and passive conditions (active minus passive) obtained averaging the spectral values of the female ($N=19$) and male ($N=18$) middle-aged WT mice. This difference of the normalized EEG power (active minus passive) refers to the frequency range between 0 and 30 Hz. (Bottom): Mean values (\pm SE) of the difference of the normalized EEG power density between the active and passive conditions (active minus passive) illustrating a statistically significant ANOVA interaction ($F(7, 238)=2.386$, $p=0.022$) between the factors Group (male, female) and Band (1-2 Hz, 2-4 Hz, 4-6 Hz, 6-8 Hz, 8-10 Hz, 10-12 Hz, 12-20 Hz, and 20-30 Hz). The asterisks indicate

Experimental part

the EEG frequency bands at which the difference of the normalized EEG power density (active minus passive) presented statistically significant differences between the female and male mice (Duncan post hoc testing, $p < 0.05$).

5.3.4 Reliability of the spectral EEG markers among the recording centers

Figure 12 (top) shows the grand average of the normalized EEG power spectra for the active and passive conditions in the WT mice of any recording center considered separately (i.e. Janssen, Lundbeck, MNI, and UNIVR). In all recording centers, these spectra showed a clear EEG power peak at 2-4 Hz (i.e. delta range) that was higher in the passive condition compared to the active one. Furthermore, there was another clear EEG power peak at 6-8 Hz (i.e. theta range), that was higher in the active condition compared to the passive one in Janssen, Lundbeck, and MNI recording centers. On the contrary, this peak at 6-8 Hz was slight in UNIVR recording center. In the figure, the difference in the EEG power between the active and passive conditions (i.e. active minus passive) is also reported for all recording centers. As in the grand average of all WT mice as a whole group, a negative peak of the EEG power difference at 2-4 Hz reflected the maximum EEG power peak in the passive condition in all recording centers. In all recording centers but one (i.e. UNIVR), there was also a clear positive peak of the EEG power difference at 6-8 Hz, reflecting the maximum EEG power peak in the active condition.

Figure 12 (bottom) shows the mean values (\pm SE) of the difference in the normalized EEG power between the active and passive conditions (i.e. active minus passive) illustrating the results of the four ANOVAs, one for any recording center considered separately (i.e. Janssen, Lundbeck, MNI, and UNIVR). In all ANOVAs, there was a statistically significant ANOVA interaction ($p < 0.00001$) between the factors Condition (passive, active) and Band (1-2 Hz, 2-4 Hz, 4-6 Hz, 6-8 Hz, 8-10 Hz, 10-12 Hz, 12-20 Hz, and 20-30 Hz). Duncan planned post hoc testing confirmed in all single ANOVA the statistical differences among the passive and active conditions observed in the main analysis in all WP mice as a whole group. Compared to the passive condition, the active condition showed a statistically significant dominant negative EEG power difference (i.e. active minus passive) at 1-2 Hz and 2-4 Hz in all recording centers ($p < 0.005$). Also, the active condition showed a statistically significant dominant positive EEG power difference at 6-8 Hz in all recording centers but UNIVR ($p < 0.05$) and the 8-10 Hz in all recording centers ($p < 0.01$). More details on the results of this statistical session are reported in Table 9. The reduced differences of the EEG power density between the behavioral active and passive states in UNIVR mice, mainly due to a very slight increase of theta rhythms during the behavioral active state of the UNIVR mice, was probably due to the relative high amount of the old mice (20 months old) of UNIVR recording center (7 old mice for a total amount of 16). As the on-going cortical EEG rhythms differed across aging (see Figure 2), the averaging between the young, middle-age, and old mice may have caused the reduced theta increase during the behavioral active state in the UNIVR mice.

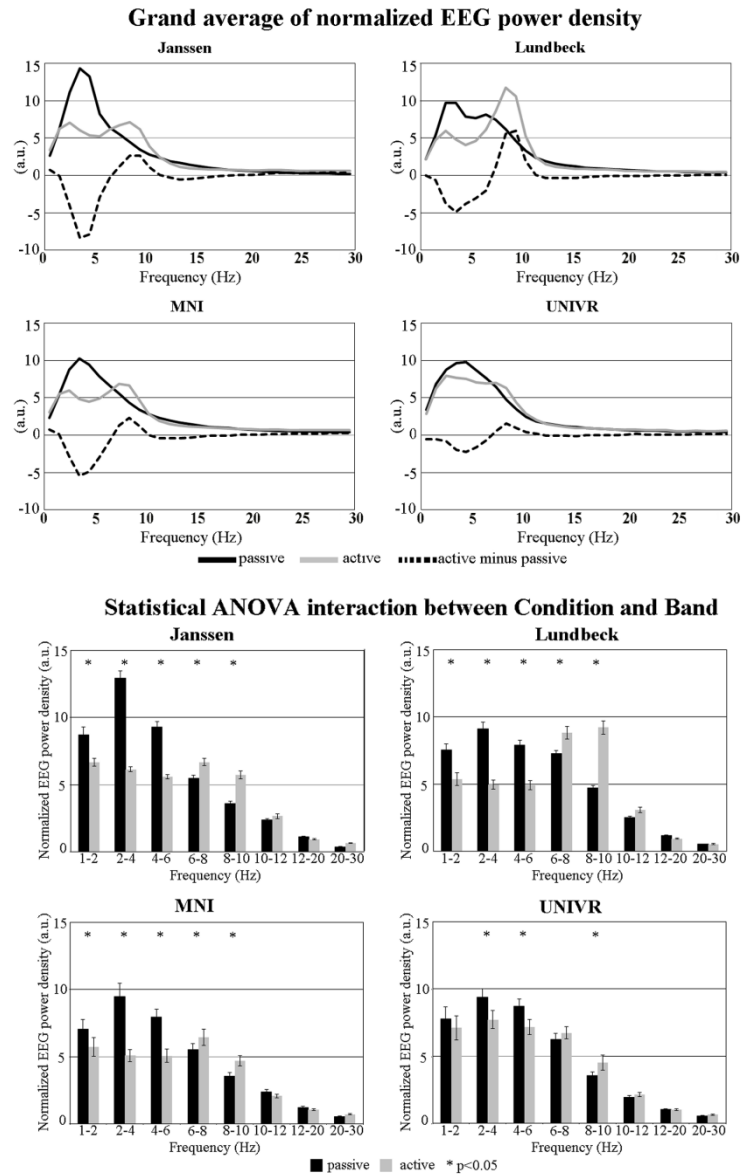


Figure 12. (Top): Grand average of the normalized EEG power density spectra for the four recording centers considered separately. Specifically, these centers were the following: Janssen Research and Development (Belgium), H. Lundbeck A/S (Denmark), Mario Negri Institute (MNI, Italy), and University of Verona (UNIVR, Italy). The EEG power density spectra range between 0 and 30 Hz for the active and passive state. The difference between the active and the passive state (active minus passive) is also reported. (Bottom): Mean values (\pm SE) of the normalized EEG power density illustrating a statistically significant ANOVA interaction effect (Janssen: $F(7, 77)=32.28$, $p=0.00001$; Lundbeck: $F(7, 231)=88.65$; MNI: $F(7, 154)=21.64$, $p=0.00001$; UNIVR: $F(7, 105)=5.80$, $p=0.00001$) between the factors Condition (passive, active) and Band (1-2 Hz, 2-4 Hz, 4-6 Hz, 6-8 Hz, 8-10 Hz, 10-12 Hz, 12-20 Hz, 20-30 Hz). Asterisks indicate the EEG bands at which the normalized EEG power density presented statistically significant differences between the passive and active conditions (Duncan post hoc testing, $p<0.05$).

ANOVA interaction between the factors Condition and Band	
Center	Duncan post hoc results
Janssen	$F(7, 77)=32.28$, $p=0.00001$ 1-2 Hz ($p=0.00003$), 2-4 Hz ($p=0.00002$), 4-6 Hz ($p=0.00002$), 6-8 Hz ($p=0.04$), 8-10 Hz
Lundbeck	$F(7, 231)=88.65$, $p=0.00001$ 1-2 Hz ($p=0.00001$), 2-4 Hz ($p=0.00004$), 4-6 Hz ($p=0.00004$), 6-8 Hz ($p=0.00003$), 8-

Experimental part

	F(7, 154)=21.64, p=0.00001
MNI	1-2 Hz (p=0.002), 2-4 Hz (p=0.00004), 4-6 Hz (p=0.00004), 6-8 Hz (p=0.03), 8-10 Hz (p=0.005)
UNIVR	F(7, 105)=5.80, p=0.00001
	2-4 Hz (p=0.00001), 4-6 Hz (p=0.00003), 8-10 Hz (p=0.01)

Table 9. Results of the statistically significant interaction ($p < 0.05$) between the factors Condition (i.e. passive, active; independent variable) and Band (1-2 Hz, 2-4 Hz, 4-6 Hz, 6-8 Hz, 8-10 Hz, 10-12 Hz, 12-20 Hz, and 20-30 Hz) of four ANOVAs using EEG power (density) as a dependent variable. ANOVA dependent variable was the normalized EEG power density. The ANOVAs refer to the following four EEG recording centers: Janssen Research and Development (Belgium), H. Lundbeck A/S (Denmark), Mario Negri Institute (MNI, Italy), and University of Verona (UNIVR, Italy). In the table, the results of a post-hoc Duncan testing are also reported ($p < 0.05$).

5.4 Discussion

In humans, resting state EEG rhythms reflect the fluctuation of cortical arousal and vigilance in a typical clinical recording setting, namely the EEG recordings for few minutes of subjects in the state of eyes closed (i.e. passive condition) and eyes open (i.e. active condition). The higher the cortical EEG power at a given frequency, the higher the synchronization of cortical pyramidal neurons at that frequency (Pfurtscheller and Lopes da Silva, 1999). Can this basic procedure be back-translated to C57BL6 (WT) mice for aging studies, this strain being the genetic basis for the mouse mutants modeling AD processes?

Here we report that the WT mice showed substantial differences in the EEG power between passive and active conditions mimicking those of the mentioned clinical setting for humans. Compared to the passive condition, the active condition exhibited a decrease of the EEG power at 1-2 Hz in the so-called delta range. Also, there was an increase in the EEG power at 6-10 Hz in the so-called extended theta range. This difference was more pronounced in female than male mice.

5.4.1 On-going cortical EEG rhythms in WT mice differ between the passive and active conditions

The present results indicate that theta power of on-going EEG rhythms is sensitive to an increased cortical arousal and vigilance in WT mice during exploratory movements. These findings lead support to previous evidence showing that on-going theta rhythms (6-9 Hz) were correlated with the amount of motor activity in mice and rats (Vanderwolf et al., 1969; Pickenhain and Klingberg, 1967; Buzsáki et al., 2003; Kelemen et al., 2005). Furthermore, these rhythms increased in power in awake states associated with attentive or motor activities in rats (Maloney et al., 1997). In the same vein, amphetamine did induce both increased theta power and hyperlocomotion in rats (Páleníček et al., 2013).

The present results also suggest that delta power of on-going EEG rhythms reflect low cortical arousal and vigilance in WT mice in awake quiet wakefulness. These findings challenge the traditional view that on-going delta rhythms are negligible in awake (healthy) rodents and primates, while they are dominant in non-rapid eye movement (NREM) stages of the sleep (Steriade et al., 1993; Steriade and Amzica, 1998; Steriade, 1993, 2000, 2003; Lörincz et al., 2009; Crunelli et al., 2015). In this regard, the present results extend the following pieces of previous evidence challenging that traditional view. In rodents, a state of quiet

Experimental part

wakefulness (i.e. similar to the current passive condition) induced dominant low-frequency (<5 Hz) and large voltage fluctuations in the membrane potential of cortical neurons and in cortical EEG and local field potentials (Timofeev et al., 2000; Petersen et al., 2003; Crochet and Petersen, 2006; Vyazovskiy et al., 2011; Zagha et al., 2013). These fluctuations interacted with incoming signals from visual, auditory, and somatosensory cortex in behaving animals (Okun et al. 2010; Bennett et al. 2013; Haider et al. 2013; Hromádka et al. 2013; Polack et al. 2013; Zhou et al. 2014). Furthermore, cortical delta rhythms exhibited increased power when rats were in quiet wakefulness with respect to states associated with attentive or motor activities (Maloney et al., 1997). Moreover, on-going delta rhythms and slow-frequency/large voltage fluctuations were reported in membrane potentials, multiunit activity, and local field potentials in the cerebral cortex of awake nonhuman primates (Lakatos et al. 2005, 2008; Tan et al. 2014). In human primates, widespread on-going delta rhythms were recorded from the scalp in relation to physiological sleep (Simon and Emmons 1956), consciousness disorders (Simon and Emmons, 1956), and pathological aging with cognitive impairment (Babiloni et al., 2007, 2009, 2014, 2015). In awake epilepsy patients, intracerebral EEG recordings showed ample on-going delta rhythms in circumscribed regions of the intact cerebral cortex during quiet wakefulness (Sachdev et al., 2015).

5.4.2 On-going cortical EEG rhythms in WT mice differ across aging

In the present study, the population of WT male mice was subdivided into three groups based on age: young (25 mice of 4.5-6 months), middle-aged (37 mice of 12-15 months), and old (23 mice of 20-24 months). EEG results showed some peculiar features in the former group. In the passive condition, EEG power in the delta band (i.e. 1-2 Hz) was higher in the old group than in the young and middle-aged groups. Whereas, the EEG power peak in the active condition was slower as frequency in the Nold group (i.e. 6-8 Hz) than in the other groups (i.e. 8-10 Hz). These results suggest a general “slowing” of the delta and theta rhythms in the old mice. In this line, they extend previous evidence showing a slowing of the frequency peak of on-going theta rhythms in awake C57 mice along physiological aging (Wimmer et al., 2013). In that previous study, there was no distinction of behavioral passive and active states during wakefulness, so it can be hypothesized that the overlapping of these states hides the aging effects on delta band.

5.4.3 Translational value of the present results

What is the translational value of the present results for the research on both physiological and pathological aging?

First, the present study unveiled the interspecies differences of on-going EEG rhythms in wakefulness between WT mice and humans. It is well known that in awake healthy humans, alpha rhythms (8-12 Hz) dominate in posterior areas of cerebral cortex in relaxed wakefulness, as a reflection of low cortical arousal and vigilance (Pfurtscheller and Klimesch, 1992; Klimesch et al., 1997; Klimesch, 1999). Power of these rhythms is dramatically reduced during perceptual, memory, and motor demands, as a reflection of increased cortical arousal and vigilance (Van Winsum et al., 1984; Sergeant et al., 1987; Babiloni et al., 1999,

Experimental part

Pfurtscheller and Klimesch, 1992; Klimesch et al., 1997; Klimesch, 1999). The same dynamic of on-going alpha rhythms is reproduced in a convenient clinical setting as the conditions of resting state eyes closed (i.e. passive condition) and eyes open (i.e. open condition), lasting few minutes each (Babiloni et al., 2010). In the present study, the pattern of the EEG activity was quite different in WT mice. The mice showed neither a power peak in the alpha range (8-12 Hz) during the passive condition nor the reduction of this power peak during the active condition. Rather, changes in the cortical arousal and vigilance were reflected by on-going delta and theta rhythms recorded for few minutes. Despite these interspecies differences, we posit that the present passive and active conditions are a useful translational paradigm for the neurophysiological study of the fluctuation of cortical arousal and vigilance in mice across aging.

Second, this translational paradigm can be used in multi-center studies on physiological aging in mice. Indeed, the present experimental procedures for the classification of the animal behavior and the EEG recordings provided results quite repeatable across four qualified recording centers. These procedures were defined in the IMI PharmaCog project (www.pharmacog.org) by researchers coming from academia and the pharmaceutical industry. Therefore, these procedures have incorporated needs and views of both perspectives. Overall, the present study represents the first cross-validation of the mentioned behavioral and EEG procedures in a public-private research network.

Third, the mentioned translational paradigm can be used in multi-centric studies on a mouse model of AD. Indeed, the present spectral EEG markers of cortical arousal in WT mice can be considered a promising back-translation of abnormal spectral EEG markers observed in AD patients placed in resting state condition (Claus et al., 1999; Huang et al., 2000; Bennys et al., 2001; Lehmann et al., 2007; Bonanni et al., 2008; Babiloni et al., 2010; Ommundsen et al., 2011). Compared to groups of normal elderly subjects, groups of AD patients with dementia were characterized by the following EEG markers: (1) higher power of widespread delta (<3 Hz) and theta rhythms (4-7 Hz); (2) lower power of posterior alpha rhythms (8-12 Hz) with a slowing of the alpha peak frequency, and (3) lower power of high-frequency beta (14-30 Hz) and gamma (around 40 Hz) rhythms (Prichep et al., 1994; Huang et al., 2000; Dierks et al., 2000; Ponomareva et al., 2003; Wolf et al., 2003; Jeong, 2004; Adeli et al., 2005; Babiloni et al., 2007, 2009, 2013, 2014, 2015); and (4) lower reduction of power of posterior alpha rhythms (Babiloni et al., 2010). In the framework of the PharmaCog project, we evaluated whether the present spectral EEG markers, reflecting changes in cortical arousal, were altered in single and double mutant transgenic mouse model of AD (i.e. PDAPP and TASTPM mice) compared to WT mice. Future studies will report the outcomes of these EEG comparisons as first positive impact of the present study (WT vs. PDAPP mice; WT vs. TASTPM mice).

6 Study III: Ongoing electroencephalographic activity associated with cortical arousal in transgenic PDAPP mice (hAPP v717f)

6.1 Introduction

Alzheimer's disease (AD) is the most diffuse progressive neurodegenerative disorder that affects aging (Braak and Braak, 1995, Bastos Leite et al., 2004, Glodzik-Sobanska et al., 2005). This disorder causes dementia, namely severe cognitive and psychiatric symptoms with a loss of autonomy in the activities of daily life ([Jelic et al., 1998, Price, 2000, Bianchetti et al., 2001). A promising biomarker of AD is ongoing electroencephalographic (EEG) activity (Schroeter et al., 2009, Babiloni et al., 2013). These rhythms of EEG activity are an emerging functional feature of the mammalian brain. They are generated by the synaptic currents related to the synchronization or desynchronization of the activation of large populations of pyramidal neurons in the cerebral cortex, due to subcortical (i.e. thalamocortical) and cortical signals (Pfurtscheller and Lopes da Silva, 1999).

A clinical setting with two experimental conditions is typically used to investigate these neurophysiological synchronization and desynchronization mechanisms in humans. In the “passive” behavioral condition, the person remains in relaxed wakefulness (resting state) with eyes closed for about 5 minutes. This mode is opposed to a more “active” behavioral condition during which the subject rests in relaxed wakefulness with the eyes open again for about 5 minutes, monitoring the environment around her or him. In the condition of resting state, EEG rhythms point to the highest power (density) at about 8-12 Hz in posterior cortical areas, namely the dominant alpha rhythms (for a review see Pfurtscheller and Lopes da Silva, 1999). After the opening of the eyes, alpha rhythms exhibit a power reduction (i.e. desynchronization) as a reflection of increased cortical arousal related to augmented vigilance (Pfurtscheller and Lopes da Silva, 1999).

Previous investigations have shown differences in EEG power in normal seniors (Nold) compared with patients with AD in the condition of resting state eyes closed. With reference to Nold seniors, AD subjects with dementia exhibited a higher power of topographically diffuse delta (<4 Hz) and/or theta (4-7 Hz) rhythms, in association with lower power of alpha (8-12 Hz) and beta (13-20 Hz) rhythms in posterior regions (Dierks et al., 2000, Huang et al., 2000, Ponomareva et al., 2003, Babiloni et al., 2007, 2009, 2014). In the same line, EEG power showed a different response to eyes opening in Nold seniors compared with AD subjects. There was a lower reduction (reactivity) of the posterior alpha power in AD and MCI patients than in Nold subjects (Stam et al., 1996, Stevens and Kircher, 1998, van der Hiele et al., 2007, Jeong 2004, Babiloni et al., 2006, 2010). This reduced reactivity of alpha power did predict a deterioration of cognitive functions in the subjects with cognitive decline (van der Hiele et al., 2008, Moretti et al., 2014).

An important question is whether EEG topographic biomarkers can be back-translated to preclinical research in the field of AD research and the drug discovery in rodents. A first requisite is that there are similar neurophysiological mechanisms at the basis of cortical arousal and vigilance in humans and rodent models. This seems to be the case, although inter-species differences exist. Indeed, active brain state was related to

Experimental part

hippocampal theta (6-9 Hz) rhythms and high cholinergic activity in both rodents and humans (Moruzzi and Magoun, 1949, Buzsáki et al., 2003, Zhang et al., 2010, Li et al., 2016). In these species, vigilance was related to enhanced power of low-voltage fast EEG frequencies (i.e. beta rhythms at about 14–30 Hz) while drowsiness and non-rapid eye movement (REM) sleep showed enhanced power of high-voltage slow EEG frequencies (i.e. delta and theta rhythms at about 1-7 Hz; Vanderwolf, 1969, Marshall and Born, 2002, Vyazovskiy et al., 2005).

A second requisite for the so-called back-translation is the availability of valid preclinical models of AD. A β injected rats (Liu et al., 2014) and transgenic mouse models with some different mutations (Webster et al., 2014) have been recently developed. A single mutation typically affects the gene regulating amyloid precursor protein (APP) in transgenic mouse models, to promote a strong brain accumulation of A β 1-42 (Sturchler-Pierrat et al., 1997, Hartman et al., 2005, Murakami et al., 2011, Cisse et al., 2011), which is one of the AD pathophysiological biomarkers (Games et al., 1995, Hsiao, 1998, Mucke et al., 2000, Chishti et al., 2001, Prut et al., 2007, Lassalle et al., 2008, Hanna et al., 2009, Oulès et al., 2012).

A bulk of studies has shown an abnormal brain electrophysiological activity in transgenic mouse models with a mutation in the gene regulating APP (Wang et al., 2002, Lalonde et al., 2005, Westmark et al., 2008, Minkeviciene et al., 2009, Sanchez et al. 2012, Verret et al. 2013, Schneider et al., 2014). These studies reported epileptiform and hypersynchronous neural activities characterizing these transgenic strains with respect to their littermates (Palop et al., 2007, Ziyatdinova et al., 2011, Corbett et al., 2013, Ziyatdinova et al., 2016). Different mouse models pointed to differences in the co-expressed transgenes, in the APP mutations they expressed, and in the promoters adopted to drive the expression of the phenotype (Born et al., 2014). In the same line, neuronal network seizures and imbalances have previously been proposed as important neural correlates of cognitive deficits in populations of patients with AD (Rabinowicz et al., 2000, Palop and Mucke, 2009).

In the IMI PharmaCog project (Innovative Medicine Initiative, <http://www.imi.europa.eu/content/pharmacog>), two convenient and back-translational conditions of EEG recordings for mice were identified. An equivalent of the “passive” condition in a clinical setting was defined as a mode of relaxed wakefulness with no or minimal animal movements in the cage (no sleep). Also, a surrogate of the “active” condition in a clinical setting was defined as a state characterized by spontaneous exploratory movements of the animals in the cage. Recently, these two behavioral conditions were successfully used as functional modes of behaving C57 wild-type -WT- mice, to probe the hypothesis that ongoing EEG activity reflects variations in cortical arousal (Del Percio et al., 2017). It was shown that, in comparison with the cited passive condition, the active one was associated with a decreased EEG power (density) at 1-2 Hz and increased EEG power at 6-10 Hz in WT mice. Also, effects of aging on those EEG biomarkers were found. The passive condition showed EEG power at 1-2 Hz greater in the old group of WT mice (20-24 months) than the middle-aged (12-15 months) and young adult (4.5-6 months) groups. Also, the active condition showed EEG power at 6-8 Hz greater in the old group and 8-10 Hz in the young group.

Experimental part

In the present exploratory study, we used the same experimental procedures of the reference investigation [59] to provide a preliminary testing of the hypothesis that ongoing EEG activity reflecting modifications in cortical arousal might be altered in a single-mutant transgenic mouse model of AD, the so called PDAPP mouse model of AD (human APP Indiana V717F mutated gene; Games et al., 1995). This AD mouse model progressively develops many of the pathological hallmarks of AD, including numerous extracellular thioflavin S-positive A β deposits, neuritic plaques, synaptic loss, astrogliosis, and microgliosis (Games et al., 1995). Even in a young age (i.e. 4-6 months), PDAPP mice show cognitive deficits in several domains such as spatial working memory (Hartman et al., 2005) and recognition of novel objects (Dodart et al., 1999). These cognitive deficits precede accumulation of A β deposition in the brain, which occurs at approximately six months of age with mature plaques appearing at 12 months and becoming intense as distribution in the cortex, thalamus, hippocampus, and striatum at 24 months (German et al., 2003). On the whole, PDAPP mice show extracellular A β deposition, gliosis, dystrophic neurites, and decreased density of synapses and dendrites in the neurons of hippocampus (Games et al., 1995, Chen et al., 2000, Galvan et al., 2006). Deficits in learning, memory, and behavioral are greater in aged PDAPP mice (Dodart et al., 1999, Galvan et al., 2006, Larson et al., 1999, Moechars et al., 1999). It is expected that these abnormalities are associated with abnormal cortical arousal as reflected by altered ongoing EEG rhythms.

6.2 Methods

6.2.1 Animals

The experiments of the present pilot study were performed in 15 PDAPP old mice (males; mean age: 22.9 months \pm 0.4 standard error, SE; range of age: 20-24 months) and 23 matched C57/BL6 WT mice (males; mean age: 22.8 months \pm 0.3 SE; range of age: 20-24 months). The transgenic homozygous PDAPP mice overexpressing human APP Indiana V717F (C57/BL6 background) were provided by Eli Lilly company (Eli Lilly Inc., Indianapolis, IN). The age of the animals ensured the presence of A β plaques deposition in the brain. The EEG data were obtained from one Danish center (i.e. H. Lundbeck A/S; 8 PDAPP and 8 WT mice) and two Italian centers (i.e. Mario Negri Institute for Pharmacological Research of Milan, MNI, 3 PDAPP and 8 WT mice; University of Verona, UNIVR, 4 PDAPP and 7 WT mice) in the framework of the work package 6 (WP6) of the IMI PharmaCog project.

Experimental procedures (management of mice, their care) were performed following institutions' guidelines, strictly in line with international and national rules, laws, and policies (EEC Council Directive 86/609, OJ L 358, 1, 12 December, 1987; Guide for the Care and Use of Laboratory Animals, U.S. National Research Council, 1996). The careful respect of the guidelines was controlled by WP8 members, in charge to control the ethics of research in the PharmaCog project.

We used independent t-testing to contrast the age of the PDAPP and WT groups (significance threshold of $p < 0.05$, two tailed). Results showed no significant difference ($p = 0.4$).

Experimental part

	Center	N	Sex (F/M)	Age
WT	Lundbeck	22	8M	24 months
	MNI	23	8M	24 months
	UNIVR	16	7M	20 months
PDAPP	Lundbeck	8	8M	24 months
	MNI	3	3M	24 months
	UNIVR	4	4M	20 months

Table 10. Features of the C57 (for the sake of simplicity, wild-type; WT) and the PDAPP mice in the following electroencephalographic (EEG) recording centers: H. Lundbeck A/S (Denmark), Mario Negri Institute (MNI, Italy), and University of Verona (UNIVR, Italy). Legend: M= male.

6.2.2 Pre-Surgery (3 weeks)

The present mice were acclimated in a period of minimum 3 weeks before surgery. In the cage, there was a constant temperature of 18-22°C, while humidity was of 55-65%. A standard 12-h light/dark cycle was used with a light-on hemi-cycle that spanned from 6:00 a.m. to 6:00 p.m. Light intensity was 90–110 lx in the room. In the cage, this intensity was 60 lx in the light period, while it was less than 1 lx in the dark period. The animals had free access to the food and water. In the post-surgical period, the mice were housed in individual cages (typical cage size of 45 cm in length × 24 cm in width × 20 cm in height) at the same conditions of temperature, humidity, light, and access to food and water.

Gentle handling was daily performed for about 5-10 minutes with the aim to reduce potential stress provoked by housing and experimenters. Stress was tested continuously across the experiments by experts (i.e. veterinary specialists) of each recording center. They tested animal muscle relaxation and standard behavioral indicators of stress in the freely behaving mice. The indicators measured the preservation of exploratory movements and instinctual activities (i.e. drinking and eating, and body weight) in the cage day-by-day before compared with after the surgery.

6.2.3 Surgery

EEG electrodes were implanted after an anesthesia performed by inhalation of isoflurane (5%) or Equithesin, pentobarbital (1%), and chloral hydrate (+4%) 3.5 ml/kg). The mice were also treated with systemic analgesics and antibiotics in line with local guidelines on surgical care.

The AP and ML stereotaxic coordinates of the electrodes from bregma were reported in Table 11 (standard mouse brain atlas; Franklin and Paxinos, 1997).

Electrode	Stereotaxic coordinates
Reference	AP:-6, ML:+2
Ground	AP:-2, ML:+2.5
Frontal	AP:+2.8, ML:-0.5

Experimental part

Parietal

AP:-2, ML:+2

Table 11. Stereotaxic coordinates for the implantation of EEG electrodes in the mouse brain according to a standard atlas (*The Mouse Brain coordinates by Franklin and Paxinos, 1997*).

For the MNI and Lundbeck recording units, a tethered system for EEG recordings was used. Stainless steel insulated surface epidural electrodes were used as exploring contacts at the frontal and parietal sites (model E363/20 with a diameter of 0.56 mm (0.022")); PlasticsOne, VA, US). One depth electrode as a reference contact was implanted in the cerebellum; another depth electrode as a ground contact was implanted in the temporal bone without the removal of the muscles (model E363/1 with a diameter of 0.280 mm (0.011")), PlasticsOne, VA, US). The electrodes were fixed to the skull with dental cement. EEG signals were transmitted through a plastic electrode pedestal and a connector cable to the amplifier with a maximal cable length of 50 cm.

For the UNIVR preclinical unit, a telemetric system for EEG recordings was used. Mice were instrumented with a radiotelemetry probe F20-EET (DSI, Minnesota, USA) containing sensors for the recording of the EEG, electromyogram (EMG), body temperature, and locomotion. The probe was implanted in the peritoneal cavity with 1 mL of sterile physiological saline to prevent desiccation. The four leads were subcutaneously tunneled from the peritoneal cavity towards a 1-cm head skin incision. Bipolar EEG recordings were performed by two miniature stainless-steel screw electrodes. These electrodes were epidurally implanted and fixed to the skull with acrylic dental cement. Bipolar EMG recordings were performed by two other electrodes placed in the dorsal neck muscles. These EEG and EMG electrodes (EEG and EMG) had an outer diameter of 0.3 mm.

All EEG experiments were carried out in the dark and light phases. In the EEG recording period, the mice did receive no handling treatment. The EEG recordings always started after the second hour from the beginning of light/darkness. The EEG sampling frequency was at least 250 Hz using anti-aliasing bandpass analog filters (Lundbeck: 1000 Hz, Janssen: 250 Hz, UNIVR: 500 Hz; MNI: 1600 Hz, 0.16 Hz-100 Hz passband filter). The impedance of the EEG recording was lower than 30 k Ω . No notch filter was employed.

Table 12 reports the time flow of the experimental procedures before and after the surgery.

TIME FLOW OF THE TREATMENTS AND PROCEDURE		
BEFORE AND AFTER THE SURGERY		
Period	Days	Treatments and Procedures
<i>Pre-surgery</i>	-21 to -1	<ul style="list-style-type: none"> ✓ Habituation to light switched on-off ✓ Gentle handling for about 5-10 minutes a day
<i>Surgery</i>	0	<ul style="list-style-type: none"> ✓ Anaesthetic procedure ✓ Therapy with systemic analgesics and antibiotics ✓ Electrode placement

Experimental part

<i>Quiet post-surgery</i>	+1 to +7	<ul style="list-style-type: none"> ✓ Therapy with systemic analgesics and antibiotics <ul style="list-style-type: none"> ✓ No gentle handling ✓ No EEG experiment
<i>Post-surgery</i>	+8 to +14	<ul style="list-style-type: none"> ✓ Facilitating the adaptation by plugging and unplugging several times the animal ✓ Gentle handling for about 5-10 minutes a day <ul style="list-style-type: none"> ✓ No EEG experiment
<i>Experimental day</i>	from +15	<ul style="list-style-type: none"> ✓ No gentle handling ✓ EEG recording

Table 12. Time flow of the experimental procedures (including EEG recordings) before and after the surgery in the mice.

Recording EEG systems of the units were as follows: telemetric wireless EEG system provided by Data Science International (DSI) in UNIVR unit; wired EEG systems provided by Grass Technologies in Lundbeck and MNI units. These systems underwent to a preliminary qualification phase before the final experimental recordings. This phase tested the quality of the EEG data recorded in a couple of WT mice. All these units obtained a successful qualification and harmonization the EEG systems by a centralized data analysis performed by the staff of University of Foggia and Sapienza University of Rome (Italy) under the supervision of Prof. Claudio Babiloni.

6.2.4 Quiet Post-surgery period of 1 week

During a standard post-surgical period lasting one week, the animals were treated by systemic analgesics and antibiotics. In the week immediately following surgery, the mice experienced a period of full recovery with neither handling nor EEG recordings.

6.2.5 Handling post-surgery period of 1 week

In the week immediately following the quiet post-surgery period, EEG recordings was not yet performed but gentle handling was done for 2-5 minutes daily. During the handling period, the mice were gently plugged and unplugged (for wired systems only) several times across one week to familiarize with the recording procedure.

6.2.6 Experimental day

All EEG experiments were carried out in the dark and light phases. In the EEG recording period, the mice did receive no handling treatment. The EEG recordings always started after the second hour from the beginning of light/darkness. The EEG sampling frequency was at least 250 Hz using anti-aliasing bandpass analog filters (Lundbeck: 1000 Hz, UNIVR: 500 Hz; MNI: 1600 Hz, 0.16 Hz-100 Hz passband filter). No notch filter was employed.

6.2.7 Determination of the animal behavior

Experimental part

An important step of the data analysis was the classification of the animal behavior during the EEG recordings. The behavioral classification was performed by independent experts (personnel enrolled by each preclinical Unit) who underwent to a preliminary phase of training for the harmonization of procedures across the three preclinical Units. This classification was based on visual inspection of the mouse behavior in the videos obtained during the EEG recordings carried out in all preclinical Units. In each preclinical Unit, the rater classified video recording epochs lasting 10 s.

In the present study, the animal behavior in each video epoch was classified into one of the following 5 behavioral classes:

- (1) Active behavior (condition). This kind of epochs showed animals performing overt exploratory movements in the cage for most of the given epoch. The exploratory movements had to be characterized by ample displacements of body parts such as trunk, head, and/or forelimbs (when videos were available). They had not to be confounded with instinctual activities (*vide infra*).
- (2) Passive behavior (condition). This kind of epochs showed animals performing no or small movements of the trunk, head, and/or forelimbs with a maximal total duration of that behavior of 20 s. The maximal immobility duration was of 10 s. These criteria were expected to minimize the risk that “passive condition” be misclassified in an epoch in which the mouse was sleeping.
- (3) Behavioral sleep state. This kind of epochs showed mice behaviourally exhibiting a sleep state from a behavioral point of view.
- (4) Instinctual behavior. This kind of epochs showed mice exhibiting instinctual activities such as drinking, cleaning, mating, eating, etc. for most of the epochs (when videos were available). Special attention was paid not to include these epochs into the class denoting active behavior.
- (5) Undefined. This kind of epochs was characterized by a lack of clarity about the behavioral condition of the animal. Such epochs were rejected from the analysis....(*omissis*)...

In the UNIVR Unit, the behavioral classification was also corroborated by additional variables such as body temperature, electromyographic (EMG) activity recorded from neck muscles, and instrumental markers of the movement (i.e. actigraphy). These variables (and EEG activity) were used as an input to DSI software automatic classification (Data Sciences International, DSI, Minnesota, USA). The DSI software classified the epochs in some behavioral classes corresponding to the above passive behavior, active behavior, and sleep.

6.2.8 EEG data analysis

The behavioral epochs (lasting 10 s) of the passive and active state were segmented in consecutive EEG epochs lasting 2 s. These EEG epochs selected for the spectral analysis were free from muscle, EEG, electrocardiographic (EKG), instrumental or other artifacts. The mice showing epileptic-like EEG activity were excluded from the following analyses. This activity was defined as the presence of spikes, spike-wave EEG patterns or the appearance of seizure activity. A seizure was defined by a high amplitude ($>2 \times$ baseline)

Experimental part

rhythmic discharge clearly representing an abnormal EEG pattern (i.e. repetitive spikes, spike-wave, and slow waves) lasting more than 5 ss (Ziyatdinova et al., 2016). To be considered as an epileptic seizure, EEG had to be also related to the behavioral manifestations described in the Racine' scales (Racine, 1972). This selection was done centrally by the group of University of Foggia and Rome (Dr. Claudio Babiloni's staff).

Artifact-free EEG epochs were re-referenced from monopolar to bipolar montage. This re-referencing was done by a mathematical procedure that consisted in the subtraction of the EEG signal collected at the monopolar parietal electrode from the EEG signal collected at the monopolar frontal electrode. These bipolar EEG epochs were used as an input for the subsequent EEG data analysis.

6.2.9 Spectral EEG data analysis

Artifact-free bipolar EEG epochs of the passive and active state represented the input for the spectral EEG data analysis, namely the computation of EEG power (density). This analysis was based on an FFT algorithm implemented in the Matlab environment (MathWorks, Massachusetts, USA). Specifically, the algorithm used Hanning windowing with no overlap of time windows and Welch technique with a frequency resolution of 0.5 Hz. FFT solutions were used to individuate two frequency bins of interest named as individual delta and theta frequencies (IDF and ITF), respectively. In a given mouse, the IDF was defined as the frequency bin showing the highest amplitude of the absolute EEG power (density) between 1 and 6 Hz (delta frequency range) at the bipolar frontoparietal electrodes during the passive state in the wakefulness. Furthermore, the ITF was defined as the frequency bin showing the highest amplitude of the absolute EEG power density between 6.5 and 10 Hz (theta frequency range) at the bipolar frontoparietal electrodes during the exploratory active state. The frequency and amplitude of the IDF and ITF peaks were considered as markers of the absolute EEG power during the passive and the active state, respectively. In the behaving old mice, the delta and theta frequency bands are of particular interest based on the results of a reference investigation performed in 85 C57 mice [59].

6.2.10 Statistical analysis

The statistical analysis was formed by four sessions (Statistica® 10.0 packages), which tested the main hypotheses of this study. In all statistical analyses, the significance threshold was $p < 0.05$. In all statistical sessions, we used the recording Unit as a covariate (e.g. Lundbeck, UNIVR, and MNI) to account for the multi-centric nature of this study.

The first session evaluated the (working) hypothesis that, in comparison with the WT mice, the current PDAPP mice showed differences in the frequency bin (Hz) of the IDF during the behavioral passive state and that of the ITF during the active state. To address this hypothesis, an ANOVA (i.e. analysis of variance) used the frequency bin of the IDF and ITF as the dependent variable. The ANOVA factors of the ANOVA were Group (WT, PDAPP) and Frequency (IDF, ITF). The confirmation of the hypothesis implied the following statistical results: (1) a statistically significant interaction between the Group and the Frequency factor ($p < 0.05$); (2) the

Experimental part

post-hoc test showing significant differences in the frequency bin of the IDF and ITF between the WT and the PDAPP group (Duncan test, $p < 0.05$).

The second session evaluated the (control) hypothesis that the WT group showed the same differences in the delta and theta EEG rhythms related to the passive vs. active state in the wakefulness as obtained in a reference investigation performed in 85 WT mice (Del Percio et al., 2017). To evaluate this hypothesis, an ANOVA used the absolute EEG power (density) of the IDF and ITF as the dependent variable. The ANOVA factors were Condition (active, passive) and Frequency (IDF, ITF). The confirmation of the hypothesis implied the following statistical results in the WT group: (1) a statistically significant interaction between the Condition and the Frequency factor ($p < 0.05$); (2) the *post-hoc* test showing significant differences in the absolute EEG power of the IDF and ITF between the active and the passive condition (Duncan test, $p < 0.05$).

The third session evaluated the (working) hypothesis that the PDAPP group showed no statistical differences ($p > 0.05$) in the absolute EEG power between the active vs. the passive state, confirming the sensitivity of the present EEG markers in this mouse model of AD. To evaluate this hypothesis, an ANOVA used the absolute EEG power of the IDF and ITF as the dependent variable. The ANOVA factors were Condition (active, passive) and Frequency (IDF, ITF) in the PDAPP group.

The fourth session evaluated the (working) hypothesis that, in comparison with the WT group, the PDAPP group showed differences in the absolute EEG power (density) between the active vs. the passive state. To evaluate this hypothesis, a preliminary step was the computation of the difference in the absolute EEG power between the two behavioral states (active minus passive) as a dependent input variable to an ANOVA. The ANOVA factors were Group (WT, PDAPP) and Frequency (IDF, ITF). The confirmation of the hypothesis implied the following statistical results: (1) a statistically significant effect including the factor Group ($p < 0.05$); (2) the *post-hoc* test showing significant differences in the EEG variable between the two groups (Duncan test, $p < 0.05$).

6.2.11 Control analysis

We performed a control analysis considering the delta (1-4 Hz) and the theta (6-9 Hz) fixed frequency bands to cross-validate the analysis based on the individual assessment of IDF and ITF peaks. This control analysis included three statistical sessions. In all statistical sessions, we used the recording Unit as a covariate (e.g. Lundbeck, UNIVR, and MNI) to account for the multi-centric nature of this study.

The first session tested the (control) hypothesis that the WT group might show differences in the delta (1-4 Hz) and theta (6-9 Hz) EEG rhythms related to the passive vs. active state in the wakefulness. To evaluate this hypothesis, an ANOVA used the absolute EEG power (density) of the delta and theta fixed bands as a dependent variable. The ANOVA factors were Condition (active, passive) and Band (delta, theta). The hypothesis would be confirmed by the following statistical results in the WT group: (1) a statistically significant interaction between the Condition and the Band factor ($p < 0.05$); (2) the *post-hoc* test showing

Experimental part

significant differences in the absolute EEG power of the delta and theta bands between the active and the passive condition (Duncan test, $p < 0.05$).

The second session tested the (working) hypothesis that the PDAPP group might exhibit no statistical differences ($p > 0.05$) in the absolute EEG power between the active vs. the passive state. To evaluate this hypothesis, an ANOVA used the absolute EEG power (density) of the delta and theta fixed bands as a dependent variable. The ANOVA factors were Condition (active, passive) and Band (delta, theta). The hypothesis would be confirmed by no statistically significant interaction between the Condition and the Band factor ($p > 0.05$).

The third session tested the (working) hypothesis that, in comparison with the WT group, the PDAPP group might unveil differences in the EEG activity between the active vs. the passive state. To evaluate this hypothesis, a preliminary step was the computation of the difference in the absolute EEG power (density) between the two behavioral states (active minus passive) as a dependent variable. The ANOVA factors were Group (WT, PDAPP) and Band (delta, theta). The hypothesis would be confirmed by the following statistical results: (1) a statistically significant interaction between the Condition and the Band factor ($p < 0.05$); (2) the post-hoc test showing significant differences in the absolute EEG power of the delta and theta bands between the two groups (Duncan test, $p < 0.05$).

6.3 Results

6.3.1 Absolute EEG power (density) during passive and active conditions in WT and PDAPP groups

Figure 13 displays the mean spectra of the frontoparietal absolute EEG power (density) for the passive and the active condition in the WT ($N=23$; Fig. 1, left) and the PDAPP group ($N=15$; Fig. 1, right). In both groups of mice, these spectra showed an EEG power peak at 1-6 Hz (i.e. delta range). This peak was greater in the passive condition when compared to the active one. For each animal, this peak identified the frequency bin (Hz) of the IDF during the passive state in the wakefulness. Besides, there was another EEG power peak within the theta range (i.e. 6.5-10 Hz), which was higher in the active than the passive condition. For each animal, this peak identified the frequency bin (Hz) of the ITF during the exploratory active state. In the EEG power difference between the active and the passive condition (i.e. active minus passive), both groups of mice showed two main peaks in the graph. There was a downward negative peak of the EEG power difference at 1-6 Hz, which reflected the higher values of the delta power in the passive than the active condition. Furthermore, there was an upward positive peak of the EEG power difference at 6-8 Hz, which reflected the higher values of the theta power in the active than the passive condition. These results indicated that both groups of mice showed changes in the EEG power during the passive vs. the active condition.

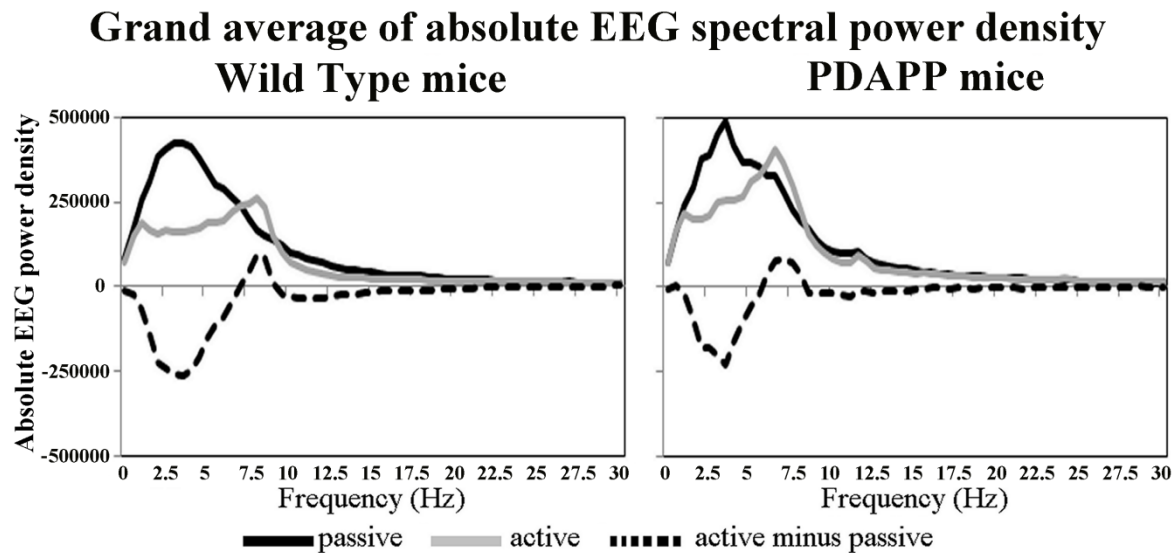


Figure 13. Grand average of the electroencephalographic (EEG) power (density) obtained averaging data of the Wild Type (WT; $N=23$, left in the figure) and the PDAPP group of mice ($N=15$, right). In particular, the graph represents the absolute EEG power at the bipolar frontoparietal electrodes for the passive and the active condition during the dark phase of the day (note that mouse is a nocturnal animal). The difference of the EEG power between the active and the passive condition (active minus passive) is also reported (dotted EEG power spectra).

6.3.2 Comparison of the frequency and absolute EEG power between the WT and the PDAPP group

Figure 14 plots the distribution of the frequency bin (Hz) of the IDF and ITF of the frontoparietal rhythms in all individual WT and PDAPP mice. Grubbs test ($p < 0.05$) was preliminary used for the evaluation of the outliers in the distribution of the IDF and ITF. No outlier was found for both frequency (IDF, ITF) and group (WT, PDAPP). The ANOVA showed a statistically significant interaction effect ($F(1, 35)=11.354$, $p=0.002$) between the factors Group (WT, PDAPP) and Frequency (IDF, ITF). Duncan post hoc testing showed that compared to the WT group, the PDAPP group was characterized by higher frequency bins of the IDF during the passive state and lower frequency bins of the ITF during the active state ($p=0.01$).

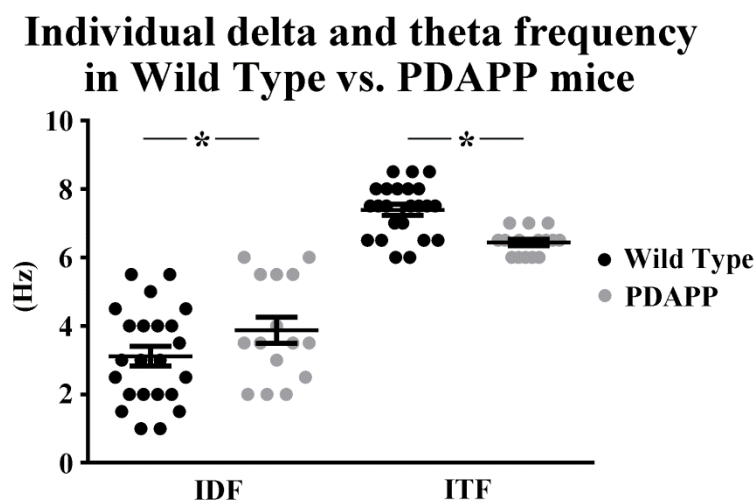


Figure 14. Individual delta and theta frequency (IDF and ITF, respectively) calculated for the WT ($N=23$, left) and PDAPP ($N=15$, right) mice. The graph represents the individual frequency peaks within the delta (1-6 Hz; individual delta frequency, IDF) and the theta (6-10 Hz; individual theta frequency, ITF) frequency bands corresponding to the highest amplitude of the absolute EEG power (density) at the bipolar frontoparietal electrodes. Statistical analysis showed a significant ANOVA interaction between

Experimental part

the factors Group (WT, PDAPP) and Frequency (IDF, ITF; $F(1, 35)=11.354$, $p=0.002$; covariate: Unit). Asterisks indicate the EEG frequency peak at which statistically significant differences were found between the WT and the PDAPP groups of mice (Duncan post hoc test, $p<0.05$).

Figure 15 illustrates the individual values of the frontoparietal absolute EEG power (density) for the WT (left) and PDAPP (right) groups of mice at the two frequency peaks (IDF and ITF) and the two behavioral conditions (active, passive). Grubbs test ($p<0.05$) was preliminary used for the evaluation of the outliers in the distribution of the absolute EEG power (density). Two outliers were found in the WT group, while only one outlier was observed in the PDAPP group (see rectangles in Figure 3). These outliers were removed from the respective groups for the ANOVA design. In the WT group, the ANOVA showed a statistically significant interaction effect ($F(1, 20)=12.200$, $p=0.002$) between the factors Condition (passive, active) and Frequency (IDF, ITF). Duncan post-hoc test indicated that the WT group was characterized by an increase of the absolute EEG power at the IDF during the passive compared to the active state ($p=0.0001$). Furthermore, this group showed a trend towards an increase of the absolute EEG power at the ITF during the active compared to the passive state ($p=0.06$). In the PDAPP group, the ANOVA did not show any significant effect ($p>0.05$).

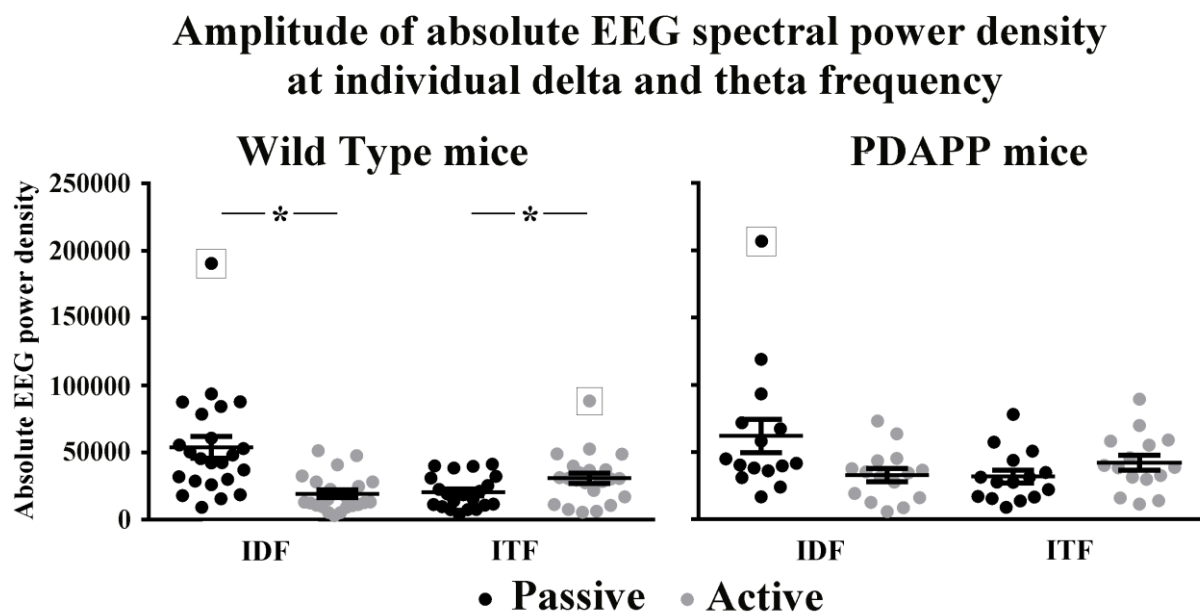


Figure 15. Individual values of the absolute EEG power (density) for the WT (left) and PDAPP (right) mice. In particular, the frontoparietal absolute EEG power is represented for the two conditions (active, passive) and the two frequency peaks (IDF and ITF). The outlier values according to Grubb's test ($p<0.05$) indicated by the squares were excluded from the subsequent statistical analyses. Statistical analysis showed a significant ANOVA interaction between the factors Condition (passive, active) and Frequency (IDF, ITF) in the WT group ($F(1, 20)=12.200$, $p=0.002$; covariate: recording Unit). Asterisks indicate the EEG frequency peaks at which statistically significant differences in the EEG power (density) were observed between the passive and the active condition in the WT group (Duncan post hoc testing, $p<0.05$). In the PDAPP group (right) no significant ANOVA interaction between the factors Condition and Frequency was found ($F(1, 12)=1.9892$, $p=0.18382$; covariate: recording Unit).

Figure 16 displays the individual difference of the frontoparietal absolute EEG power (density) between the active and the passive condition (active *minus* passive) at the two frequency peaks (IDF, ITF) for the WT and PDAPP groups of mice. Grubbs test ($p<0.05$) was preliminary used for the evaluation of the outliers in the distribution of this difference. One outlier was found in the WT group, while two outliers were observed in the PDAPP group (see rectangles in Figure 4). These outliers were removed from the respective groups for the

Experimental part

ANOVA design. The ANOVA did not show any significant effect between the factors Group and Frequency ($p>0.05$) despite the lower difference values of the IDF in the PDAPP group when compared to the WT group.

Amplitude of absolute EEG spectral power density in Wild Type vs PDAPP mice

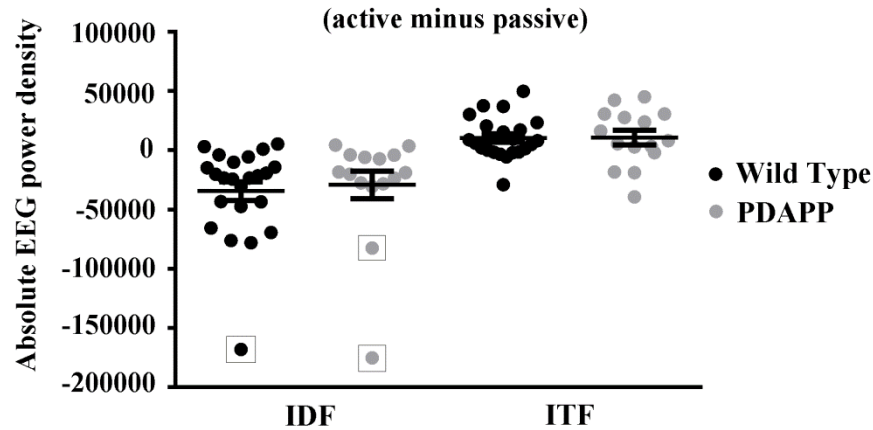
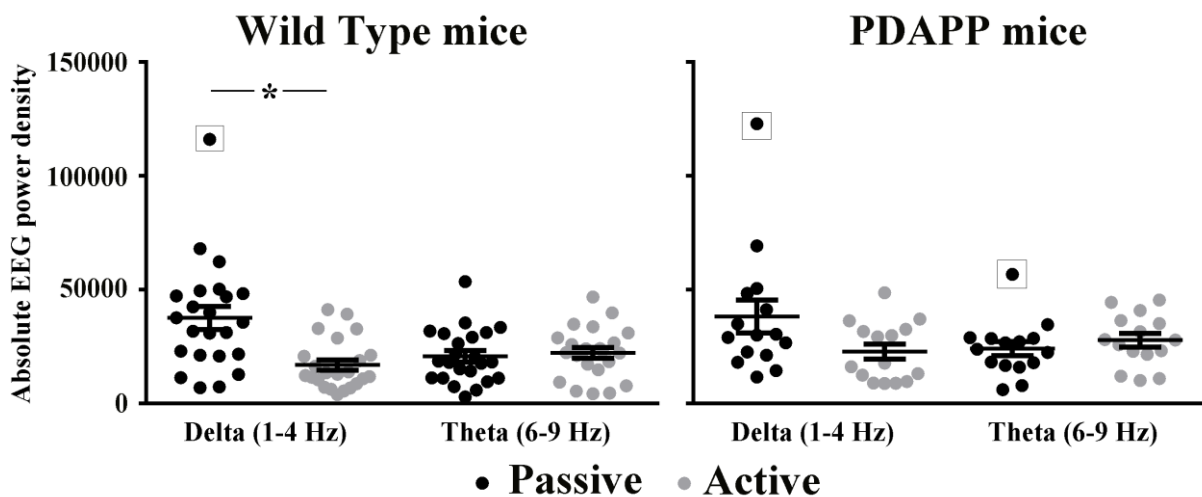


Figure 16. Individual values of the difference of the absolute EEG power (density) between the active and the passive condition (active minus passive) at the two frequency peaks (IDF and ITF) for the WT ($N=23$) and PDAPP ($N=15$) mice. The outlier values according to Grubb's test ($p<0.05$) indicated by the squares were excluded from the subsequent statistical analysis. No significant ANOVA interaction between the factors Group (WT, PDAPP) and Frequency (IDF, ITF) was found ($F(1, 32)=.80668$, $p=0.376$; covariate: recording Unit).

6.3.3 Control analysis

Figure 17 illustrates the individual values of the frontoparietal absolute EEG power (density) for the WT (left) and PDAPP (right) groups of mice for the two fixed frequency bands (delta, theta) and the two behavioral conditions (active, passive). Grubbs test ($p<0.05$) was preliminary used for the evaluation of the outliers in the distribution of the absolute EEG power (density). One outlier was found for each group of mice (see rectangles in Figure 5). These outliers were removed from the respective groups for the ANOVA design.

Amplitude of absolute EEG power density at delta and theta frequency bands



Experimental part

Figure 17. Individual values of the absolute EEG power (density) for the WT (left) and PDAPP (right) mice. In particular, the frontoparietal absolute EEG power is represented for the two conditions (active, passive) and the two fixed frequency bands (delta, 1-4 Hz and theta, 6-9 Hz). The outlier values according to Grubb's test ($p < 0.05$) indicated by the squares were excluded from the subsequent statistical analyses. Statistical analysis showed a significant ANOVA interaction between the factors Condition (passive, active) and Band (delta, theta) in the WT group ($F(1, 20) = 15.9$, $p = 0.0007$; covariate: recording Unit) between the factors Condition (passive, active) and Band (delta, theta). Asterisks indicate the EEG fixed frequency bands at which statistically significant differences in the EEG power (density) were observed between the passive and the active condition in the WT group (Duncan post hoc testing, $p < 0.05$). Duncan post-hoc test indicated that the WT group was characterized by an increase of the absolute EEG power at the delta band during the passive compared to the active state ($p = 0.00006$). In the PDAPP group (right), the ANOVA did not show any statistically significant interaction effect ($p > 0.05$).

In the WT group, the ANOVA showed a statistically significant interaction effect ($F(1, 20) = 15.9$, $p = 0.0007$) between the factors Condition (passive, active) and Band (delta, theta). Duncan post-hoc test indicated that the WT group was characterized by a decrease in the absolute EEG power at the delta band during the active compared to the passive state ($p = 0.00006$) in line with the results of the main analysis based on individual frequencies. In the PDAPP group, the ANOVA showed no statistically significant interaction effect between the factors Condition and Band ($p > 0.05$) in line with the results of the main analysis based on individual frequencies.

Figure 18 displays the individual difference of the frontoparietal absolute EEG power (density) between the active and the passive condition (active minus passive) for the two fixed frequency bands (delta, theta) in the WT and PDAPP groups of mice. Grubbs test ($p < 0.05$) revealed that one outlier was found for each group of mice (see rectangles in Figure 6). These outliers were removed from the respective groups for the ANOVA design. The ANOVA exhibited no significant effect between the factors Group and Band ($p > 0.05$), although the difference in the frontoparietal absolute EEG power (density) between the active and the passive condition (active minus passive) was lower in the PDAPP group when compared to the WT group. This finding was in line with the results of the main analysis based on individual frequencies.

Amplitude of absolute EEG spectral power density in Wild Type vs PDAPP mice

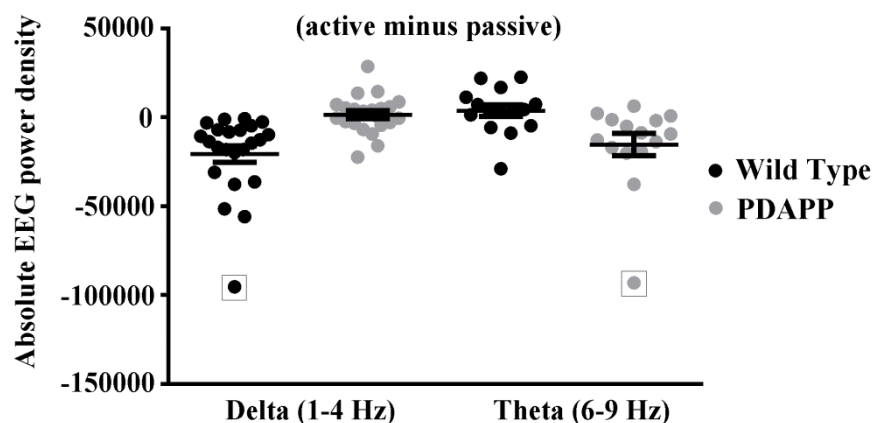


Figure 18. Individual values of the difference of the absolute EEG power (density) between the active and the passive condition (active minus passive) at the two fixed frequency bands (delta and theta) for the WT and PDAPP mice. The outlier values according to Grubb's test ($p < 0.05$) indicated by the squares were excluded from the subsequent statistical analysis. No significant ANOVA interaction between the factors Group (WT, PDAPP) and Frequency (delta, theta) was found ($p > 0.05$; covariate: recording Unit).

Experimental part

These control results using the fixed delta (1-4 Hz) and theta (6-9 Hz) bands globally cross-validated those obtained with the individual frequency analysis

6.4 Discussion

It is well-known that wakeful resting state EEG rhythms in humans reflect the fluctuation of cortical arousal and vigilance in quiet wakefulness. These rhythms are typically investigated through a simple clinical setting of EEG recording. In this setting, EEG data are collected while subjects lay in the wakeful resting state condition for few minutes with eyes closed (i.e. passive condition) and, then, for few minutes with eyes open (i.e. active condition). EEG rhythms recorded in the two conditions are usually compared, and results would reflect cortical neural synchronization and desynchronization related to the mentioned fluctuation of cortical arousal. Specifically, the higher the EEG power at a given frequency, the higher the cortical neural synchronization at that frequency (Babiloni et al., 2013). In the present study, such protocol of clinical EEG research was back-translated to a preclinical setting in freely behaving old PDAPP mice (i.e. human APP Indiana V717F mutated gene, Games et al., 1995). The PDAPP mouse strain was chosen as it models some aspects of AD such as extracellular dystrophic neurites, A β deposition, gliosis, and impaired density of dendritic and synaptic function in brain structures in the hippocampus and cerebral cortex (see relevant bibliographic references quoted in the Introduction of this article). In the present exploratory study, we hypothesized that compared with old WT mice, PDAPP mouse peers might exhibit abnormal ongoing EEG rhythms in behavioral passive (i.e. quiet wakefulness with immobility or small displacement of the head, forelimbs, and trunk) vs. active (i.e. exploration of the cage) conditions as a reflection of an altered regulation of the neurophysiological mechanisms underpinning cortical arousal.

From a descriptive point of view, the present findings showed that both groups of old WT and PDAPP mice displayed a reduction in the frontoparietal EEG power in the extended delta range (i.e. 1-6 Hz) during the active compared with the passive condition. Furthermore, both groups unveiled that EEG power in the extended theta range (i.e. 6.5-10 Hz) was greater during the active than the passive condition. It is speculated that these features of frontoparietal EEG rhythms in the wakefulness may reflect the changes in cortical arousal during different behavioral and vigilance states of the mice. These results are in line with previous evidence of a reference study using 85 WT mice [59] and other findings in the literature (Bland, 1986, Orzeł-Gryglewska et al., 2014, Vyazovskiy et al., 2005). They reported an amplitude increase of brain theta rhythms during active (e.g. waking) over passive conditions (Bland, 1986, Orzeł-Gryglewska et al., 2014, Vyazovskiy et al., 2005).

From a statistical point of view, the present study showed some significant differences in the frontoparietal EEG frequency and power between the WT and PDAPP groups of mice. Noteworthy, these results were obtained with an analysis of EEG rhythms on individual basis. In a given mouse, the IDF peak was defined as the frequency bin showing the highest amplitude of the frontoparietal EEG power between 1 and 6 Hz (extended delta frequency range) during the passive state. In the same vein, the ITF peak was defined as the frequency bin showing the highest amplitude of the frontoparietal EEG power between 6.5 and 10 Hz

Experimental part

(extended theta frequency range) during the exploratory active state. A similar methodological approach has previously shown abnormalities in the dominant EEG frequencies in patients with dementia due to AD (Moretti et al., 2014). In the present study, results of that procedure showed that compared with the WT mice, the PDAPP mice unveiled higher frequency of the IDF peak during the behavioral passive state and lower frequency of the ITF peak during the exploratory active state. Concerning the amplitude of these EEG rhythms, the WT -but not the PDAPP- group exhibited significant differences in the frontoparietal EEG power of both IDF and ITF peaks between the two behavioral states. These results suggest that in the wakefulness, PDAPP mice are characterized by minimal changes in those frontoparietal EEG rhythms as a reflection of a poor transition in the brain arousal.

What is the neurophysiological meaning and the translational clinical value of the present findings? Previous EEG studies in healthy humans have shown that an eyes-closed relaxed wakefulness (i.e. equivalent to the present passive condition in the mice) is associated with dominant posterior alpha rhythms (8-12 Hz). In that behavioral condition, these rhythms possibly reflect a low cortical arousal and vigilance, regulated by reciprocal thalamic-cortical interactions and brainstem ascending cholinergic and monoaminergic inputs (Klimesch et al., 1997, Klimesch, 1999). Of note, alpha rhythms decrease in power during eyes opening and cognitive-motor demands (i.e. the active condition), reflecting an increased cortical arousal and vigilance (Klimesch et al., 1997, Klimesch, 1999, Van Winsum et al., 1984, Sergeant et al., 1987, Babiloni et al., 1999, Pfurtscheller G, Klimesch, 1992). In AD patients, eyes opening as a moderately active state is related to a weaker decrease in the posterior alpha rhythms compared to what observed in matched healthy subjects (Claus et al., 1999, Bennys et al., 2001, Lehmann et al., 2007, Bonanni et al., 2008, Ommundsen et al., 2011).

Keeping in mind the above evidence in humans, clear interspecies differences of cortical ongoing EEG rhythms appear. Both groups of WT and PDAPP mice showed neither dominant alpha rhythms (8-12 Hz) during the passive condition nor the power reduction of these rhythms during the active condition. Rather, the active condition in the WT mice was related to a decrease of the delta rhythms and an increase of the theta rhythms as a possible cortical up regulation of the arousing thalamic-cortical brainstem ascending inputs (Del Percio et al., 2017). In the PDAPP mice, such state-related modulation of the delta and theta rhythms was less straightforward.

Despite the mentioned inter-species differences in the frequency bands and EEG power modulation, there is an intriguing back-translational similarity. Compared to the corresponding control groups, both the mouse model of AD and AD patients would show less reactivity of cortical on-going EEG rhythms < 10-12 Hz to activating events in the wakefulness (the active condition). A fascinating speculation is that AD processes might impair the fine-tuning of the cortical arousal in the wakefulness and would induce a tonic cerebral over-excitation that could reduce the selectivity in the information processing. This over-excitation could not be necessarily associated with epileptic-like EEG activity (note that the EEG data of the present spectral analysis were not affected by that activity). In this speculation line, it has been shown that the incidence of convulsive seizures is 10 times higher in AD patients than the age-matched general population (Horváth et al., 2016).

Experimental part

Furthermore, epileptic-like EEG activities have been described in both AD patients (Magaki et al., 2046) and transgenic mice (Minkeviciene et al., 2009). Concerning its pathophysiological substrate, the effect of Abeta1-42 on the neural over-excitation and epilepsy is still open as one recent study in transgenic mouse models of AD demonstrated that cortical spiking increased when the transgene was active and disappeared over a couple of weeks when it was turned off, despite persisting amyloid plaques (Born et al., 2014).

The present analysis of the individual EEG frequencies complements the traditional analysis with the fixed EEG frequency bands. At the present stage of the research, it is still unclear whether IDR and ITR peaks provide better measures than fixed EEG bands. As methodological critical aspects, IDR and ITR peaks were selected in broad bands of 1–6 Hz and 6.5-10 Hz, respectively. In contrast, narrower fixed frequency bands are typically used in rodents (Ziyatdinova et al, 2011). The fixed delta band is usually selected in the 1-4 Hz range. Furthermore, the fixed theta band is frequently designated in the 4-6 Hz and 7-11 Hz ranges when animals are immobile and in-motion, respectively. In this theoretical framework, the present choice of extended 1–6 Hz and 6.5-10 Hz bands was based on a preliminary analysis of the results. Indeed, individual values of the IDF and ITF peaks were observed in the 1-6 Hz (mean of 3-4 Hz) and the 6.5-10 Hz range (mean of 6.5-7 Hz) in all mice of the present experiments (Figure 2). In the same line, the grand average of the EEG power spectra “active minus passive condition” pointed to a downward drop from 1 to 6 Hz and an upward drop from 6.5 to 10 Hz (Figure 1).

For cross-validation purposes, we performed a control analysis using two fixed frequency bands at 1-4 (delta) and 6-9 Hz (theta). The results globally cross-validated those obtained with the individual frequency analysis. As a unique exception, the control results showed that the WT group exhibited substantial differences in the frontoparietal EEG power at the fixed delta but not theta band between the two behavioral states. It can be speculated that the individual frequency analysis is able to reveal these differences not only in delta but also in theta dominant rhythms as it can take into account the variability of that theta reactivity during the active condition. Indeed, some WT mice showed a maximum increase in the EEG power from 9 to 10.5 Hz in that condition, namely beyond the standard 1-9 Hz range of the fixed frequency band.

In the interpretation of the present preliminary findings, some important methodological limitations should be taken into account. Firstly, the different EEG frequency pattern between mice and humans might be at least in part due to the effects of head volume conduction in the cortical EEG recordings in mice. Indeed, mice typically show an ample theta oscillatory activity in the hippocampus during exploratory movements. Due to the small dimension of the mouse brain, that theta oscillatory activity could be volume conducted to near electrodes located in the parietal cortex (Kahana et al., 2001, Vinogradova, 1995). Future studies should cross-validate this effect with very near bipolar recording contacts in the parietal cortex.

Secondly, the rating of the mouse behavior (active, passive, etc.) was done after a very careful preliminary phase of harmonization and standardization of the procedure in the three preclinical recording Units involved in the present study (e.g. Lundbeck, UNIVR, and MNI). Here an indirect sign of the success of that phase is the fact that the main results did not change using the recording Unit as a covariate. Furthermore, a relatively

Experimental part

low variance of the EEG results in the present preclinical recording Units has been shown elsewhere with the same methodology of the current study (Del Percio et al., 2017). However, we acknowledge the intrinsic limitations of the behavioral rating based mainly on visual inspection. One might argue that behavioral data analysis did not account for the velocity and extension of the exploratory movements or other quantitative indexes of that exploration. As a result, the difference in the EEG rhythms between the WT and PDAPP groups might be at least in part due to some difference between the two groups in the quantitative features of the movements during the active condition. Indeed, previous studies have reported that hippocampal theta oscillations might code information on motor behavior (Shin and Talnov, 2001). Furthermore, different patterns of hippocampal theta rhythms code various types of locomotion in animals (Arnolds et al., 1984, Gengler et al., 2005, Sinnamon, 2005). Therefore, future studies should cross-validate the present results with a rigorous quantitative control of the exploratory movements.

Thirdly, the present study has been carried out on a relatively small number of WT (N=15) and PDAPP (N=23) mice. Future studies should cross-validate the present results in a larger cohort of animals.

Fourthly, the present experimental procedure allows only a partial back-translation from AD patients to mice in the understanding of the neurophysiological mechanisms underlying to the modulation of global cortical arousal. In human resting state EEG rhythms recorded with eyes-closed and –open, cortical arousal is mostly due to visuo-spatial processes. In the EEG rhythms recorded in the present passive and active conditions, cortical arousal in mice was mostly due to both visuo-spatial and somatomotor processes.

As a final remark, it should be stressed that the present experimental procedure cannot substitute the other traditional preclinical neurophysiological procedures in mice such the evaluation of wake-cycle sleep, the application of stressful or anxiety situations, and the use of virtual reality techniques to study the EEG correlates of exploration and spatial navigation. On one hand, each of the mentioned procedures offers attractive opportunities to the neurophysiology research. On the other hand, there are some limitations in the back-translation for all of them. For example, sleep studies in patients with AD are generally considered as too time consuming. They typically require a night for the patient to familiarize with continuous EEG sleep recordings and avoid any spurious emotional contamination. Reactions to stress and anxiety testing are biased by the individual susceptibility and behavioral state. These reactions appear very variable between mice and humans and even in the individuals belonging to the same species. Finally, virtual reality may be useful to evaluate the spatial learning and integration processing in both species, but it requires a preliminary long training that might be challenging for patients with impaired cognition. Furthermore, it needs personnel with a specific high degree of specialization for those technological applications in mice.

7 Study IV: Ongoing electroencephalographic rhythms related to cortical arousal in transgenic TASTPM mice

7.1 Introduction

Alzheimer's disease (AD) is the most prevalent progressive neurodegenerative dementing disorder across aging (Braak and Braak, 1995; Bastos Leite et al., 2004; Glodzik-Sobanska et al., 2005). In the new diagnostic criteria (Dubois et al., 2014), AD can be diagnosed before any cognitive or behavioral symptoms (preclinical stage) and in the mild cognitive impairment (MCI, prodromal stage) and dementia stage (ADD).

Among the topographic markers for tracking the AD progression, a promising variable derives from ongoing cortical electroencephalographic (EEG) rhythms in wakefulness (Ponomareva et al., 2003, Jeong, 2004). Those EEG rhythms might be generated by the spatial summation of post-synaptic potentials, which might be provoked by the temporal synchronization/desynchronization at given frequencies of a large number of cortical pyramidal neurons by neurotransmitters released by cortical and subcortical (i.e. thalamic, basal forebrain, brainstem) neurons (Niedermayer and Lopes da Silva, 2005). In wakefulness, this temporal synchronization/desynchronization depends on the reciprocal interactions between cortical pyramidal neurons and ascending cholinergic, dopaminergic, noradrenergic, and serotonergic neuromodulatory systems (Niedermayer and Lopes da Silva, 2005). In this framework, spatial selectivity and frequency contents of EEG rhythms might be affected by cortical and thalamic GABAergic interneurons (Niedermayer and Lopes da Silva, 2005).

Two main conditions are typically used to probe these neurophysiological synchronization and desynchronization mechanisms in a clinical setting in humans. In a “passive” behavioral condition, the subject remains in relaxed wakefulness (resting state) with eyes closed for a few minutes. This mode is contrasted with a more “active” behavioral condition in which the subject remains in relaxed wakefulness with eyes open for a few minutes (monitoring the surrounding environment). In the resting state eyes-closed condition, EEG rhythms show the highest power (density) at about 8 and 12 Hz in posterior cortical areas, the so-called dominant alpha rhythms, which originate from the inhibitory mode of visual, spatial, auditory, and somatomotor areas (Pfurtscheller and Lopes da Silva, 1999). The higher the alpha power, the lower the cortical arousal, the lower the vigilance. After eyes opening, alpha rhythms exhibit a power reduction (i.e. desynchronization) as a reflection of increased cortical arousal related to augmented vigilance (Pfurtscheller and Lopes da Silva, 1999).

Previous studies have reported differences in absolute and relative EEG power in normal elderly (Nold) subjects compared with AD patients in the clinical setting of resting state eyes-closed condition. With respect to Nold subjects, AD patients with dementia showed a higher power of widespread delta (<4 Hz) and/or theta (4-7 Hz) rhythms, associated with lower power of posterior alpha (8-12 Hz) and beta (13-20 Hz) rhythms

Experimental part

(Dierks et al., 2000, Huang et al., 2000, Ponomareva et al., 2003, Jeong, 2004, Babiloni et al., 2006, 2007, 2009).

Absolute and relative resting-state EEG power exhibited differences between AD and Nold subjects also in the “reactivity” from the eyes-closed to the eyes-open condition. Compared with Nold subjects, AD patients with dementia and MCI showed a lower “reactivity” of posterior alpha rhythms, namely a reduced difference between the EEG power during the eyes-open and -closed condition (Stam et al., 1996, Stevens and Kircher, 1998, van der Hiele et al., 2007, Babiloni et al., 2010). This poor reactivity of alpha power predicted a deterioration of higher functions in subjects with cognitive decline (van der Hiele et al., 2008). This predictive value of that poor reactivity was confirmed by magnetoencephalographic evidence (Berendse et al., 2000, Kurimoto et al., 2008).

An open issue is whether those resting state EEG topographic markers can be back-translated to preclinical AD research and drug discovery in rodents. At least two requirements should be necessary for that use.

The first requirement might be the demonstration of consistent changes in ongoing EEG rhythms during active and passive conditions in wakefulness not only in humans but also in mice. This requirement seems to be met globally by the neurophysiological mechanisms generating delta (< 4 Hz) to beta (> 14 Hz) rhythms, despite some inter-species differences.

In both humans and rodents, increased vigilance and focused attention were associated with enhanced power of high-voltage phasic, theta rhythms (4-8 Hz) and low-voltage beta (14–30 Hz) rhythms as opposed to a drowsiness low-vigilance condition characterized by high-voltage tonic and widespread delta and theta (< 8 Hz) rhythms (Marshall and Born, 2002, Vyazovskiy, 2005). In an anxiety state, increased vigilance was related to increased power of low-voltage beta rhythms in both humans and rodents (Sviderskaia et al., 2001, Oathes et al., 2008). Cholinergic and monoaminergic drugs caused similar effects on ongoing EEG rhythms in both humans and rodents (Dimpfel et al., 1992, Coenen and Van Luijtelaar, 2003, Dimpfel, 2005).

Neurophysiological features of theta rhythms are of special interest for back-translational purposes. In wakefulness, rodents show ample and regular brain theta rhythms (6-9 Hz) during exploratory movements, with a maximum amplitude in the hippocampus and related temporal lobe structures (Buzsáki et al., 1983). Noteworthy, these theta rhythms are volume conducted to the near dorsal surfaces in the small brain of rodents. In humans, theta rhythms increase in amplitude in the hippocampus, frontal, and midline cortical regions during tasks requiring attention and memory (Jacobs, 2014). Hippocampal theta rhythms are driven by GABAergic and cholinergic inputs received from the medial septum playing the role of the pacemaker of that oscillatory activity (Brown et al., 2012).

The second requirement for an ideal back-translation of EEG rhythms to preclinical research might be the existence of valid rodent models of AD showing abnormalities in those neurophysiological biomarkers. In the last years, several transgenic mouse models with single, double, and triple mutations have been developed (Webster et al., 2014). These mutations typically affect the gene regulating amyloid precursor protein (APP)

Experimental part

and/or that of presenilin 1 (PS1) to induce an abnormal accumulation of A β 1-42 in the brain, one of the pathophysiological markers of AD.

A wealth of studies has documented an abnormal brain electrical activity in the APP- and PS1-mutated transgenic models for AD (Wang et al., 2002, Lalonde et al., 2005, Palop et al., 2007, Westmark et al., 2008, Minkeviciene et al., 2009, Ziyatdinova et al., 2011, Sanchez et al., 2012, Verret et al., 2013, Corbett et al., 2013, Schneider et al., 2014). These studies focused on hyper-synchronous and epileptiform neural activities and EEG rhythms that characterized these animals as compared to their littermates. Different mouse models differ in the APP and/or PS1 mutations they express, in the co-expressed transgenes, and in the promoters used to drive expression (Born et al., 2014). Similarly, neuronal network imbalances and seizures have recently been implicated in the development of cognitive deficit in a subset of AD patients (Rabinowicz et al., 2000, Palop and Mucke, 2009). In those mice, EEG rhythms were investigated. In the European Innovative Medicine Initiative (IMI) project shortly entitled “PharmaCog” (Grant Agreement n°115009, www.pharmacog.org), to this purpose, two convenient and back-translational behavioral conditions of EEG recordings for mice were studied. The first condition was an equivalent of the “passive” condition commonly used in clinical settings, namely a relaxed wakefulness with no or minimal animal movements in the cage (no sleep). The second condition was a surrogate of the “active” condition in clinical settings, namely the occurrence of spontaneous exploratory movements in the cage.

In detail, the preclinical EEG studies of the PharmaCog project were carried out in C57 mice (for the sake of simplicity, we call this strain as wild-type, WT) as a control group and transgenic PDAPP and TASTPM mice as models of AD-like A β aggregation in the brain. PDAPP mice are obtained by the mutation of human APP while TASTPM mice by a double mutation in APP KM670/671NL (Swedish) and PSEN1 M146V (Howlett et al., 2004, 2008). In the EEG study performed in WT mice, ongoing EEG rhythms showed differences in the passive vs. the active behavioral condition. Compared with the former, the latter condition showed decreased EEG power (density) at delta rhythms (1-2 Hz) and increased EEG power at theta rhythms (6-10 Hz, Del Percio et al., 2017a). Furthermore, the passive condition exhibited delta rhythms greater in amplitude in an older sub-group of WT mice (i.e. 20-24 months) compared with the middle-aged (i.e. 12-15 months) and the young adult group (i.e. 4.5-6 months, Del Percio et al., 2017a). Finally, the active condition was related to theta rhythms with maximum theta power at 6-8 Hz in the old group and 8-10 Hz in the young group (Del Percio et al., 2017).

In the PharmaCog EEG studies, the mentioned ongoing EEG rhythms showed abnormalities in PDAPP mice (e.g. mutation of human APP, Del Percio et al., 2017b). When likened to the WT group, the PDAPP one exhibited higher frequency of the delta rhythms in the 1-4 Hz range during the passive condition and lower frequency of theta rhythms in the 5-12 Hz range during the active condition. Furthermore, the PDAPP group showed no changes in the EEG power during the active compared with the passive condition (Del Percio et al., 2017b).

Experimental part

The present article reports the results of a PharmaCog exploratory EEG study carried out in the TASTPM mice. The overexpression of human mutant forms of APP and PS1 in TASTPM mice leads to amyloidosis beginning at 3-4 months in the cerebral cortex, with mature plaques forming by 6-8 months, and eventually severe A β plaque deposition by 10 months (Howlett et al., 20004, 2008). TASTPM mice show both age-related neuropathology and early and progressive cognitive impairment, thus reproducing features of the pathophysiological and clinical presentation of familial AD (Howlett et al., 20004, 2008). In this study, we used the same experimental procedures of the reference PharmaCog investigations (Del Percio et al., 2017a,b) to provide a proof of the concept that ongoing EEG rhythms accompanying passive and active behavioral conditions are altered in the TASTPM mice when compared to the WT mice as a control group. In the passive and active condition, the mice were freely behaving, so we termed the EEG “ongoing” as opposed to the “event-related”. In “event-related” procedures, EEG activity is recorded during some standardized sensory or motor events repeated many times, and recorded data are analyzed off-line in time (e.g. event-related potentials) and frequency (e.g. event-related EEG oscillations) domains.

7.2 Methods

7.2.1 Animals

In the present study, 33 TASTPM mice (14 females; mean age: 14.9 months \pm 0.8 standard error, SE; range of age: 5-24 months) and 73 matched C57 WT mice were included (19 females; mean age: 15 months \pm 0.7 SE; range of age: 4.5-24 months) were used. The data were collected from 1 Belgian center (Janssen Research and Development; 9 TASTPM and 12 WT mice), 1 Danish center (H. Lundbeck A/S; 10 TASTPM and 22 WT mice), and 2 Italian centers (Mario Negri Institute for Pharmacological Research of Milan, 9 TASTPM and 23 WT mice; University of Verona, 5 TASTPM and 16 WT mice). Of note, the WT group was a subset of that used in a previous study (N = 85), selected to match age and gender of the TASTPM mice (Del Percio et al., 2017a).

Procedures involving mice and their care were conducted in line with the institutions' guidelines, in strict conformity with national and international laws and policies (EEC Council Directive 86/609, OJ L 358, 1, 12 December 1987; U.S. National Research Council, 1996, Guide for the Care and Use of Laboratory Animals). The respect of these guidelines was carefully controlled by the members of WP8 of the IMI PharmaCog project, devoted to ethics of research.

The independent t-test was used to compare the age of the two mouse groups (i.e. TASTPM and WT; significance threshold: $p < 0.05$, two tailed). Furthermore, the Fisher exact test was used to compare the sex of the two mouse groups, and no significant difference was found (age: $p = 0.9$; sex: $p = 0.1$).

	Center	N	Sex (F/M)	Age
WT	Janssen	12	5F/7M	12 months
	Lundbeck	22	14F/8M	15, 24 months

Experimental part

TASTPM	MNI	23	23M	6, 12, 14, 24 months
	UNIVR	16	16M	5, 12, 20 months
	Janssen	9	5F/4M	12 months
	Lundbeck	9	9F	15 months
	MNI	10	10M	14, 24 months
	UNIVR	5	5M	5, 20 months

Table 13. Features of the C57 mice (for the sake of simplicity, wild-type, WT) for the following electroencephalographic (EEG) recording centers: Janssen Research and Development (Belgium), H. Lundbeck A/S (Denmark), Mario Negri Institute (Italy), and University of Verona (UNIVR, Italy). Legend: F= female; M= male

7.2.2 Pre-Surgery (3 weeks)

For at least 3 weeks prior to surgery, the mice were acclimated. They were housed at a constant temperature (18-22°C) and relative humidity (55-65%) under a standard 12-h light/dark cycle (light-on hemi-cycle typically spanning from 6:00 a.m. to 6:00 p.m.) with free access to food and water. After surgery, the animals were housed in individual cages at the same conditions (typical cage size was 45 cm [length] × 24 cm [width] × 20 cm [height]). Light intensity was 90–110 lx in the room, 60 lx in the cage during the light period, and less than 1 lx during the dark period. Gentle handling for about 5-10 minutes was applied daily to reduce the potential stress due to housing and experimenters. Such stress was evaluated continuously along all the duration of the experiments by veterinary experts of each centre. These experts tested animal muscle relaxation and standard behavioral indices of stress in freely behaving mice (i.e. preservation of exploratory movements in the cage, preservation of instinctual activities such as drinking and eating, and body weight across pre- and post-surgical days).

7.2.3 Surgery

EEG electrodes were implanted after an anesthesia performed by inhalation of isoflurane (5%) or Equithesin, pentobarbital (1%), and chloral hydrate (+4%) 3.5 ml/kg). The mice were also treated with systemic analgesics and antibiotics in line with local guidelines on surgical care.

The AP and ML stereotaxic coordinates of the electrodes from bregma were reported in Table 2 (standard mouse brain atlas; Franklin and Paxinos, 1997).

For the MNI and Lundbeck preclinical Units, a tethered system for EEG recordings was used. Stainless steel insulated surface epidural electrodes were used as exploring contacts at the frontal and parietal sites (model E363/20 with a diameter of 0.56 mm (0.022"); PlasticsOne, VA, US). One depth electrode as a reference contact was implanted in the cerebellum; another depth electrode as a ground contact was implanted in the temporal bone without the removal of the muscles (model E363/1 with a diameter of 0.280 mm (0.011"), PlasticsOne, VA, US). The electrodes were fixed to the skull with dental cement. EEG signals were transmitted through a plastic electrode pedestal and a connector cable to the amplifier with a maximal cable length of 50 cm.

Experimental part

For the Janssen and UNIVR preclinical Units, a telemetric system for EEG recordings was used. Mice were instrumented with a radiotelemetry probe F20-EET (DSI, Minnesota, USA) containing sensors for the recording of the EEG, electromyogram (EMG), body temperature, and locomotion. The probe was implanted in the peritoneal cavity with 1 mL of sterile physiological saline to prevent desiccation. The four leads were subcutaneously tunneled from the peritoneal cavity towards a 1-cm head skin incision. Bipolar EEG recordings were performed by two miniature stainless-steel screw electrodes. These EEG electrodes were epidurally implanted on parietal and frontal cortical areas and fixed to the skull with acrylic dental cement. Bipolar EMG recordings were performed by two other electrodes placed in the dorsal neck muscles. These EEG and EMG electrodes (EEG and EMG) had an outer diameter of 0.3 mm.

The stereotaxic coordinates of that electrode montages in the four preclinical Units are reported in Table 14.

Electrode	Stereotaxic coordinates
Reference	AP:-6, ML:+2
Ground	AP:-2, ML:+2.5
Frontal	AP:+2.8, ML:-0.5
Parietal	AP:-2, ML:+2

Table 14. Stereotaxic coordinates for the implantation of EEG electrodes in the mouse brain according to a standard stereotaxic atlas (i.e. *The Mouse Brain coordinates* by Franklin and Paxinos, 1997). The frontal and parietal electrodes were used in all preclinical Units (i.e. Mario Negri Institute, Lundbeck, University of Verona, and Janssen). The reference and ground electrodes were used for the monopolar electrode montage in the Mario Negri Institute and Lundbeck preclinical Units.

7.2.4 Quiet Post-surgery period (1 week)

The mice were treated with systemic analgesics and antibiotics, during a standard post-surgical period of one week. The week immediately after surgery, animals underwent a period of recovery with neither handling treatment nor EEG recordings.

7.2.5 Handling post-surgery period (1 week)

In the week after the quiet post-surgery period, EEG was not recorded but gentle handling was applied for about 2-5 minutes daily and the animals were gently plugged and unplugged several times (for wired systems only) across that week to familiarize with the procedure.

7.2.6 Experimental day

EEG experiments were performed during both the dark and light phases. During the EEG recording period, the mice received no handling treatment. EEG recordings started after the second hour of the beginning of light or darkness. Sampling frequency of EEG recordings was performed at least 250 Hz with anti-aliasing bandpass analog filters (Janssen: 250 Hz, Lundbeck: 1000 Hz, MNI: 1600 Hz, UNIVR: 500 Hz; 0.16 Hz-100 Hz passband filter). No notch filter was used.

Experimental part

7.2.7 Determination of the behavioral mode

An important step of the data analysis was the classification of the animal behavior during the EEG recordings. The behavioral classification was performed by independent experts (personnel enrolled by each preclinical Unit). These experts underwent to a preliminary phase of training for the harmonization of procedures across the four recording Units. They performed in blind this exercise and were not involved in the EEG data analysis. The behavioral classification was based on visual inspection of the mouse behavior in the videos obtained during the EEG recordings. In each preclinical Unit, the rater classified video recording epochs lasting 10 s in each video epoch. The animal behavior was classified into “active” and “passive” conditions based on the following definitions:

(1) Active behavior (condition). Animals perform overt exploratory movements in the cage for most of the given epoch. The exploratory movements are characterized by ample displacements of body parts such as trunk, head, and/or forelimbs (when videos were available). They have not to be confounded with instinctual activities (*vide infra*).

(2) Passive behavior (condition). Animals perform no or small movements of the trunk, head, and/or forelimbs with a maximal total duration of that behavior of 20 seconds. The maximal immobility duration lasts 10 seconds. These criteria are expected to minimize the risk that “passive condition” be misclassified as sleep and viceversa.

In the UNIVR and Janssen Unit, the behavioral classification was also corroborated by additional variables such as body temperature, electromyographic (EMG) activity recorded from neck muscles, and instrumental markers of the movement (i.e. actigraphy). These variables (and EEG activity) were used as an input to DSI software automatic classification (Data Sciences International, DSI, Minnesota, USA). The DSI software classified the epochs in some behavioral classes corresponding to the above passive behavior, active behavior, and sleep. With this procedure, epochs whose classification as a passive state was not considered reliable enough were discarded from the following analysis (less than 10%).

Particular attention was devoted to distinguishing the “active” and “passive” conditions as compared to other states based on the following definitions:

(1) Behavioral sleep state. Each epoch of the sleep state, as behaviorally defined, corresponds to immobility of the animals for the entire period of observation (when videos were available) and during longer periods of immobility lasting several minutes with signs of muscle relaxation. As mentioned above, particular attention is devoted to avoiding misinterpretation of the passive condition and sleep state. The sleep condition is also denoted by lowest values of body temperature and EMG activity compared to the other behavioral states.

(2) Instinctual behavior. This behavioral class is detected when the animal shows movements such as cleaning, drinking, eating, mating, etc. for most of the period (when videos were available). The instinctual condition is also denoted by increased body temperature and EMG activity compared to the passive behavior or sleep. As mentioned above, special attention is paid not to include these epochs in the active behavior epochs.

Experimental part

(3) Undefined. Each epoch classified as undefined shows a mix of the other behavioral classes or lack of clarity about the behavioral situation of the animal. Such epochs are excluded from the analysis.

The inter-reliability of the behavioral rating (e.g. passive, active) was tested on the classifications performed by two experimenters authoring this article (A.F. and S.L.). The concordance of the rating was substantially higher than 80%.

According to PharmaCog guidelines, the experiment should not use EEG data to classify the epochs to avoid circular logic. Based on the above analysis of behavioral states, the first 5 minutes of artifact-free EEG epochs classified as active condition were selected for the EEG data analysis. The same procedure of selection was followed by the epochs of the passive condition.

7.2.8 EEG data analysis

The behavioral epochs of the active and passive state were segmented off-line in consecutive epochs lasting 2 s each. The 2-s EEG epochs with muscle, EEG, electrocardiographic (EKG), instrumental or other artifacts (no epileptic-like EEG activity) were excluded from the centralized EEG data analysis. In the WT mice group, the rejected EEG epochs were 1.19% (± 0.57 , SEM, standard error mean) for the active state and 1.90% (± 0.69 SEM) for the passive state. In the TASTPM mice group, they were 7.77% (± 0.41 , SEM) for the active state and 11.12% (± 2.82 SEM) for the passive state.

In the Janssen and UNIVR preclinical units, the EEG data were recorded with a bipolar electrode montage providing frontoparietal EEG signals. In the Lundbeck and MNI preclinical units, the EEG data were recorded with a monopolar electrode montage providing frontal and parietal EEG signals, separately. To uniform all montages for the group data analysis, EEG data of the Lundbeck and MNI preclinical Units were re-referenced to obtain bipolar frontoparietal EEG signals. The re-referencing to that bipolar electrode montage was computed offline with a mathematical procedure consisting in the subtraction of the signal recorded by the monopolar parietal channel from the signal recorded by the frontal monopolar channel. The bipolar frontoparietal EEG signals were then inspected for the artefact rejection and used as an input for the subsequent statistical analysis.

7.2.9 Spectral analysis of the EEG data

The artifact-free EEG epochs of the active and passive state were used as an input for the analysis of EEG power (density). This analysis was performed by a standard (Matlab; MathWorks, Natick, Massachusetts USA) FFT algorithm using Welch technique and Hanning windowing (no overlap of the time windows) function with 1-Hz frequency resolution. A normalization of the results of FFT analysis was obtained by computing the ratio between EEG power at each frequency bin with the EEG power value averaged across all frequency bins (0-100 Hz). After this normalization, the EEG power lost the original physical dimension and was represented by an arbitrary unit scale, in which the value of “1” was equal to the power value averaged across all frequency bins. The following EEG frequency bands were selected for the statistical comparisons: 1-2 Hz, 3-4 Hz, 5-6

Experimental part

Hz, 7-8 Hz, 9-10 Hz, 11-12 Hz, 13-20 Hz, and 21-30 Hz. These narrow bands were selected to avoid any *a priori* assumption on the composition of EEG frequency bands in mice.

7.2.10 Statistical analysis

Three statistical designs, performed by Statistica® 10.0 packages, were executed to address the main scientific issues of the present study. In all analyses, the significance threshold was set at $p < 0.05$. In all statistical sessions, we used the preclinical Unit as a covariate (e.g. Lundbeck, Janssen, UNIVR, and MNI) to account for the multi-centric nature of this study.

The first session tested the control hypothesis that the 73 WT mice of the present study were characterized by the same changes in EEG rhythms in the active vs. the passive condition obtained in a previous reference study carried out in 85 WT mice (Del Percio et al., 2017a). Noteworthy, those 73 WT mice were sampled from the 85 WT mice to match the demographic features of the present TASTPM mice.

To test this hypothesis, an analysis of variance (ANOVA) considered the normalized EEG power as a dependent variable. The ANOVA factors were Condition (passive, active) and Band (1-2 Hz, 3-4 Hz, 5-6 Hz, 7-8 Hz, 9-10 Hz, 11-12 Hz, 13-20 Hz, and 21-30 Hz). The hypothesis would be confirmed by the following two statistical results: (1) a significant ANOVA interaction effect between the two factors ($p < 0.05$); (2) a post-hoc test (Duncan test) indicating significant differences in the normalized EEG power between the active and passive condition at the different frequency bands.

The second session tested the first main scientific issue that the TASTPM mice could show differences in EEG power between the active and the passive condition, in line with what observed in the WT mice. To test this hypothesis, an ANOVA used the normalized EEG power as a dependent variable. The ANOVA factors were Condition (passive, active) and Band (as above). The working hypothesis would be confirmed by the following two statistical results: (1) a significant ANOVA interaction effect between the two factors ($p < 0.05$); (2) a post-hoc test (as above) indicating significant differences in the normalized EEG power between the active and passive condition at the different frequency bands.

The third session tested the working hypothesis that, compared with the WT mice, the TASTPM mice might show diminished differences in EEG power between the active and the passive state, as an index of a reduced tuning of cortical arousal and information processing during exploratory movements. To test this hypothesis, the ANOVA used the difference in the normalized EEG power between the active and the passive condition (active minus passive) as a dependent variable. We used the same procedure in previous PharmaCog studies in WT [49] and PDAPP [50] mice as well as AD patients [74]. The ANOVA factors were Genotype (WT, TASTPM) and Band (as above). The hypothesis would have been confirmed by: (1) significant ANOVA interaction effect including the factors Genotype and Band ($p < 0.05$); (2) a post hoc test (as above) indicating a significant reduction in the normalized EEG power (active minus passive) in the TASTPM group with reference to the WT group ($p < 0.05$ one-tailed).

Experimental part

7.2.11 Control analysis

We performed a control analysis session selecting a subgroup of the WT and TASTPM mice, matched by age and gender. The sample was of 32 mice per group (18 males and 14 females), with a mean age of 14.7 (± 0.8) and 14.8 (± 0.8) months for WT and TASTPM mice, respectively. The working hypothesis was that, also with these matched subgroups, compared with the WT mice, the TASTPM mice might show differences in EEG power, possibly reflecting the effect of brain deposition of amyloid induced by the genetic mutations. To test this hypothesis, we computed the difference in the normalized EEG power between the active and the passive conditions (active minus passive). The ANOVA used this difference as a dependent variable. The ANOVA factors were Genotype (WT, TASTPM) and Band (1-2 Hz, 3-4 Hz, 5-6 Hz, 7-8 Hz, 9-10 Hz, 11-12 Hz, 13-20 Hz, 21-30 Hz). The hypothesis would be confirmed by: (1) significant ANOVA interaction effect including the factor Genotype ($p < 0.05$); (2) a post hoc test (as above) indicating significant differences in the normalized EEG power (active minus passive) in the TASTPM group when compared to the WT group.

7.3 Results

7.3.1 Normalized EEG power density during active and passive conditions in WT and TASTPM mice

Figure 19 shows the grand average of the normalized EEG power spectra for the active and passive conditions in the WT ($N=73$; Fig. 1, left) and TASTPM mice ($N=33$; Fig. 1, right). These spectra exhibited an EEG power peak at 2-4 Hz (i.e. delta range) that was higher in the passive condition compared to the active one. An additional EEG power peak at 6-8 Hz (i.e. theta range) was greater in the active condition compared to the passive one. Concerning the difference in the EEG power between the active and passive conditions (i.e. active *minus* passive), a negative peak of the EEG power difference was observed at 2-4 Hz, reflecting the maximal EEG power peak in the passive condition. Furthermore, there was a positive peak of the EEG power difference at 6-8 Hz, reflecting the highest EEG power peak in the active condition.

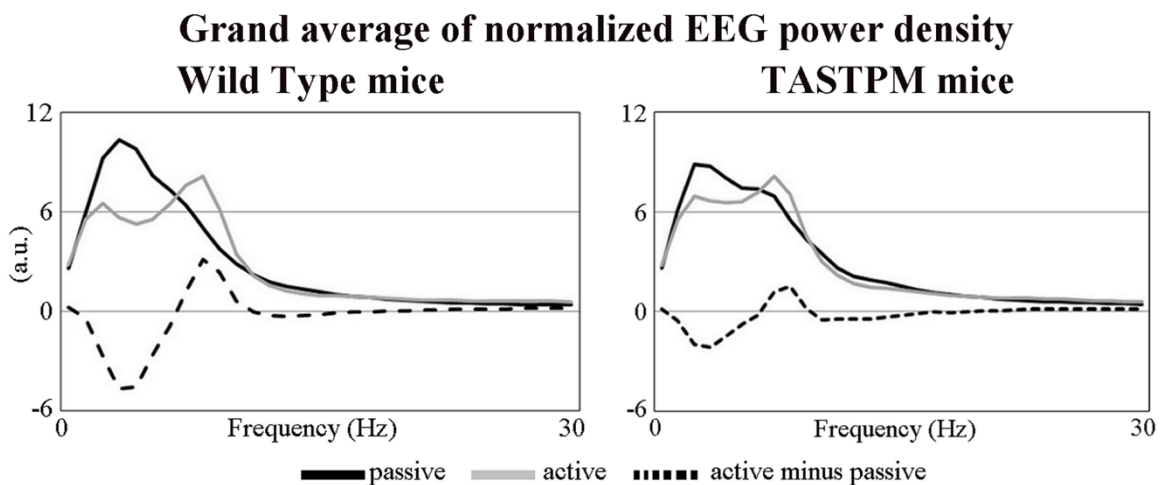


Figure 19. Grand average of the normalized electroencephalographic (EEG) power density obtained averaging data of the WT ($N=73$, left) and TASTPM ($N=33$, right) mice. The graph represents the normalized EEG power density to the frequency range

Experimental part

between 0 and 30 Hz at the bipolar fronto-parietal electrode for the passive and active condition during the dark phase of the day (note that mouse is a nocturnal animal). The difference between active and passive condition (active minus passive) is also reported.

It is noteworthy that the distribution of individual values of the normalized EEG power (represented by the active and passive conditions and the 8 EEG frequency bands) showed no outliers both in the WT (Figure 20, left) and the TASTPM mice (Figure 20, right). Specifically, 3 mice for WT group and 1 mouse for TASTPM group were individuated as outlier values according to the Grubb's test ($p > 0.05$) and were excluded for the subsequent analyses.

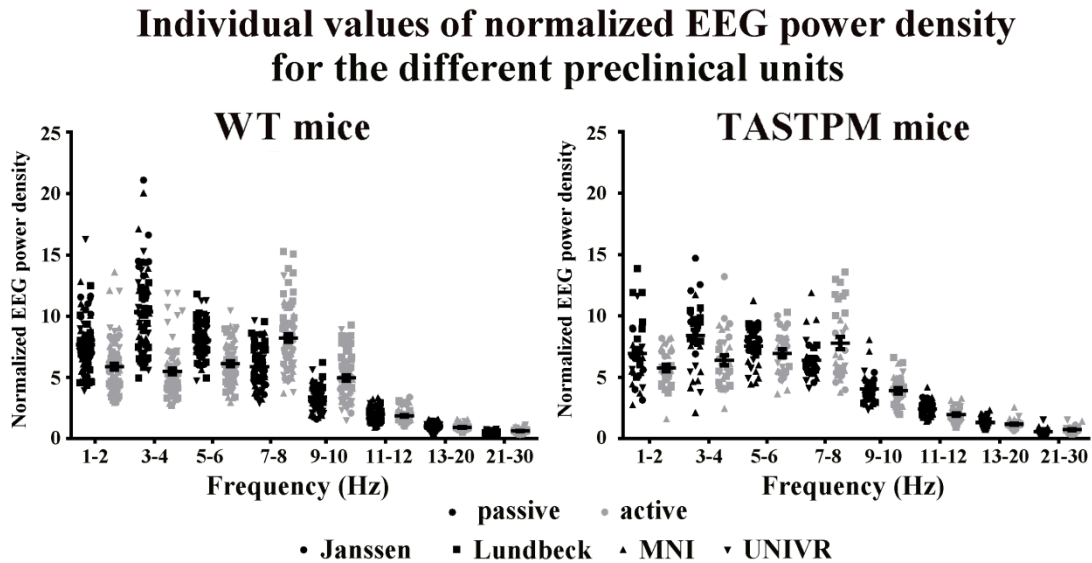


Figure 20. Individual values of the normalized EEG power density for the WT (left) and TASTPM (right) mice. In particular, the normalized EEG power density is represented for the two conditions (active, passive) and the eight bands (1-2 Hz, 3-4 Hz, 5-6 Hz, 7-8 Hz, 9-10 Hz, 11-12 Hz, 13-20 Hz, and 21-30 Hz). Of note, different symbols were used for the four preclinical Units to appreciate the inter-Unit variability. Few outlier values according to the Grubb's test (3 mice for WT group and 1 mouse for TASTPM group; $p > 0.05$) were excluded for the subsequent analysis.

Figure 21 showed significant differences in the EEG power between the passive and active condition in the WT (left) and TASTPM (right) mice. Figure 3 (left) shows the mean values (\pm SE) of the normalized EEG power in the WT group illustrating the results of a significant ANOVA interaction ($F(7, 476) = 9.3204$, $p = 0.00001$) between the factors Condition (passive, active) and Band (1-2 Hz, 3-4 Hz, 5-6 Hz, 7-8 Hz, 9-10 Hz, 11-12 Hz, 13-20 Hz, and 21-30 Hz). The Duncan post-hoc testing indicated that the EEG power was significantly higher in the passive compared to the active condition at 1-2 Hz ($p = 0.000011$), 3-4 Hz ($p = 0.000005$), and 5-6 Hz ($p = 0.000011$). In contrast, the EEG power was significantly higher in the active compared to the passive condition at 7-8 Hz ($p = 0.000004$) and 9-10 Hz ($p = 0.000009$). Figure 3 (right) shows the mean values (\pm SE) of the normalized EEG power in the TASTPM group illustrating the results of a significant ANOVA interaction ($F(7, 210) = 4.2866$, $p = 0.00019$) between the factors Condition (passive, active) and Band (as above). The Duncan post-hoc testing showed that the EEG power was significantly higher in the passive compared to the active condition at 1-2 Hz ($p = 0.0037$), 3-4 Hz ($p = 0.000004$). In contrast, the EoEG power was significantly higher in the active compared to the passive condition at 7-8 Hz ($p = 0.00048$).

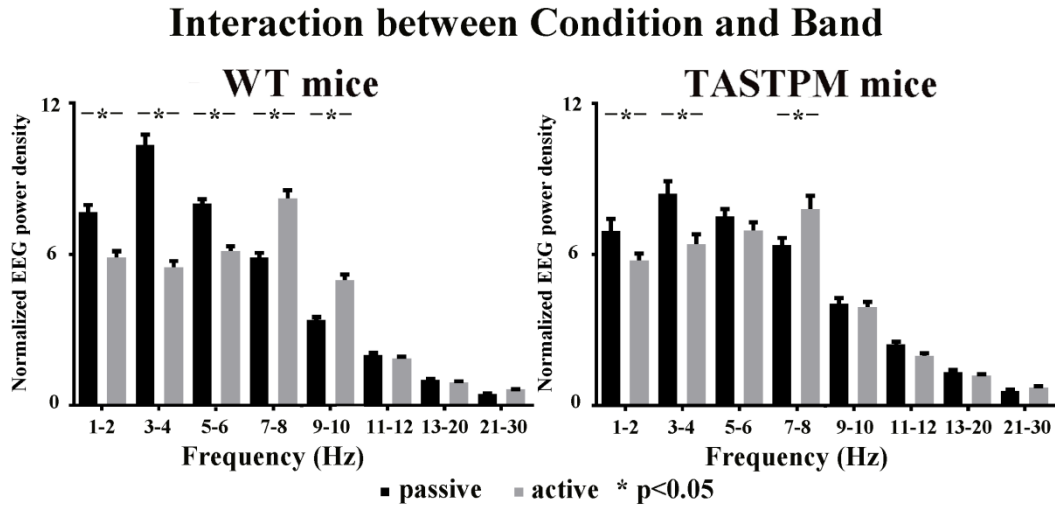


Figure 21. LEFT. Mean values (\pm standard error, SE) of the normalized EEG power density relative to a significant ANOVA interaction effect ($F(7, 476)= 9.3204$, $p=0.00001$) between the factors Condition (passive, active) and Band (1-2 Hz, 3-4 Hz, 5-6 Hz, 7-8 Hz, 9-10 Hz, 11-12 Hz, 13-20 Hz, and 21-30 Hz) in the WT group. RIGHT. Mean values (\pm standard error, SE) of the normalized EEG power density relative to a statistically significant ANOVA interaction effect ($F(7, 210)=4.2866$, $p=0.00019$) between the factors Condition (passive, active) and Band (1-2 Hz, 3-4 Hz, 5-6 Hz, 7-8 Hz, 9-10 Hz, 11-12 Hz, 13-20 Hz, and 21-30 Hz) in the TASTPM group. Asterisks indicate the EEG frequency bands at which normalized EEG power density presented statistically significant differences between the passive and active condition (Duncan post hoc testing, $p < 0.05$).

7.3.2 Comparison of the normalized EEG power between WT and TASTPM mice

Figure 22 shows the grand average of the difference in the normalized EEG power between active and passive condition (active *minus* passive) in the WT (N=73) and TASTPM (N=33) mice. The difference in the normalized EEG power refers to the frequency range between 0 and 30 Hz with 1 Hz of frequency resolution. Compared to the WT mice, the TASTPM mice exhibited a decrease of the negative peak of the EEG power difference at 2-4 Hz and a decrease of the positive peak of the EEG power difference at 8-10 Hz.

Grand average of normalized EEG power density (active minus passive)

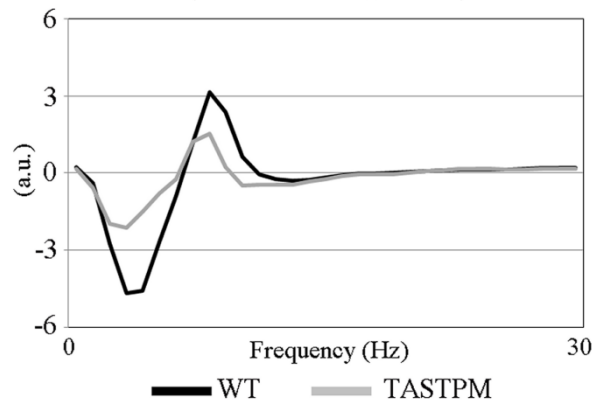


Figure 22. Grand-average of the difference of the normalized EEG power density between the active and passive condition (active minus passive) obtained averaging the data of the WT ($N=73$) and TASTPM ($N=33$) mice. The normalized EEG power density (active minus passive) refers to the frequency range between 0 and 30 Hz.

Figure 23 shows the mean values (\pm SE) of the difference in the normalized EEG power between the active and passive conditions (i.e. active minus passive) illustrating a statistically significant ANOVA interaction ($F(7, 693)=12.645$, $p=0.00001$) between the factors Genotype (WT, TASTPM) and Band (as above). The Duncan post-hoc testing unveiled the specific statistical differences between the two genotypes. Compared to the WT mice, the TASTPM mice were characterized by a decrease of EEG power difference (i.e. active minus passive) at 3-4 Hz ($p=0.000008$), 5-6 Hz ($p=0.0026$), 7-8 Hz ($p=0.035$) and 9-10 Hz ($p=0.0001$). The results suggest that the TASTPM mice showed abnormally low EEG markers reflecting cortical arousal.

Interaction between Genotype and Band

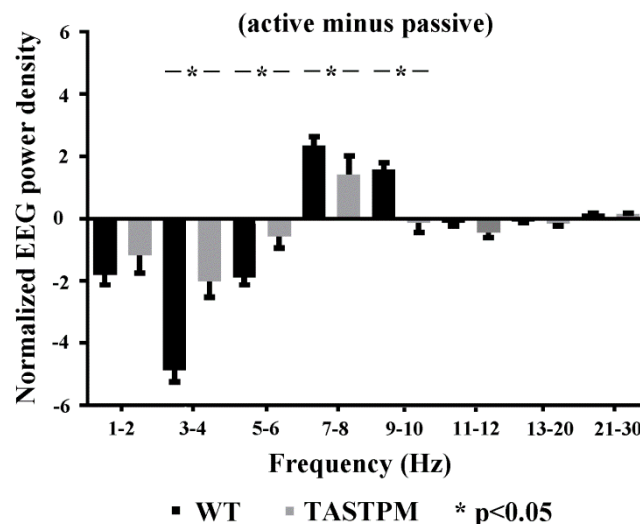


Figure 23. Mean values (\pm SE) of the difference of the normalized EEG power density between the active and passive condition (active minus passive) illustrating a significant ANOVA interaction effect ($F(7, 693)=12.645$, $p=0.00001$) between the factors Genotype (WT, TASTPM) and Band (1-2 Hz, 3-4 Hz, 5-6 Hz, 7-8 Hz, 9-10 Hz, 11-12 Hz, 13-20 Hz, and 21-30 Hz). Asterisks indicate the EEG bands at which normalized EEG power density (active minus passive) presented statistically significant differences between the WT and TASTPM mice (Duncan post hoc testing, $p < 0.05$).

Experimental part

Figure 24 shows the mean values (\pm SE) of the difference in the normalized EEG power between the active and passive conditions (i.e. active minus passive) illustrating a statistically significant ANOVA interaction $F(7, 427)=8.3418$, $p=0.000001$) between the factors Genotype (WT, TASTPM) and Band (as above). The Duncan post-hoc testing unveiled the specific statistical differences between the two genotypes. Compared to the WT mice, the TASTPM mice were characterized by a decrease of EEG power difference (i.e. active minus passive) at 3-4 Hz ($p=0.00001$), 5-6 Hz ($p=0.0036$) and 9-10 Hz ($p=0.0022$). In conclusion, we found similar results to those obtained in the main statistical analysis.

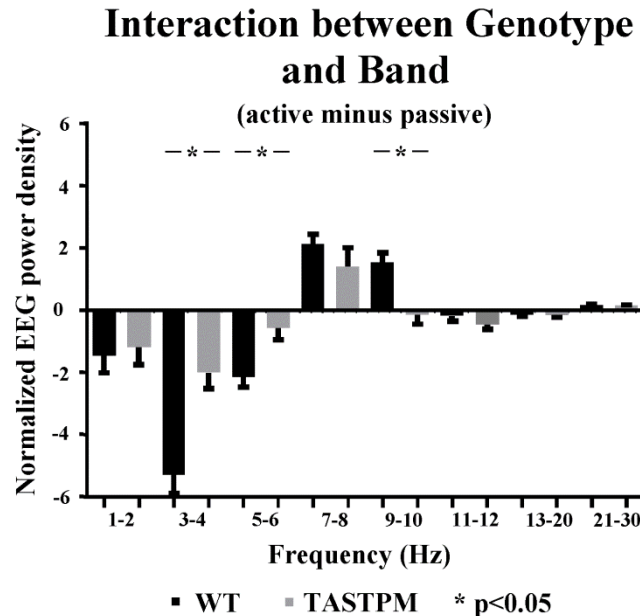


Figure 24. Mean values (\pm SE) of the difference of the normalized EEG power density between the active and passive condition (active minus passive) illustrating a significant ANOVA interaction effect ($F(7, 427)=8.3418$, $p=0.000001$) between the factors Genotype (WT, TASTPM) and Band (1-2 Hz, 3-4 Hz, 5-6 Hz, 7-8 Hz, 9-10 Hz, 11-12 Hz, 13-20 Hz, and 21-30 Hz). Specifically, this analysis refers to a subgroup of 32 mice (18 males and 14 females), with a mean age of $14.7 (\pm 0.8)$ and $14.8 (\pm 0.8)$ months for WT and TASTPM mice, respectively. Asterisks indicate the EEG bands at which normalized EEG power density (active minus passive) presented statistically significant differences between the WT and TASTPM mice (Duncan post hoc testing, $p < 0.05$).

7.4 Discussion

In humans, resting state EEG rhythms reflect the fluctuation of cortical arousal and vigilance in quiet wakefulness. These rhythms are investigated in a typical clinical setting, namely the EEG recording in neurological patients relaxed in the state of eyes closed (i.e. passive condition) and eyes open (i.e. active condition). From a neurophysiological point of view, it is supposed that the higher the power of cortical EEG rhythms at a given frequency, the higher the synchronization of cortical pyramidal neurons at that frequency (Pfurtscheller and Lopes da Silva, 1999). In the present study, we adapted and back-translated the above clinical EEG protocol to TASTPM mice (i.e. double mutated in APP KM670/671NL (Swedish) and PSEN1 M146V), characterized by a progressive deposition of A β 1-42 in the brain across aging. Specifically, ongoing EEG rhythms were investigated in the passive (i.e. quiet wakefulness with immobility or small movements of the trunk, head, and forelimbs) and the active condition (i.e. dynamic exploration of the cage).

Experimental part

The findings of the current study showed that both the WT and TASTPM mouse groups exhibited higher EEG power at delta rhythms (1-6 Hz) in the passive than the active condition. Furthermore, there was a higher EEG power at theta rhythms (6-10 Hz) in the active compared with the passive condition. These differences might reflect changes in cortical arousal, vigilance, and cognitive processes underlying exploration of the cage in mice. Neurophysiological mechanisms at the basis of these effects have been recently discussed (Del Percio et al., 2017a). In the passive condition, the dominant delta rhythms might be partially generated by widespread thalamo-cortical and thalamo-reticular frontoparietal circuits inducing widespread EEG slow waves in the cerebral cortex during non-REM sleep (Steriade, 2003, Rector et al., 2005, 2009, Lörincz et al., 2009, Krueger et al., 1993). Instead, the dominant theta rhythms during the active condition might be generated by selective reciprocal thalamo-cortical and hippocampal-cortico circuits involved in the regulation of the vigilance for cognitive processes including the visuospatial navigation and the somatomotor integration (Del Percio et al., 2017a).

The current findings unveiled different EEG rhythms in TASTPM and WT mice. In the passive condition, the delta power (i.e. 2-6 Hz) was lower in the TASTPM group compared with the WT group. In the active condition, the theta power (i.e. 8-10 Hz) was lower in the former than the latter as well. These findings suggest that TASTPM mice are characterized by reduced variations of frontoparietal EEG rhythms from passive to active conditions. Noteworthy, they are in agreement with the findings reported in a parallel EEG study performed in PDAPP mice expressing a single mutation of human APP [50]. In that parallel study, the PDAPP group showed abnormalities in both delta and theta rhythms, with a poor reactivity of those rhythms in the active condition (Del Percio et al., 2017b).

The mentioned findings of the present study arise at least the following two main questions.

What is the neuropathophysiological mechanism underlying the poor EEG reactivity in TASTPM mice in the present experimental conditions? The current findings might reflect the deleterious effect of A β 1-42 on cholinergic and GABAergic brain neurons involved in the modulation of cortical arousal, visuo-spatial navigation and memory, and somatomotor integration, although other neurotransmitter systems are affected as AD progresses (e.g. those using corticotrophin-releasing factor, somatostatin, dopamine, and serotonin, Mura et al., 2010). Indeed, it has been proposed that cortical theta rhythms in mice are generated from brain circuits involving hippocampal and basal forebrain cholinergic neurons (Rubio et al., 2012). These circuits subserve visuospatial processing, spatial navigation, object recognition, and somatomotor integration (Crunelli et al., 2015, Hasselmo et al., 2005, Vertes, 2005, Hamlin et al., 2013, Dashniani et al., 2015). Moreover, theta rhythms are modulated by the septohippocampal pathway controlling the activity of GABAergic interneurons, especially in the hippocampus (Rubio et al., 2012, [60]. Ekstrom et al., 2005, Watrous et al., 2013). These neurons might underlie pathological alterations contributing to cognitive dysfunctions in AD (Li et al., 2016).

What is the translational value of the present results for the research about pathological aging? AD patients and the present TASTPM mice show both inter-species differences and similarities in the effects of the active and passive conditions on EEG rhythms.

Experimental part

Concerning the differences, previous studies have shown that in healthy subjects, resting state eyes-closed (i.e. passive) condition is associated with alpha rhythms (8-12 Hz) dominating in posterior areas of cerebral cortex, as a reflection of sensory deprivation, muscle relaxation, and low cortical arousal and vigilance (Pfurtscheller and Klimesch, 1992, Klimesch et al., 1997, Klimesch, 1999). These rhythms decrease in power during perceptual, memory, and motor demands (i.e. active condition, as defined here), as a reflection of increased cortical arousal, vigilance, and higher cognitive processes (Pfurtscheller and Klimesch, 1992, Klimesch et al., 1997, Klimesch, 1999, Van Winsum et al., 1984, Sergeant et al., 1987, Babiloni et al., 1999). Compared with Nold subjects, AD patients were characterized by lower power of posterior alpha rhythms in the resting state eyes-closed condition and lower reduction of these rhythms after the eyes opening as a mildly active condition (Claus et al., 1999, Huang et al., 2000, Bennys et al., 2001, Lehmann et al., 2007, Bonanni et al., 2008, Babiloni et al., 2015, Ommundsen et al., 2011). Compared with AD patients, the present TASTPM mice showed different features of the EEG rhythms. They exhibited neither a power peak in the alpha range (8-12 Hz) during the passive condition nor the reduction of this power peak during the active condition. As far as the inter-species similarity is concerned, both AD patients (Babiloni et al., 2010) and the present TASTPM mice pointed to a poor reactivity of EEG rhythms <12 Hz to activating conditions in the wakefulness. A fascinating speculation is that AD processes might impair the fine tuning of the cortical arousal in activating conditions. In the experimental condition of resting state EEG recordings in AD patients, prominent effects might reflect poor changes in vigilance despite eyes opening and related visual information processing (Babiloni et al., 2010). In the experimental condition of ongoing EEG recordings in TASTPM mice, prominent effects during exploratory movements might reflect not only poor changes in vigilance but also abnormal visuospatial navigation, memory, and sensorimotor integration (Lassalle et al., 2008).

In the light of the above data and considerations, the concept of back-translation from AD patients to TASTPM mice should be considered at large in the interpretation of the present findings. Here the use of this concept should take into account the clear differences in the underlying cognitive processes and relative effects in the experiments carried out in the two species. It can be speculated that some similarity in the neurophysiological effects might consist in a tonic cerebral overexcitation (e.g. a sort of background neural noise) that might reduce the graduated increment in the cortical arousal and peculiar information processing from the passive to the active condition. This overexcitation might share some underlying neurophysiological mechanisms with preclinical epileptic-like processes. In line with this speculation, epileptic-like EEG activities have been described in both AD patients (Steriade et al., 1993) and transgenic mice accumulating A β 1-42 in the brain (Rector et al., 2009). Furthermore, convulsive seizures have an incidence 10 times higher in AD patients than healthy subjects (Steriade and Amzica, 1998). Finally, a recent fascinating evidence showed that in transgenic mice developing neuritic plaques, epileptic-like EEG activities appeared only when the transgene was active (Steriade et al., 1993). Noteworthy, these EEG activities ceased in about two weeks when the transgene was turned off, although amyloid plaques persisted (Cramer et al., 2012).

The present results should be just considered as a “proof of concept” due to the following methodological limitations of the study.

Experimental part

First of all, the present experimental procedures permit only a partial translational understanding of the neurophysiological mechanisms modulating cortical arousal in physiological and pathological (e.g. AD neuropathology) conditions. In physiological conditions, human resting state EEG rhythms reflect the cortical arousal due to visual processes induced by the eyes opening and the effects on vigilance. In contrast, those of the present experiments reflected visuo-spatial, memory, and somatomotor integrating processes related to the exploration of the cage. In AD patients, the brain is affected not only by the accumulation of A β 1-42 but also by tauopathy and often a certain degree of cerebrovascular disease.

Secondly, the different dominant frequencies of cortical EEG rhythms between mice and humans might be partially provoked by the head as a volume conductor. In fact, mice are typically characterized by prominent theta rhythms mainly generated in the hippocampus and surrounding structures about exploratory behaviors. In the small mouse brain, hippocampal theta activity might propagate to near electrodes located in the parietal cortex. As a consequence, changes in ongoing theta rhythms at those cortical electrodes (especially in the parietal cortex) might be partially affected by hippocampal oscillatory neural currents produced at theta frequencies during exploratory movements (Steriade, 2000, 2003). As two preclinical Units used a telemetric system allowing only a single bipolar (e.g. frontoparietal) EEG electrode montage, we could not perform a group analysis of EEG rhythms at the frontal electrode (less affected by the hippocampal theta oscillations) with a monopolar montage. In contrast, hippocampal neural currents cannot reach patients' scalp electrodes due to the relatively long distance in the human brain. Keeping in mind the above considerations, the back-translation value of the present procedure does not rely on the identical brain origin and nature of (1) resting state alpha rhythms estimated in AD patients in parietal source and (2) theta rhythms related to exploratory movements recorded with a frontoparietal bipolar montage in the present TASTPM mice (e.g.). As mentioned above, that translational value relies on the evidence of a reduced reactivity of EEG rhythms from the passive to the active condition in both species, possibly in relation to AD neuropathology.

Thirdly, the mouse behavior was qualitatively rated as active vs. passive based on a harmonized visual rating protocol in the four research Units of this study (e.g. Lundbeck, Janssen, UNIVR, and MNI). In that protocol, movement velocity and extension were not considered. Therefore, the reported EEG differences in the two mouse groups (i.e. WT and TASTPM) might partially depend on different quantitative motor features in the active condition. This limitation is relevant as hippocampal theta rhythms might reflect some features of movements (Rector et al., 2005, 2009, Lörincz et al., 2009). Another limitation is that due to the scope of the study, the discrimination of the passive condition in wakefulness vs. initial sleep stages was done relying on behavioral observations only to avoid circular logics in the study of EEG rhythms as a dependent variable affected by passive and active behavioral conditions. The disadvantage of this approach is that the state of passive wakefulness vs. initial sleep is very challenging to determine reliably without the assistance of EEG and EOG readouts. To mitigate the misclassification, we defined strict criteria to discriminate explorative vs. automatic behavior vs. initial sleep, considering that eyes closure is not a good criterion for sleep, and the experimenter did not score as "passive condition" epochs in which the animals stayed continuously still for 10 s or with small movements for 20 s or longer. Furthermore, the relative reliability of the classifications across

Experimental part

the four preclinical Units might be supported by the fact that the EEG results were not affected by the variable “Unit” used as a covariate.

As a final consideration, the current methodology cannot substitute other classical neurophysiological methodologies applied in mice, namely long EEG recordings investigating wake-cycle sleep, the experimental inoculation of stress or anxiety, and new technologies of virtual reality to simulate spatial navigation in animals during EEG recordings.

8 Conclusions

The aim of the present Ph.D. project, developed in the framework of the IMI PharmaCog project, consisted in the identification of EEG biomarkers most suitable to be backtranslated from prodromal AD patients to transgenic mouse models of the disease such as PDAPP and TASTPM strains. The integration of several functional biomarkers in a multimodal matrix (EEG, MRI, blood, etc.) may help the development of more effective pharmacological interventions and enrich our understanding of the AD progression and therapy response. To date, much of the work has been directed toward validating and qualifying biomarkers of the prodromal stage of AD disease (Hampel et al., 2011, Blennow et al., 2010, Mattsson et al., 2009). A biomarker matrix of the prodromal AD status and progression may facilitate an early stratification of AD patients for clinical trials using disease-modifying drugs, based on the prediction of the disease evolution and therapy monitoring.

8.1 *EEG biomarkers in prodromal AD patients with aMCI*

Candidate backtranslational AD biomarkers have been firstly characterized in aMCI patients with abnormal CSF levels of A β 42 and P-tau measured at baseline, namely the prodromal AD patients of this study. To take into account the confounding effects of different disease stages and cognitive grades, we used 5 serial recording sessions over 2 years, controlling for cognitive status using a control group of aMCI patients supposed not due to AD based on CSF levels of A β 42 and P-tau. Some functional biomarkers including fMRI and EEG were able to detect significant Group effects stable over time in the prodromal AD patients compared with the control aMCI subgroup: (1) reduced fMRI functional connectivity in the DMN and in the PCC node; (2) increased EEG source activity at delta (< 4 Hz) and theta (4-8 Hz) rhythms and decreased source activity at alpha (8-10.5 Hz) rhythms; and (3) reduced parietal and posterior cingulate source activities of P3b peak of ERPs. Some functional fMRI and EEG biomarkers were also able to show Time X Group effects, giving differential progression profiles over time in the prodromal AD subgroup relative to the control aMCI subgroup: (1) increased rsfMRI functional connectivity in the LPC node of the DMN and (2) increased limbic source activity at theta rhythms. These functional biomarkers can be considered as topographical biomarkers of prodromal AD status and progression according to a moder theory of AD biomarkers (Dubois et al., 2014, Frisoni et al., 2010) and future studies may test the hypothesis of different sensitivity of those biomarkers at different phases of the disease progression. At the present stage of the knowledge, we cannot explain why some rsfMRI and EEG biomarkers were found to be sensitive only to Group effects and others to Group X Time effects over 24 months of the monitoring. Future studies correlating those biomarkers with PET maps of A β 1-42 and P-tau accumulation in the brain may enlighten such an explanation.

As an absolute novelty, the present findings represent the first longitudinal characterization of functional topographic biomarkers of prodromal AD when the cognitive status of aMCI is controlled as a possible confound (by using a control group of aMCI patients possibly not due to AD). If cross-validated, these findings may be used for the stratification and monitoring of the effects of disease-modifying drugs in aMCI patients

Conclusions

suffering from AD. Indeed, topographic biomarkers of brain function as those derived from rsfMRI and EEG (or the magnetoencephalographic counterpart) may be more likely to respond to an effective disease-modifying intervention relative to structural neuroimaging atrophy markers (e.g., cortical or hippocampus atrophy) or topographic biomarkers of brain hypometabolism (e.g., those measured by FDG-PET), which may only partially recover as they are markedly dependent on neurodegeneration (Dubois et al., 2014).

The resting state EEG results of this study were used as a reference for their backtranslation to ongoing EEG activity recorded in mouse models of AD such as TASTPM and PDAPP strains when compared to WT littermates.

8.2 EEG biomarkers in AD mouse models

As mentioned above, EEG biomarkers identified in prodromal AD patients were evaluated along physiological ageing in WT mice. According to the behavioural state of the animal in the wakefulness, compared to the passive condition, the active condition induced a decrease of EEG power at 1-6 Hz and its increase at 6-10 Hz in all mice as a group. The different cortical synchronization was affected by ageing, in particular the passive condition showed higher EEG power at 1-2 Hz in the old group than the young and middle-aged groups. Furthermore, the active condition exhibited a maximum EEG power at 6-8 Hz in the former group and 8-10 Hz in the latter groups. Delta and theta EEG rhythms reflected changes in cortical arousal and vigilance in freely behaving WT mice across aging. These changes resemble the so-called slowing of resting state EEG rhythms observed in humans across physiological and pathological aging.

Once identified, the EEG biomarkers at delta and theta bands reflecting fluctuations in cortical arousal were tested in PDAPP and TASTPM mice in two studies. These studies showed that both mouse models of AD were characterized by a poor change in the frequency and power of the frontoparietal on-going delta and theta rhythms during the active vs. passive states in the wakefulness. These results would suggest that the “reactivity” of ongoing delta and theta rhythms in wakefulness might be sensitive to AD neuropathology in PDAPP and TASTPM mice. In this sense, they are reminiscent of the poor “reactivity” of EEG rhythms in AD patients, observed switching from resting state eyes-closed to -open. Of course, the cerebral origin of that EEG reactivity and the underlying brain functions might be different in humans and mice, but some analogists may exist between the two species in the impairment in brain circuits underpinning the regulation and switches in general cerebral arousal. Future studies should (1) cross-validate the present results on large animal groups monitoring quantitative features of the animal movements, (2) clarify the neurophysiological underpinning of the effect in relation to neuritic plaques and A β species, and (3) test if the disease modifying drugs against AD amyloidosis normalize those candidate EEG biomarkers in transgenic mouse models of the pathology.

In conclusion, this Ph.D. thesis provide first significant evidence that the mentioned EEG variables are promising backtranslational topographic biomarkers useful for the instrumental neurophysiological assessment of brain function in prodromal AD patients diagnosed based on standard pathophysiological disease markers (Dubois et al., 2014). This outcome is particularly important as EEG technique is cost-effective, diffuse, non-invasive, and perfectly translatable to preclinical research as shown in the present study. In the framework of

Conclusions

the PharmaCog project and this Ph.D thesis, the backtranslation was realized by identifying EEG biomarkers in aMCI patients positive to CSF biomarkers (prodromal AD) and by realizing a simple behavioural paradigm able to reproduce in AD mouse models generalized brain arousal due to the fluctuation of the vigilance. Taken together, these results provide the rational for the use of the present EEG biomarkers in future studies involving clinical and preclinical testing of new disease-modifying drugs against AD.

9 References

- Adeli H, Ghosh-Dastidar S, Dadmehr N. Alzheimer's disease: models of computation and analysis of EEGs. *Clin EEG Neurosci*. 2005 Jul; 36(3):131-40.
- Agosta F, Dalla Libera D, Spinelli EG, Finardi A, Canu E, Bergami A, Bocchio Chiavetto L, Baronio M, Comi G, Martino G, Matteoli M, Magnani G, Verderio C, Furlan R (2014) Myeloid microvesicles in cerebrospinal fluid are associated with myelin damage and neuronal loss in mild cognitive impairment and Alzheimer disease. *Ann Neurol* 76, 813–825.
- Agosta F, Scola E, Canu E, Marcone A, Magnani G, Sarro L, Copetti M, Caso F, Cerami C, Comi G, Cappa SF, Falini A, Filippi M (2012) White matter damage in frontotemporal lobar degeneration spectrum. *Cereb Cortex* 22, 2705–2714.
- Albert MS, DeKosky ST, Dickson D, Dubois B, Feldman HH, Fox NC, Gamst A, Holtzman DM, Jagust WJ, Petersen RC, Snyder PJ, Carrillo MC, Thies B, Phelps CH. *Alzheimers Dement*. 2011 May;7(3):270-9. The diagnosis of mild cognitive impairment due to Alzheimer's disease: recommendations from the National Institute on Aging-Alzheimer's Association workgroups on diagnostic guidelines for Alzheimer's disease.
- Albi A, Pasternak O, Minati L, Marizzoni M, Bartres-Faz D, Bargallo N, Bosch B, Rossini PM, Marra C, Muller B, Fiedler U, Wiltfang J, Roccatagliata L, Picco A, Nobili FM, Blin O, Sein J, Ranjeva JP, Didic M, Bombois S, Lopes R, Bordet R, Gros-Dagnac H, Payoux P, Zoccatelli G, Alessandrini F, Beltramello A, Ferretti A, Caulo M, Aiello M, Cavaliere C, Soricelli A, Parnetti L, Tarducci R, Floridi P, Tsolaki M, Constantinidis M, Drevelegas A, Frisoni G, Jovicich J (2017) Free water elimination improves test-retest reproducibility of diffusion tensor imaging indices in the brain: A longitudinal multisite study of healthy elderly subjects. *Hum Brain Mapp* 38, 12–26.
- Allsop D, Mayes J. Amyloid β -peptide and Alzheimer's disease. *Essays in Biochemistry* Aug 18, 2014, 56 99-110.
- Alzheimer A: Uber einen eigenartigen schweren erkrankungsprozeß der hirnrinde. *Neurol Cent* 1906; 25: 1134.
- Amieva H, Letenneur L, Dartigues J-F, Rouch-Leroyer I, Sourgen C, D'Alchee-Biree F, Dib M, Barberger-Gateau P, Orgogozo J-M, Fabrigoule C (2004) Annual rate and predictors of conversion to dementia in subjects presenting mild cognitive impairment criteria defined according to a population-based study. *Dement. Geriatr. Cogn. Disord*. 18, 87–93.
- Arendt T, Brückner MK, Morawski M, Jäger C, Gertz HJ. Early neurone loss in Alzheimer's disease: cortical or subcortical? *Acta Neuropathol Commun*. 2015 Feb 10;3:10..
- Arnolds DE, Lopes da Silva FH, Boeijinga P, Kamp A, Aitink W. Hippocampal EEG and motor activity in the cat: the role of eye movements and body acceleration. *Behav Brain Res*. 12(2):121-35 (1984).
- Babiloni C, Benussi L, Binetti G, Bosco P, Busonero G, Cesaretti S, Dal Forno G, Del Percio C, Ferri R, Frisoni G, Ghidoni R, Rodriguez G, Squitti R, Rossini PM. Genotype (cystatin C) and EEG phenotype in Alzheimer disease and mild cognitive impairment: a multicentric study. *Neuroimage*. 2006 Feb 1;29(3):948-64.
- Babiloni C, Binetti G, Cassetta E, Dal Forno G, Del Percio C, Ferreri F, Ferri R, Frisoni G, Hirata K, Lanuzza B, Miniussi C, Moretti D V, Nobili F, Rodriguez G, Romani GL, Salinari S, Rossini PM (2006) Sources of cortical rhythms change as a function of cognitive impairment in pathological aging: a multicenter study. *Clin Neurophysiol* 117, 252–268.
- Babiloni C, Carducci F, Cincotti F, Rossini PM, Neuper C, Pfurtscheller G, Babiloni F. Human movement-related potentials vs desynchronization of EEG alpha rhythm: a high-resolution EEG study. *Neuroimage*. 1999 Dec;10(6):658-65.
- Babiloni C, Cassetta E, Binetti G, Tombini M, Del Percio C, Ferreri F, Ferri R, Frisoni G, Lanuzza B, Nobili F, Parisi L, Rodriguez G, Frigerio L, Gurzi M, Prestia A, Vernieri F, Eusebi F, Rossini PM. Resting EEG sources correlate with attentional span in mild cognitive impairment and Alzheimer's disease. *Eur J Neurosci*. 2007 Jun;25(12):3742-57.
- Babiloni C, Del Percio C, Boccardi M, Lizio R, Lopez S, Carducci F, Marzano N, Soricelli A, Ferri R, Triggiani AI, Prestia A, Salinari S, Rasser PE, Basar E, Fama F, Nobili F, Yener G, Emek-Savas DD, Gesualdo L, Mundi C, Thompson PM, Rossini PM, Frisoni GB (2015) Occipital sources of resting-state alpha rhythms are related to local gray matter density in subjects with amnesic mild cognitive impairment and Alzheimer's disease. *Neurobiol Aging* 36, 556–570.
- Babiloni C, Del Percio C, Caroli A, Salvatore E, Nicolai E, Marzano N, Lizio R, Cavedo E, Landau S, Chen K, Jagust W, Reiman E, Tedeschi G, Montella P, De Stefano M, Gesualdo L, Frisoni GB, Soricelli A (2016) Cortical sources of resting state EEG rhythms are related to brain hypometabolism in subjects with Alzheimer's disease: an EEG-PET study. *Neurobiol Aging* 48, 122–134.
- Babiloni C, Del Percio C, Lizio R, Infarinato F, Blin O, Bartres-Faz D, Dix SL, Bentivoglio M, Soricelli A, Bordet R, Rossini PM, Richardson JC. A review of the effects of hypoxia, sleep deprivation and transcranial magnetic stimulation on EEG activity in humans: challenges for drug discovery for Alzheimer's disease. *Curr Alzheimer Res*. 2014;11(5):501-18.

References

- Babiloni C, Del Percio C, Lizio R, Marzano N, Infarinato F, Soricelli A, Salvatore E, Ferri R, Bonforte C, Tedeschi G, Montella P, Baglieri A, Rodriguez G, Fama F, Nobili F, Vernieri F, Ursini F, Mundi C, Frisoni GB, Rossini PM (2014) Cortical sources of resting state electroencephalographic alpha rhythms deteriorate across time in subjects with amnesic mild cognitive impairment. *Neurobiol Aging* 35, 130–142.
- Babiloni C, Frisoni G, Steriade M, Bresciani L, Binetti G, Del Percio C, Geroldi C, Miniussi C, Nobili F, Rodriguez G, Zappasodi F, Carfagna T, Rossini PM (2006) Frontal white matter volume and delta EEG sources negatively correlate in awake subjects with mild cognitive impairment and Alzheimer's disease. *Clin Neurophysiol* 117, 1113–1129.
- Babiloni C, Frisoni GB, Pievani M, Vecchio F, Lizio R, Buttiglione M, Geroldi C, Fracassi C, Eusebi F, Ferri R, Rossini PM. Hippocampal volume and cortical sources of EEG alpha rhythms in mild cognitive impairment and Alzheimer disease. *Neuroimage*. 2009 Jan 1;44(1):123-35.
- Babiloni C, Frisoni GB, Pievani M, Vecchio F, Lizio R, Buttiglione M, Geroldi C, Fracassi C, Eusebi F, Ferri R, Rossini PM. Hippocampal volume and cortical sources of EEG alpha rhythms in mild cognitive impairment and Alzheimer disease. *Neuroimage*. 2009 Jan 1;44(1):123-35.
- Babiloni C, Infarinato F, Aujard F, Bastlund JF, Bentivoglio M, Bertini G, Del Percio C, Fabene PF, Forloni G, Herrero Ezquerro MT, Noè FM, Pifferi F, Ros-Bernal F, Christensen DZ, Dix S, Richardson JC, Lamberty Y, Drinkenburg W, Rossini PM. Effects of pharmacological agents, sleep deprivation, Hypoxia and transcranial magnetic stimulation on electroencephalographic rhythms in rodents: Towards translational challenge models for drug discovery in Alzheimer's disease. *Clin Neurophysiol*. 2013 Mar;124(3):437-51.
- Babiloni C, Lizio R, Del Percio C, Marzano N, Soricelli A, Salvatore E, Ferri R, Cosentino FI, Tedeschi G, Montella P, Marino S, De Salvo S, Rodriguez G, Nobili F, Vernieri F, Ursini F, Mundi C, Richardson JC, Frisoni GB, Rossini PM (2013) Cortical sources of resting state EEG rhythms are sensitive to the progression of early stage Alzheimer's disease. *J Alzheimers Dis* 34, 1015–1035.
- Babiloni C, Lizio R, Marzano N, Capotosto P, Soricelli A, Triggiani AI, Cordone S, Gesualdo , Del Percio C. Brain neural synchronization and functional coupling in Alzheimer's disease as revealed by resting state EEG rhythms. *Int J Psychophysiol*. 2015 Feb 7. pii: S0167-8760(15)00038-0.
- Babiloni C, Lizio R, Vecchio F, Frisoni GB, Pievani M, Geroldi C, Claudia F, Ferri R, Lanuzza B, Rossini PM. Reactivity of cortical alpha rhythms to eye opening in mild cognitive impairment and Alzheimer's disease: an EEG study. *J Alzheimers Dis*. 2010;22(4):1047-64.
- Babiloni C, Pievani M, Vecchio F, Geroldi C, Eusebi F, Fracassi C, Fletcher E, De Carli C, Boccardi M, Rossini PM, Frisoni GB (2009) White-matter lesions along the cholinergic tracts are related to cortical sources of EEG rhythms in amnesic mild cognitive impairment. *Hum Brain Mapp* 30, 1431–1443.
- Babiloni C, Vecchio F, Del Percio C, Montagnese S, Schiff S, Lizio R, Chini G, Serviddio G, Marzano N, Soricelli A, Frisoni GB, Rossini PM, Amodio P (2013) Resting state cortical electroencephalographic rhythms in covert hepatic encephalopathy and Alzheimer's disease. *J Alzheimers Dis* 34, 707–725.
- Babiloni C, Vecchio F, Lizio R, Ferri R, Rodriguez G, Marzano N, Frisoni GB, Rossini PM (2011) Resting state cortical rhythms in mild cognitive impairment and Alzheimer's disease: electroencephalographic evidence. *J Alzheimers Dis* 26 Suppl 3, 201–214.
- Bai F, Liao W, Watson DR, Shi Y, Yuan Y, Cohen AD, Xie C, Wang Y, Yue C, Teng Y, Wu D, Jia J, Zhang Z (2011) Mapping the altered patterns of cerebellar resting-state function in longitudinal amnesic mild cognitive impairment patients. *J Alzheimers Dis* 23, 87–99.
- Barnes LL, Leurgans S, Aggarwal NT, Shah RC, Arvanitakis Z, James BD, et al. Mixed pathology is more likely in black than white decedents with Alzheimer dementia. *Neurology*. 2015;85:528–34.
- Barry RJ, Clarke AR, Johnstone SJ. Caffeine and opening the eyes have additive effects on resting arousal measures. *Clin Neurophysiol*. 2011 Oct;122(10):2010-5. doi: 10.1016/j.clinph.2011.02.036. Epub 2011 Apr 12.
- Bastos Leite AJ, Scheltens P, Barkhof F. Pathological aging of the brain: an overview. *Top Magn Reson Imaging*. 2004 Dec;15(6):369-89.
- Bennett C, Arroyo S, Hestrin S. Subthreshold mechanisms underlying state-dependent modulation of visual responses. *Neuron*. 2013 Oct 16;80(2):350-7.
- Bennys K, Rondouin G, Vergnes C, Touchon J. Diagnostic value of quantitative EEG in Alzheimer disease. *Neurophysiol Clin*. 2001 Jun;31(3):153-60.
- Berendse HW, Verbunt JP, Scheltens P, van Dijk BW, Jonkman EJ. Magnetoencephalographic analysis of cortical activity in Alzheimer's disease: a pilot study. *Clin Neurophysiol*. 2000 Apr;111(4):604-12.

References

- Berger H (1929): Über das Elektroenkephalogramm des Menschen. Arch. f. Psychiat. 87: 527-70.
- Berryhill ME (2012) Insights from neuropsychology: pinpointing the role of the posterior parietal cortex in episodic and working memory. Front Integr Neurosci 6, 31.
- Bianchetti A, Trabucchi M. Clinical aspects of Alzheimer's disease. Aging (Milano). 13(3):221-30 (2001).
- Binnewijzend MA, Schoonheim MM, Sanz-Arigita E, Wink AM, van der Flier WM, Tolboom N, Adriaanse SM, Damoiseaux JS, Scheltens P, van Berckel BN, Barkhof F (2012) Resting-state fMRI changes in Alzheimer's disease and mild cognitive impairment. Neurobiol Aging 33, 2018–2028.
- Biswal B, Yetkin FZ, Haughton VM, Hyde JS (1995) Functional connectivity in the motor cortex of resting human brain using echo-planar MRI. Magn Reson Med 34, 537–541.
- Bland BH. The physiology and pharmacology of hippocampal formation theta rhythms. Prog Neurobiol. 26(1):1-54 (1986).
- Blennow K. Dementia in 2010: Paving the way for Alzheimer disease drug development. Nat Rev Neurol. 2011 Feb;7(2):65-6. doi: 10.1038/nrneurol.2010.214. Review.
- Boccaletti S, Kurths J, Osipov G, Valladares DL, Zhou CS. The synchronization of chaotic systems. Phys Rep 2002;366:1–101.
- Bonanni L, Thomas A, Tiraboschi P, Perfetti B, Varanese S, Onofri M. EEG comparisons in early Alzheimer's disease, dementia with Lewy bodies and Parkinson's disease with dementia patients with a 2-year follow-up. Brain. 2008 Mar;131(Pt 3):690-705.
- Born HA, Kim JY, Savjani RR, Das P, Dabaghian YA, Guo Q, Yoo JW, Schuler DR, Cirrito JR, Zheng H, Golde TE, Noebels JL, Jankowsky JL. Genetic suppression of transgenic APP rescues Hypersynchronous network activity in a mouse model of Alzheimer's disease. J Neurosci. 2014 Mar 12;34(11):3826-40.
- Boustani M, Peterson B, Hanson L, Harris R, Lohr KN. Screening for dementia in primary care: A summary of the evidence for the U.S. Preventive Services Task Force. Ann Intern Med 2003;138(11):927-37.
- Braak H, Braak E. Staging of Alzheimer's disease-related neurofibrillary changes. Neurobiol Aging. 1995 May-Jun;16(3):271-8; discussion 278-84.
- Bradford A, Kunik ME, Schultz P, Williams SP, Singh H. Missed and delayed diagnosis of dementia in primary care: Prevalence and contributing factors. Alz Dis Assoc Disord 2009;23(4):306-14.
- Brassen S, Adler G (2003) Short-term effects of acetylcholinesterase inhibitor treatment on EEG and memory performance in Alzheimer patients: an open, controlled trial. Pharmacopsychiatry 36, 304–308.
- Brenner RP, Ulrich RF, Spiker DG, Scabassi RJ, Reynolds 3rd CF, Marin RS, Boller F (1986) Computerized EEG spectral analysis in elderly normal, demented and depressed subjects. Electroencephalogr Clin Neurophysiol 64, 483–492.
- Brown RE, Basheer R, McKenna JT, Strecker RE, McCarley RW. Control of sleep and wakefulness. Physiol Rev. 2012 Jul;92(3):1087-187. doi: 10.1152/physrev.00032.2011.
- Buzsáki G, Buhl DL, Harris KD, Csicsvari J, Czeh B, Morozov A. Hippocampal network patterns of activity in the mouse. Neuroscience. 2003;116(1):201-11.
- Buzsáki G, Leung LW, Vanderwolf CH. Cellular bases of hippocampal EEG in the behaving rat. Brain Res. 1983 Oct;287(2):139-71.
- Calhoun VD, Adali T, Pearlson GD, Pekar JJ (2001) A method for making group inferences from functional MRI data using independent component analysis. Hum Brain Mapp 14, 140–151.
- Chen G, Chen KS, Knox J, Inglis J, Bernard A, Martin SJ, et al. A learning deficit related to age and beta-amyloid plaques in a mouse model of Alzheimer's disease. Nature. 408(6815):975-9 (2000).
- Chishti MA, Yang DS, Janus C, Phinney AL, Horne P, Pearson J, et al. Early-onset amyloid deposition and cognitive deficits in transgenic mice expressing a double mutant form of amyloid precursor protein 695. J Biol Chem. 15;276(24):21562-70 (2001).
- Cisse M, Braun U, Leitges M, Fisher A, Pages G, Checler F, et al. ERK1-independent α -secretase cut of β -amyloid precursor protein via M1 muscarinic receptors and PKC α/ϵ . Mol Cell Neurosci. 47(3):223-32 (2011).
- Claus JJ, Strijers RL, Jonkman EJ, Ongerboer de Visser BW, Jonker C, Walstra GJ, Scheltens P, van Gool WA. The diagnostic value of electroencephalography in mild senile Alzheimer's disease. Clin Neurophysiol 1999;110:825–832.
- Coben LA, Danziger W, Storandt M (1985) A longitudinal EEG study of mild senile dementia of Alzheimer type: changes at 1 year and at 2.5 years. Electroencephalogr Clin Neurophysiol 61, 101–112.

References

- Coenen AM, Van Luijckelaar EL. Genetic animal models for absence epilepsy: a review of the WAG/Rij strain of rats. *Behav Genet*. 2003 Nov;33(6):635-55.
- Corbett BF, Leiser SC, Ling HP, Nagy R, Breyse N, Zhang X, Hazra A, Brown JT, Randall AD, Wood A, Pangalos MN, Reinhart PH, Chin J. Sodium channel cleavage is associated with aberrant neuronal activity and cognitive deficits in a mouse model of Alzheimer's disease. *J Neurosci*. 2013 Apr 17;33(16):7020-6.
- Cramer PE, Cirrito JR, Wesson DW, Lee CY, Karlo JC, Zinn AE, Casali BT, Restivo JL, Goebel WD, James MJ, Brunden KR, Wilson DA, Landreth GE. ApoE-directed therapeutics rapidly clear β -amyloid and reverse deficits in AD mouse models. *Science*. 2012 Mar 23;335(6075):1503-6.
- Crochet S, Petersen CC. Correlating whisker behavior with membrane potential in barrel cortex of awake mice. *Nat Neurosci*. 2006 May;9(5):608-10.
- Crunelli V, David F, Lőrincz ML, Hughes SW. The thalamocortical network as a single slow wave-generating unit. *Curr Opin Neurobiol*. 2015 Apr;31:72-80.
- Cummings JL, Back C. The cholinergic hypothesis of neuropsychiatric symptoms in Alzheimer's disease. *Am J Geriatr Psychiatry*. 1998 Spring;6(2 Suppl 1):S64-78.
- Czigler B, Csikos D, Hidasi Z, Anna Gaal Z, Csibri E, Kiss E, Salacz P, Molnar M (2008) Quantitative EEG in early Alzheimer's disease patients - power spectrum and complexity features. *Int J Psychophysiol* 68, 75–80.
- Damoiseaux JS (2012) Resting-state fMRI as a biomarker for Alzheimer's disease? *Alzheimers Res Ther* 4, 8.
- Damoiseaux JS, Prater KE, Miller BL, Greicius MD (2012) Functional connectivity tracks clinical deterioration in Alzheimer's disease. *Neurobiol Aging* 33, 828 e19-30.
- Dashniani MG, Burjanadze MA, Naneishvili TL, Chkhikvishvili NC, Beselia GV, Kruashvili LB, Pochkhidze NO, Chighladze MR. Exploratory behavior and recognition memory in medial septal electrolytic, neuro- and immunotoxic lesioned rats. *Physiol Res*. 2015 Mar 24.
- de Pasquale F, Corbetta M, Betti V, Della Penna S (2017) Cortical cores in network dynamics. *Neuroimage*.
- Del Percio C, Drinkenburg W, Lopez S, Infarinato F, Bastlund JF, Clausen B, Pedersen JT, Christensen DZ, Forloni G, Frasca A, Noè FM, Bentivoglio M, Fabene PF, Bertini G, Colavito V, Kelley J, Dix S, Richardson JC, Babiloni C. On-going electroencephalographic rhythms related to cortical arousal in wild type mice: the effect of aging. Under revision by *Neurobiology of Aging*.
- Del Percio C, Drinkenburg W, Lopez S, Limatola C, Bastlund JF, Christensen DZ, Pedersen JT, Forloni G, Frasca A, Noè FM, Bentivoglio M, Fabene PF, Bertini G, Colavito V, Dix S, Ferri R, Bordet R, Richardso JC, Babiloni C. Ongoing electroencephalographic activity associated with cortical arousal in transgenic PDAPP mice (hAPP v717f). *Curr Alzheimer Res*. 2017 Jul 4. doi: 10.2174/1567205014666170704113405.
- Delli Pizzi S, Franciotti R, Taylor JP, Esposito R, Tartaro A, Thomas A, Onofrj M, Bonanni L (2015) Structural Connectivity is Differently Altered in Dementia with Lewy Body and Alzheimer's Disease. *Front Aging Neurosci* 7, 208.
- Delli Pizzi S, Maruotti V, Taylor JP, Franciotti R, Caulo M, Tartaro A, Thomas A, Onofrj M, Bonanni L (2014) Relevance of subcortical visual pathways disruption to visual symptoms in dementia with Lewy bodies. *Cortex* 59, 12–21.
- Delli Pizzi S, Padulo C, Brancucci A, Bubbico G, Edden RA, Ferretti A, Franciotti R, Manippa V, Marzoli D, Onofrj M, Sepede G, Tartaro A, Tommasi L, Puglisi-Allegra S, Bonanni L (2016) GABA content within the ventromedial prefrontal cortex is related to trait anxiety. *Soc Cogn Affect Neurosci* 11, 758–766.
- Dennis EL, Thompson PM (2014) Functional brain connectivity using fMRI in aging and Alzheimer's disease. *Neuropsychol Rev* 24, 49–62.
- Dierks T, Ihl R, Frolich L, Maurer K (1993) Dementia of the Alzheimer type: effects on the spontaneous EEG described by dipole sources. *Psychiatry Res* 50, 151–162.
- Dierks T, Jelic V, Pascual-Marqui RD, Wahlund L, Julin P, Linden DE, Maurer K, Winblad B, Nordberg A. Spatial pattern of cerebral glucose metabolism (PET) correlates with localization of intracerebral EEG-generators in Alzheimer's disease. *Clin Neurophysiol*. 2000 Oct;111(10):1817-24.
- Dierks T, Jelic V, Pascual-Marqui RD, Wahlund L, Julin P, Linden DE, Maurer K, Winblad B, Nordberg A. Spatial pattern of cerebral glucose metabolism (PET) correlates with localization of intracerebral EEG-generators in Alzheimer's disease. *Clin Neurophysiol*. 2000 Oct;111(10):1817-24.
- Dimpfel W, Spüler M, Wessel K. Different neuroleptics show common dose and time dependent effects in quantitative field potential analysis in freely moving rats. *Psychopharmacology (Berl)*. 1992;107(2-3):195-202.

References

- Dimpfel W. Pharmacological modulation of cholinergic brain activity and its reflection in special EEG frequency ranges from various brain areas in the freely moving rat (Tele-Stereo-EEG). *Eur Neuropsychopharmacol*. 2005 Dec;15(6):673-82.
- Dodart JC, Mathis C, Saura J, et al. Neuroanatomical abnormalities in behaviorally characterized APP(V717F) transgenic mice. *Neurobiol Dis*. 2000; 7:71–85.
- Dodart JC, Meziane H, Mathis C, Bales KR, Paul SM, Ungerer A. Behavioral disturbances in transgenic mice overexpressing the V717F beta-amyloid precursor protein. *Behav Neurosci*. 113(5):982-90 (1999).
- Dubois B, Albert ML. Amnestic MCI or prodromal Alzheimer's disease? *Lancet Neurol* 2004; 3: 246–48.
- Dubois B, Feldman HH, Jacova C, Cummings JL, Dekosky ST, Barberger-Gateau P, et al. Revising the definition of Alzheimer's disease: a new lexicon. *Lancet Neurol*. 2010;9:1118–27.
- Dubois B, Feldman HH, Jacova C, Hampel H, Molinuevo JL, Blennow K, DeKosky ST, Gauthier S, Selkoe D, Bateman R, Cappa S, Crutch S, Engelborghs S, Frisoni GB, Fox NC, Galasko D, Habert MO, Jicha GA, Nordberg A, Pasquier F, Rabinovici G, Robert P, Rowe C, Salloway S, Sarazin M, Epelbaum S, de Souza LC, Vellas B, Visser PJ, Schneider L, Stern Y, Scheltens P, Cummings JL. Advancing research diagnostic criteria for Alzheimer's disease: the IWG-2 criteria. *Lancet Neurol*. 2014 Jun;13(6):614-29.
- Ekstrom AD, Caplan JB, Ho E, Shattuck K, Fried I, Kahana MJ. Human hippocampal theta activity during virtual navigation. *Hippocampus*. 2005;15(7):881-9.
- Ertekin-Taner N. Genetics of Alzheimer's disease: a centennial review. *Neurol Clin*. 2007; 25:611–667.
- Feinberg DA, Moeller S, Smith SM, Auerbach E, Ramanna S, Gunther M, Glasser MF, Miller KL, Ugurbil K, Yacoub E (2010) Multiplexed echo planar imaging for sub-second whole brain fMRI and fast diffusion imaging. *PLoS One* 5, e15710.
- Fernandez A, Arrazola J, Maestu F, Amo C, Gil-Gregorio P, Wienbruch C, Ortiz T (2003) Correlations of hippocampal atrophy and focal low-frequency magnetic activity in Alzheimer disease: volumetric MR imaging-magnetoencephalographic study. *AJNR Am J Neuroradiol* 24, 481–487.
- Förstl H, Kurz A. Clinical features of Alzheimer's disease. *Eur Arch Psychiatry Clin Neurosci*. 1999;249(6):288-90.
- Fox MD, Raichle ME (2007) Spontaneous fluctuations in brain activity observed with functional magnetic resonance imaging. *Nat Rev Neurosci* 8, 700–711.
- Franklin KBJ, Paxinos G. *The Mouse Brain in Stereotaxic Coordinates*. San Diego: Academic Press; 1997.
- Franzmeier N, Gottler J, Grimmer T, Drzezga A, Araque-Caballero MA, Simon-Vermot L, Taylor ANW, Burger K, Catak C, Janowitz D, Muller C, Duering M, Sorg C, Ewers M (2017) Resting-State Connectivity of the Left Frontal Cortex to the Default Mode and Dorsal Attention Network Supports Reserve in Mild Cognitive Impairment. *Front Aging Neurosci* 9, 264.
- Frisoni GB, Fox NC, Jack CR, Scheltens P, Thompson PM (2010) The clinical use of structural MRI in Alzheimer disease. *Nat. Rev. Neurol*. 6, 67–77.
- Galluzzi S, Marizzoni M, Babiloni C, Albani D, Antelmi L, Bagnoli C, Bartres-Faz D, Cordone S, Didic M, Farotti L, Fiedler U, Forloni G, Girtler N, Hensch T, Jovicich J, Leeuwis A, Marra C, Molinuevo JL, Nobili F, Pariente J, Parnetti L, Payoux P, Del Percio C, Ranjeva JP, Rolandi E, Rossini PM, Schonknecht P, Soricelli A, Tsolaki M, Visser PJ, Wiltfang J, Richardson JC, Bordet R, Blin O, Frisoni GB (2016) Clinical and biomarker profiling of prodromal Alzheimer's disease in workpackage 5 of the Innovative Medicines Initiative PharmaCog project: a "European ADNI study." *J Intern Med* 279, 576–591.
- Galvan V, Gorostiza OF, Banwait S, Ataie M, Logvinova AV, Sitaraman S, et al. Reversal of Alzheimer's-like pathology and behavior in human APP transgenic mice by mutation of Asp664. *Proc Natl Acad Sci U S A*. 103(18):7130-5 (2006).
- Games D, Adams D, Alessandrini R, Barbour R, Berthelette P, Blackwell C, et al. Alzheimer-type neuropathology in transgenic mice overexpressing V717F beta-amyloid precursor protein. *Nature*. 9;373(6514):523-7 (1995).
- Geifman N, Brinton RD, Kennedy RE, Schneider LS, Butte AJ (2017) Evidence for benefit of statins to modify cognitive decline and risk in Alzheimer's disease. *Alzheimers. Res. Ther.* 9, 10.
- Gengler S, Mallot HA, Hölscher C. Inactivation of the rat dorsal striatum impairs performance in spatial tasks and alters hippocampal theta in the freely moving rat. *Behav Brain Res*. 164(1):73-82 (2005).
- German DC, Yazdani U, Speciale SG, Pasbakhsh P, Games D, Liang CL. Cholinergic neuropathology in a mouse model of Alzheimer's disease. *J Comp Neurol*. 462(4):371-81 (2003).
- Gili T, Cercignani M, Serra L, Perri R, Giove F, Maraviglia B, Caltagirone C, Bozzali M (2011) Regional brain atrophy and functional disconnection across Alzheimer's disease evolution. *J Neurol Neurosurg Psychiatry* 82, 58–66.

References

- Glodzik-Sobanska L, Rusinek H, Mosconi L, Li Y, Zhan J, de Santi S, Convit A, Rich K, Brys M, de Leon MJ. The role of quantitative structural imaging in the early diagnosis of Alzheimer's disease. *Neuroimaging Clin N Am*. 2005 Nov;15(4):803-26, x.
- Golob EJ, Irimajiri R, Starr A (2007) Auditory cortical activity in amnesic mild cognitive impairment: relationship to subtype and conversion to dementia. *Brain* 130, 740–752.
- Graff-Radford J, Madhavan M, Vemuri P, Rabinstein AA, Cha RH, Mielke MM, Kantarci K, Lowe V, Senjem ML, Gunter JL, Knopman DS, Petersen RC, Jack Jr. CR, Roberts RO (2016) Atrial fibrillation, cognitive impairment, and neuroimaging. *Alzheimers Dement* 12, 391–398.
- Haider B, Häusser M, Carandini M. Inhibition dominates sensory responses in the awake cortex. *Nature*. 2013 Jan 3;493(7430):97-100.
- Hamlin AS, Windels F, Boskovic Z, Sah P, Coulson EJ. Lesions of the basal forebrain cholinergic system in mice disrupt idiothetic navigation. *PLoS One*. 2013;8(1):e53472.
- Hampel H, Broich K, Hoessler Y, Pantel J. Biological markers for early detection and pharmacological treatment of Alzheimer's disease. *Dialogues Clin Neurosci*. 2009;11(2):141-57. Review.
- Hanna A, Horne P, Yager D, Eckman C, Eckman E, Janus C. Amyloid beta and impairment in multiple memory systems in older transgenic APP TgCRND8 mice. *Genes Brain Behav*. 8(7):676-84 (2009).
- Hardy J, Selkoe DJ. The amyloid hypothesis of Alzheimer's disease: progress and problems on the road to therapeutics. *Science*. 2002 Jul 19;297(5580):353-6. Review.
- Hartman RE, Izumi Y, Bales KR, Paul SM, Wozniak DF, Holtzman DM. Treatment with an amyloid-beta antibody ameliorates plaque load, learning deficits, and hippocampal long-term potentiation in a mouse model of Alzheimer's disease. *J Neurosci*. 29;25(26):6213-20 (2005).
- Hasselmo ME, Eichenbaum H. Hippocampal mechanisms for the context-dependent retrieval of episodes. *Neural Netw*. 2005;18(9):1172-90.
- Horváth A, Szűcs A, Barcs G, Noebels JL, Kamondi A. Epileptic Seizures in Alzheimer Disease: A Review. *Alzheimer Dis Assoc Disord*. 30(2):186-92 (2016).
- Howlett DR, Bowler K, Soden PE, Riddell D, Davis JB, Richardson JC, Burbidge SA, Gonzalez MI, Irving EA, Lawman A, Miglio G, Dawson EL, Howlett ER, Hussain I. Abeta deposition and related pathology in an APP x PS1 transgenic mouse model of Alzheimer's disease. *Histol Histopathol*. 2008 Jan;23(1):67-76.
- Howlett DR, Richardson JC, Austin A, Parsons AA, Bate ST, Davies DC, Gonzalez MI. Cognitive correlates of Abeta deposition in male and female mice bearing amyloid precursor protein and presenilin-1 mutant transgenes. *Brain Res*. 2004 Aug 13;1017(1-2):130-6.
- Hromádka T, Zador AM, DeWeese MR. Up states are rare in awake auditory cortex. *J Neurophysiol*. 2013 Apr;109(8):1989-95.
- Hsiao K, Chapman P, Nilsen S, et al. Correlative memory deficits, Abeta elevation, and amyloid plaques in transgenic mice. *Science*. 1996; 274:99–102.
- Hsiao K. Transgenic mice expressing Alzheimer amyloid precursor proteins. *Exp Gerontol*. 33(7-8):883-9 (1998).
- Huang C, Wahlund L, Dierks T, Julin P, Winblad B, Jelic V. Discrimination of Alzheimer's disease and mild cognitive impairment by equivalent EEG sources: a cross-sectional and longitudinal study. *Clin Neurophysiol*. 2000 Nov;111(11):1961-7.
- Hughes SW, Crunelli V (2005) Thalamic mechanisms of EEG alpha rhythms and their pathological implications. *Neuroscientist* 11, 357–372.
- Jacobs J. Hippocampal theta oscillations are slower in humans than in rodents: implications for models of spatial navigation and memory. *Philos Trans R Soc Lond B Biol Sci*. 2014 Feb 5; 369(1635): 20130304. doi: 10.1098/rstb.2013.0304
- Jelic V, Dierks T, Amberla K, Almkvist O, Winblad B, Nordberg A. Longitudinal changes in quantitative EEG during long-term tacrine treatment of patients with Alzheimer's disease. *Neurosci Lett*. 25;254(2):85-8 (1998).
- Jelic V, Johansson SE, Almkvist O, Shigeta M, Julin P, Nordberg A, Winblad B, Wahlund LO (2000) Quantitative electroencephalography in mild cognitive impairment: longitudinal changes and possible prediction of Alzheimer's disease. *Neurobiol Aging* 21, 533–540.
- Jelles B, Scheltens P, van der Flier WM, Jonkman EJ, da Silva FH, Stam CJ (2008) Global dynamical analysis of the EEG in Alzheimer's disease: frequency-specific changes of functional interactions. *Clin Neurophysiol* 119, 837–841.
- Jeong J. EEG dynamics in patients with Alzheimer's disease. *Clin Neurophysiol*. 2004 Jul;115(7):1490-505.

References

- Jervis BW, Belal S, Cassar T, Besleaga M, Bigan C, Michalopoulos K, Zervakis M, Camilleri K, Fabri S (2010) Waveform analysis of non-oscillatory independent components in single-trial auditory event-related activity in healthy subjects and Alzheimer's disease patients. *Curr Alzheimer Res* 7, 334–347.
- Jobert M, Wilson FJ, Ruigt GS, Brunovsky M, Prichep LS, Drinkenburg WH; IPEG Pharmacology-EEG Guidelines Committee. Guidelines for the recording and evaluation of pharmacology-EEG data in man: the International Pharmacology-EEG Society (IPEG). *Neuropsychobiology*. 2012;66(4):201-20.
- Jovicich J, Marizzoni M, Bosch B, Bartres-Faz D, Arnold J, Benninghoff J, Wiltfang J, Roccatagliata L, Picco A, Nobili F, Blin O, Bombois S, Lopes R, Bordet R, Chanoine V, Ranjeva JP, Didic M, Gros-Dagnac H, Payoux P, Zoccatelli G, Alessandrini F, Beltramello A, Bargallo N, Ferretti A, Caulo M, Aiello M, Ragucci M, Soricelli A, Salvadori N, Tarducci R, Floridi P, Tsolaki M, Constantinidis M, Drevelegas A, Rossini PM, Marra C, Otto J, Reiss-Zimmermann M, Hoffmann KT, Galluzzi S, Frisoni GB (2014) Multisite longitudinal reliability of tract-based spatial statistics in diffusion tensor imaging of healthy elderly subjects. *Neuroimage* 101, 390–403.
- Jovicich J, Marizzoni M, Sala-Llonch R, Bosch B, Bartres-Faz D, Arnold J, Benninghoff J, Wiltfang J, Roccatagliata L, Nobili F, Hensch T, Trankner A, Schonknecht P, Leroy M, Lopes R, Bordet R, Chanoine V, Ranjeva JP, Didic M, Gros-Dagnac H, Payoux P, Zoccatelli G, Alessandrini F, Beltramello A, Bargallo N, Blin O, Frisoni GB (2013) Brain morphometry reproducibility in multi-center 3T MRI studies: a comparison of cross-sectional and longitudinal segmentations. *Neuroimage* 83, 472–484.
- Jovicich J, Minati L, Marizzoni M, Marchitelli R, Sala-Llonch R, Bartres-Faz D, Arnold J, Benninghoff J, Fiedler U, Roccatagliata L, Picco A, Nobili F, Blin O, Bombois S, Lopes R, Bordet R, Sein J, Ranjeva JP, Didic M, Gros-Dagnac H, Payoux P, Zoccatelli G, Alessandrini F, Beltramello A, Bargallo N, Ferretti A, Caulo M, Aiello M, Cavaliere C, Soricelli A, Parnetti L, Tarducci R, Floridi P, Tsolaki M, Constantinidis M, Drevelegas A, Rossini PM, Marra C, Schonknecht P, Hensch T, Hoffmann KT, Kuijter JP, Visser PJ, Barkhof F, Frisoni GB (2016) Longitudinal reproducibility of default-mode network connectivity in healthy elderly participants: A multicentric resting-state fMRI study. *Neuroimage* 124, 442–454.
- Kahana MJ, Seelig D, Madsen JR. Theta returns. *Curr Opin Neurobiol*. 11(6):739-44 (2001).
- Kelemen E, Morón I, Fenton AA. Is the hippocampal theta rhythm related to cognition in a non-locomotor place recognition task? *Hippocampus*. 2005;15(4):472-9.
- Killiany RJ, Moss MB, Albert MS, Sandor T, Tieman J, Jolesz F (1993) Temporal lobe regions on magnetic resonance imaging identify patients with early Alzheimer's disease. *Arch Neurol* 50, 949–954.
- Klein SB, Thorne BM. *Biological Psychology*. Worth Publishers, 2006.
- Klimesch W (1999) EEG alpha and theta oscillations reflect cognitive and memory performance: a review and analysis. *Brain Res Brain Res Rev* 29, 169–195.
- Klimesch W, Doppelmayr M, Schimke H, Ripper B. Theta synchronization and alpha desynchronization in a memory task. *Psychophysiology*. 34(2):169-76 (1997).
- Klimesch W, Doppelmayr M, Schimke H, Ripper B. Theta synchronization and alpha desynchronization in a memory task. *Psychophysiology*. 1997 Mar;34(2):169-76.
- Klimesch W, Schimke H, Doppelmayr M, Ripper B, Schwaiger J, Pfurtscheller G. Event-related desynchronization (ERD) and the Dm effect: does alpha desynchronization during encoding predict later recall performance? *Int J Psychophysiol*. 1996; 24:47-60.
- Klimesch W. EEG alpha and theta oscillations reflect cognitive and memory performance: a review and analysis. *Brain Res Brain Res Rev*. 1999 Apr;29(2-3):169-95.
- Klimesch W. EEG alpha and theta oscillations reflect cognitive and memory performance: a review and analysis. *Brain Res Brain Res Rev*. 1999 Apr;29(2-3):169-95.
- Koenig T, Prichep L, Dierks T, Hubl D, Wahlund LO, John ER, Jelic V (2005) Decreased EEG synchronization in Alzheimer's disease and mild cognitive impairment. *Neurobiol Aging* 26, 165–171.
- Kogan EA, Korczyn AD, Virchovsky RG, Klimovizky Ss, Treves TA, Neufeld MY (2001) EEG changes during long-term treatment with donepezil in Alzheimer's disease patients. *J Neural Transm* 108, 1167–1173.
- Kotagal V, Langa KM, Plassman BL, Fisher GG, Giordani BJ, Wallace RB, et al. Factors associated with cognitive evaluations in the United States. *Neurology* 2015;84(1):64-71.
- Krueger JM, Obal F. A neuronal group theory of sleep function. *J Sleep Res*. 1993 Jun;2(2):63-69.

References

- Kurimoto R, Ishii R, Canuet L, Ikezawa K, Azechi M, Iwase M, Yoshida T, Kazui H, Yoshimine T, Takeda M. Event-related synchronization of alpha activity in early Alzheimer's disease and mild cognitive impairment: an MEG study combining beamformer and group comparison. *Neurosci Lett*. 2008 Oct 3;443(2):86-9. doi: 10.1016/j.neulet.2008.07.015.
- Kwa VI, Weinstein HC, Posthumus Meyjes EF, van Royen EA, Bour LJ, Verhoeff PN, Ongerboer de Visser BW (1993) Spectral analysis of the EEG and 99m-Tc-HMPAO SPECT-scan in Alzheimer's disease. *Biol Psychiatry* 33, 100–107.
- Lakatos P, Karmos G, Mehta AD, Ulbert I, Schroeder CE. Entrainment of neuronal oscillations as a mechanism of attentional selection. *Science*. 2008 Apr 4;320(5872):110-3.
- Lakatos P, Shah AS, Knuth KH, Ulbert I, Karmos G, Schroeder CE. An oscillatory hierarchy controlling neuronal excitability and stimulus processing in the auditory cortex. *J Neurophysiol*. 2005 Sep;94(3):1904-11.
- Lalonde R, Dumont M, Staufenbiel M, Strazielle C. Neurobehavioral characterization of APP23 transgenic mice with the SHIRPA primary screen. *Behav Brain Res*. 2005 Feb 10;157(1):91-8.
- Larson J, Lynch G, Games D, Seubert P. Alterations in synaptic transmission and long-term potentiation in hippocampal slices from young and aged PDAPP mice. *Brain Res*. 840(1-2):23-35 (1999).
- Lassalle JM, Halley H, Dumas S, Verret L, Francés B. Effects of the genetic background on cognitive performances of TG2576 mice. *Behav Brain Res*. 2008 Aug 5;191(1):104-10.
- Lau WK, Leung MK, Lee TM, Law AC (2016) Resting-state abnormalities in amnesic mild cognitive impairment: a meta-analysis. *Transl Psychiatry* 6, e790.
- Lehmann C, Koenig T, Jelic V, Prichep L, John RE, Wahlund LO, Dodge Y, Dierks T. Application and comparison of classification algorithms for recognition of Alzheimer's disease in electrical brain activity (EEG). *J Neurosci Methods* 2007;161:342–350.
- Li JM, Zhang Y, Tang L, Chen YH, Gao Q, Bao MH, Xiang J, Lei DL. Effects of triptolide on hippocampal microglial cells and astrocytes in the APP/PS1 double transgenic mouse model of Alzheimer's disease. *Neural Regen Res*. 2016 Sep;11(9):1492-1498.
- Li JY, Kuo TB, Yang CC. Aged rats show dominant modulation of lower frequency hippocampal theta rhythm during running. *Exp Gerontol*. 83:63-70 (2016).
- Liu T, Bai W, Yi H, Tan T, Wei J, Wang J, Tian X. Functional connectivity in a rat model of Alzheimer's disease during a working memory task. *Curr Alzheimer Res*. 11(10):981-91 (2014).
- Lörincz ML, Crunelli V, Hughes SW. Cellular dynamics of cholinergically induced alpha (8-13 Hz) rhythms in sensory thalamic nuclei in vitro. *J Neurosci*. 2008 Jan 16;28(3):660-71.
- Lörincz ML, Geall F, Bao Y, Crunelli V, Hughes SW. ATP-dependent infra-slow (<0.1 Hz) oscillations in thalamic networks. *PLoS One*. 2009;4(2):e4447.
- Lörincz ML, Kékesi KA, Juhász G, Crunelli V, Hughes SW. Temporal framing of thalamic relay-mode firing by phasic inhibition during the alpha rhythm. *Neuron*. 2009 Sep 10;63(5):683-96.
- Magaki S, Yong WH, Khanlou N, Tung S, Vinters HV. Comorbidity in dementia: update of an ongoing autopsy study. *J Am Geriatr Soc*. 62(9):1722-8 (2014).
- Maloney KJ, Cape EG, Gotman J, Jones BE. High-frequency gamma electroencephalogram activity in association with sleep-wake states and spontaneous behaviors in the rat. *Neuroscience*. 1997 Jan;76(2):541-55.
- Marchitelli R, Minati L, Marizzoni M, Bosch B, Bartres-Faz D, Muller BW, Wiltfang J, Fiedler U, Roccatagliata L, Picco A, Nobili F, Blin O, Bombois S, Lopes R, Bordet R, Sein J, Ranjeva JP, Didic M, Gros-Dagnac H, Payoux P, Zoccatelli G, Alessandrini F, Beltramello A, Bargallo N, Ferretti A, Caulo M, Aiello M, Cavaliere C, Soricelli A, Parnetti L, Tarducci R, Floridi P, Tsolaki M, Constantinidis M, Drevelegas A, Rossini PM, Marra C, Schonknecht P, Hensch T, Hoffmann KT, Kuijter JP, Visser PJ, Barkhof F, Frisoni GB, Jovicich J (2016) Test-retest reliability of the default mode network in a multi-centric fMRI study of healthy elderly: Effects of data-driven physiological noise correction techniques. *Hum Brain Mapp* 37, 2114–2132.
- Marizzoni M, Antelmi L, Bosch B, Bartres-Faz D, Muller BW, Wiltfang J, Fiedler U, Roccatagliata L, Picco A, Nobili F, Blin O, Bombois S, Lopes R, Sein J, Ranjeva JP, Didic M, Gros-Dagnac H, Payoux P, Zoccatelli G, Alessandrini F, Beltramello A, Bargallo N, Ferretti A, Caulo M, Aiello M, Cavaliere C, Soricelli A, Salvadori N, Parnetti L, Tarducci R, Floridi P, Tsolaki M, Constantinidis M, Drevelegas A, Rossini PM, Marra C, Hoffmann KT, Hensch T, Schonknecht P, Kuijter JP, Visser PJ, Barkhof F, Bordet R, Frisoni GB, Jovicich J (2015) Longitudinal reproducibility of automatically segmented hippocampal subfields: A multisite European 3T study on healthy elderly. *Hum Brain Mapp* 36, 3516–3527.
- Marizzoni M, Ferrari C, Galluzzi S, Jovicich J, Albani D, Babiloni C, Didic M, Forloni G, Molinuevo JL, Nobili FM, Parnetti L, Payoux P, Rossini PM, Schönknecht P, Soricelli A, Tsolaki M, Visser PJ, Wiltfang J, Bordet R, Cavaliere L, Richardson J, Blin O,

References

- Frisoni GB (2017) CSF biomarkers and effect of apolipoprotein E genotype, age and sex on cut-off derivation in mild cognitive impairment. *Alzheimer's Dement.* 13, P1319.
- Marshall L, Born J. Brain-immune interactions in sleep. *Int Rev Neurobiol* 2002;52:93–131.
- Mattsson N, Zetterberg H, Hansson O, Andreasen N, Parnetti L, Jonsson M, Herukka SK, van der Flier WM, Blankenstein MA, Ewers M, Rich K, Kaiser E, Verbeek M, Tsolaki M, Mulugeta E, Rosén E, Aarsland D, Visser PJ, Schröder J, Marcusson J, de Leon M, Hampel H, Scheltens P, Pirttilä T, Wallin A, Jönköping ME, Minthon L, Winblad B, Blennow K. CSF biomarkers and incipient Alzheimer disease in patients with mild cognitive impairment. *JAMA.* 2009 Jul 22;302(4):385-93. doi: 10.1001/jama.2009.1064.
- McKhann G, Drachman D, Folstein M, Katzman R, Price D, Stadlan EM. Clinical diagnosis of Alzheimer's disease: report of the NINCDS-ADRDA Work Group under the auspices of Department of Health and Human Services Task Force on Alzheimer's Disease. *Neurology* 1984; 34: 939–44.
- McKhann GM, Knopman DS, Chertkow H, Hyman BT, Jack CR Jr, Kawas CH, Klunk WE, Koroshetz WJ, Manly JJ, Mayeux R, Mohs RC, Morris JC, Rossor MN, Scheltens P, Carrillo MC, Thies B, Weintraub S, Phelps CH. The diagnosis of dementia due to Alzheimer's disease: recommendations from the National Institute on Aging-Alzheimer's Association workgroups on diagnostic guidelines for Alzheimer's disease. *Alzheimer's Dement.* 2011 May;7(3):263-9.
- Minkeviciene R, Rheims S, Doboszay MB, Zilberter M, Hartikainen J, Fülöp L, Penke B, Zilberter Y, Harkany T, Pitkänen A, Tanila H. Amyloid beta-induced neuronal hyperexcitability triggers progressive epilepsy. *J Neurosci.* 2009 Mar 18;29(11):3453-62.
- Moechars D, Dewachter I, Lorent K, Reversé D, Baekelandt V, Naidu A, et al. Early phenotypic changes in transgenic mice that overexpress different mutants of amyloid precursor protein in brain. *J Biol Chem.* 274(10):6483-92 (1999).
- Moretti D V, Babiloni F, Carducci F, Cincotti F, Remondini E, Rossini PM, Salinari S, Babiloni C (2003) Computerized processing of EEG-EOG-EMG artifacts for multi-centric studies in EEG oscillations and event-related potentials. *Int J Psychophysiol* 47, 199–216.
- Moretti DV, Paternicò D, Binetti G, Zanetti O, Frisoni GB. EEG upper/low alpha frequency power ratio and the impulsive disorders network in subjects with mild cognitive impairment. *Curr Alzheimer Res.* 11(2):192-9 (2014).
- Morgan CD, Murphy C (2002) Olfactory event-related potentials in Alzheimer's disease. *J Int Neuropsychol Soc* 8, 753–763.
- Moruzzi G, Magoun HW. Brain stem reticular formation and activation of the EEG. *Electroencephalogr Clin Neurophysiol.* 1949 Nov;1(4):455-73.
- Mucke L, Masliah E, Yu GQ, Mallory M, Rockenstein EM, Tatsuno G, et al. High-level neuronal expression of abeta 1-42 in wild-type human amyloid protein precursor transgenic mice: synaptotoxicity without plaque formation. *J Neurosci.* 1;20(11):4050-8 (2000).
- Mura E, Lanni C, Preda S, Pistoia F, Sarà M, Racchi M, Schettini G, Marchi M, Govoni S. Beta-amyloid: a disease target or a synaptic regulator affecting age-related neurotransmitter changes? *Curr Pharm Des.* 2010;16(6):672-83.
- Murakami K, Murata N, Noda Y, Tahara S, Kaneko T, Kinoshita N, et al. SOD1 (copper/zinc superoxide dismutase) deficiency drives amyloid β protein oligomerization and memory loss in mouse model of Alzheimer disease. *J Biol Chem.* 30;286(52):44557-68 (2011).
- Murray ME, Graff-Radford NR, Ross OA, Petersen RC, Duara R, Dickson DW. Neuropathologically defined subtypes of Alzheimer's disease with distinct clinical characteristics: a retrospective study. *Lancet Neurol.* 2011;10:785–96.
- Nathan PJ, Lim YY, Abbott R, Galluzzi S, Marizzoni M, Babiloni C, Albani D, Bartres-Faz D, Didic M, Farotti L, Parnetti L, Salvadori N, Muller BW, Forloni G, Girtler N, Hensch T, Jovicich J, Leeuwis A, Marra C, Molinuevo JL, Nobili F, Pariente J, Payoux P, Ranjeva JP, Rolandi E, Rossini PM, Schonknecht P, Soricelli A, Tsolaki M, Visser PJ, Wiltfang J, Richardson JC, Bordet R, Blin O, Frisoni GB (2017) Association between CSF biomarkers, hippocampal volume and cognitive function in patients with amnesic mild cognitive impairment (MCI). *Neurobiol Aging* 53, 1–10.
- Nelson PT, Head E, Schmitt FA, Davis PR, Neltner JH, Jicha GA, et al. Alzheimer's disease is not "brain aging": neuropathological, genetic, and epidemiological human studies. *Acta Neuropathol.* 2011;121:571–87. [PMC free article] [PubMed]
- Niedermayer E, Lopes da Silva FH. *Electroencephalography: Basic Principles, Clinical Applications, And Related Fields.* 5th. Wolters Kluwer; 2005.
- Niedermayer E (1997) Alpha rhythms as physiological and abnormal phenomena. *Int J Psychophysiol* 26, 31–49.
- Niedermayer E and Lopes da Silva F, *Electroencephalography: Basic Principles, Clinical Applications, and Related Fields,* 2004
- Northoff G, Bermpohl F (2004) Cortical midline structures and the self. *Trends Cogn Sci* 8, 102–107.
- Northoff G, Heinzel A, de Greck M, Bermpohl F, Dobrowolny H, Panksepp J (2006) Self-referential processing in our brain--a meta-analysis of imaging studies on the self. *Neuroimage* 31, 440–457.
- Nunez PL. *Electric field of the brain: the neurophysics of EEG.* Oxford University Press, 1981.

References

- Oathes DJ, Ray WJ, Yamasaki AS, Borkovec TD, Castonguay LG, Newman MG, Nitschke J. Worry, generalized anxiety disorder, and emotion: evidence from the EEG gamma band. *Biol Psychol.* 2008 Oct;79(2):165-70.
- Ochsner KN, Beer JS, Robertson ER, Cooper JC, Gabrieli JD, Kihlstrom JF, D'Esposito M (2005) The neural correlates of direct and reflected self-knowledge. *Neuroimage* 28, 797–814.
- Okun M, Naim A, Lampl I. The subthreshold relation between cortical local field potential and neuronal firing unveiled by intracellular recordings in awake rats. *J Neurosci.* 2010 Mar 24;30(12):4440-8.
- Ommundsen N, Engedal K, Øksengård AR. Validity of the quantitative EEG statistical pattern recognition method in diagnosing Alzheimer's disease. *Dement Geriatr Cogn Disord* 2011;31:195-201.
- Onofrj M, Thomas A, Iacono D, Luciano AL, Di Iorio A (2003) The effects of a cholinesterase inhibitor are prominent in patients with fluctuating cognition: a part 3 study of the main mechanism of cholinesterase inhibitors in dementia. *Clin Neuropharmacol* 26, 239–251.
- Orzeł-Gryglewska J, Matulewicz P, Jurkowlaniec E. Theta activity in local field potential of the ventral tegmental area in sleeping and waking rats. *Behav Brain Res.* 15;265:84-92 (2014).
- Oulès B, Del Prete D, Greco B, Zhang X, Lauritzen I, Sevalle J, et al. Ryanodine receptor blockade reduces amyloid- β load and memory impairments in Tg2576 mouse model of Alzheimer disease. *J Neurosci.* 32(34):11820-34 (2012).
- Páleníček T, Fujáková M, Brunovský M, Horáček J, Gorman I, Balíková M, Rambousek L, Syslová K, Kačer P, Zach P, Bubeníková-Valešová V, Tylš F, Kubešová A, Puskarčíková J, Höschl C. Behavioral, neurochemical and pharmac-EEG profiles of the psychedelic drug 4-bromo-2,5-dimethoxyphenethylamine (2C-B) in rats. *Psychopharmacology (Berl).* 2013 Jan;225(1):75-93.
- Palop JJ, Chin J, Roberson ED, Wang J, Thwin MT, Bien-Ly N, Yoo J, Ho KO, Yu GQ, Kreitzer A, Finkbeiner S, Noebels JL, Mucke L. Aberrant excitatory neuronal activity and compensatory remodeling of inhibitory hippocampal circuits in mouse models of Alzheimer's disease. *Neuron.* 2007 Sep 6;55(5):697-711.
- Palop JJ, Mucke L. Epilepsy and Cognitive Impairments in Alzheimer Disease. *Arch Neurol.* 2009;66(4):435-440.
- Papaliagkas V, Kimiskidis V, Tsolaki M, Anogianakis G (2008) Usefulness of event-related potentials in the assessment of mild cognitive impairment. *BMC Neurosci* 9, 107.
- Papaliagkas VT, Anogianakis G, Tsolaki MN, Koliakos G, Kimiskidis VK (2010) Combination of P300 and CSF beta-amyloid(1-42) assays may provide a potential tool in the early diagnosis of Alzheimer's disease. *Curr Alzheimer Res* 7, 295–299.
- Papaliagkas VT, Kimiskidis VK, Tsolaki MN, Anogianakis G (2011) Cognitive event-related potentials: longitudinal changes in mild cognitive impairment. *Clin Neurophysiol* 122, 1322–1326.
- Pascual-Marqui (2007) Discrete, 3D distributed, linear imaging methods of electric neuronal activity. Part 1: exact, zero error localization. *Clin Neurophysiol* 112, 7.
- Passero S, Rocchi R, Vatti G, Burgalassi L, Battistini N (1995) Quantitative EEG mapping, regional cerebral blood flow, and neuropsychological function in Alzheimer's disease. *Dementia* 6, 148–156.
- Petersen CC, Hahn TT, Mehta M, Grinvald A, Sakmann B. Interaction of sensory responses with spontaneous depolarization in layer 2/3 barrel cortex. *Proc Natl Acad Sci U S A.* 2003 Nov 11;100(23):13638-43.
- Petrella JR, Sheldon FC, Prince SE, Calhoun VD, Doraiswamy PM (2011) Default mode network connectivity in stable vs progressive mild cognitive impairment. *Neurology* 76, 511–517.
- Pfurtscheller G, Klimesch W. Functional topography during a visuoverbal judgment task studied with event-related desynchronization mapping. *J Clin Neurophysiol.* 1992 Jan;9(1):120-31.
- Pfurtscheller G, Lopes da Silva FH. Event-related EEG/MEG synchronization and desynchronization: basic principles. *Clin. Neurophysiol.* 1999;110:1842–1857.
- Pickenhain L, Klingberg F. Hippocampal slow wave activity as a correlate of basic behavioral mechanisms in the rat. *Prog Brain Res.* 1967;27:218-27.
- Polack PO, Friedman J, Golshani P. Cellular mechanisms of brain state-dependent gain modulation in visual cortex. *Nat Neurosci.* 2013 Sep;16(9):1331-9.
- Polich J, Comerchero MD (2003) P3a from visual stimuli: typicality, task, and topography. *Brain Topogr* 15, 141–152.
- Polich J, Corey-Bloom J (2005) Alzheimer's disease and P300: review and evaluation of task and modality. *Curr Alzheimer Res* 2, 515–525.

References

- Polich J, Pitzer A (1999) P300 and Alzheimer's disease: oddball task difficulty and modality effects. *Electroencephalogr Clin Neurophysiol Suppl* 50, 281–287.
- Ponomareva NV, Selesneva ND, and Jarikov GA. EEG alterations in subjects at high familial risk for Alzheimer's disease. *Neuropsychobiology*. 2003;48(3):152-9.
- Preibisch C, Castrillon GJ, Buhner M, Riedl V (2015) Evaluation of Multiband EPI Acquisitions for Resting State fMRI. *PLoS One* 10, e0136961.
- Price DL. Aging of the brain and dementia of the Alzheimer type. In: Kandel ER, Schwartz JH, Jessell TM, editors. *Principles of Neural Science*. 4th edition. New York, NY, USA: McGraw-Hill; pp. 1149–1168 (2000).
- Prichet LS, John ER, Ferris SH, Reisberg B, Almas M, Alper K, Cancro R. Quantitative EEG correlates of cognitive deterioration in the elderly. *Neurobiol Aging*. 1994 Jan-Feb;15(1):85-90.
- Prut L, Abramowski D, Krucker T, Levy CL, Roberts AJ, Staufenbiel M, et al. Aged APP23 mice show a delay in switching to the use of a strategy in the Barnes maze. *Behav Brain Res*. 16;179(1):107-10 (2007).
- Qi Z, Wu X, Wang Z, Zhang N, Dong H, Yao L, Li K (2010) Impairment and compensation coexist in amnesic MCI default mode network. *Neuroimage* 50, 48–55.
- Rabinovici GD, Jagust WJ, Furst AJ, Ogar JM, Racine CA, Mormino EC, et al. Abeta amyloid and glucose metabolism in three variants of primary progressive aphasia. *Ann Neurol*. 2008;64:388–401.[PMC free article] [PubMed]
- Rabinowicz AL, Starkstein SE, Leiguarda RC, Coleman AE. Transient epileptic amnesia in dementia: a treatable unrecognized cause of episodic amnesic wandering. *Alzheimer Dis Assoc Disord*. 2000 Oct-Dec;14(4):231-3.
- Racine RJ. Modification of seizure activity by electrical stimulation. II. Motor seizure. *Electroencephalogr Clin Neurophysiol*. 1972 Mar;32(3):281-94.
- Rae-Grant A, Blume W, Lau C, Hachinski VC, Fisman M, Merskey H (1987) The electroencephalogram in Alzheimer-type dementia. A sequential study correlating the electroencephalogram with psychometric and quantitative pathologic data. *Arch Neurol* 44, 50–54.
- Raichle ME (2015) The brain's default mode network. *Annu Rev Neurosci* 38, 433–447.
- Rector DM, Schei JL, Van Dongen HP, Belenky G, Krueger JM. Physiological markers of local sleep. *Eur J Neurosci*. 2009 May;29(9):1771-8.
- Rector DM, Topchii IA, Carter KM, Rojas MJ. Local functional state differences between rat cortical columns. *Brain Res*. 2005 Jun 14;1047(1):45-55.
- Reeves RR, Struve FA, Patrick G (2002) The effects of donepezil on quantitative EEG in patients with Alzheimer's disease. *Clin Electroencephalogr* 33, 93–96.
- Reilly JF, Games D, Rydel RE, et al. Amyloid deposition in the hippocampus and entorhinal cortex: quantitative analysis of a transgenic mouse model. *Proc Natl Acad Sci U S A*. 2003; 100:4837–4842.
- Rodriguez G, Copello F, Vitali P, Perego G, Nobili F (1999) EEG spectral profile to stage Alzheimer's disease. *Clin Neurophysiol* 110, 1831–1837.
- Rodriguez G, Vitali P, De Leo C, De Carli F, Girtler N, Nobili F (2002) Quantitative EEG changes in Alzheimer patients during long-term donepezil therapy. *Neuropsychobiology* 46, 49–56.
- Rossini PM, Rossi S, Babiloni C, Polich J (2007) Clinical neurophysiology of aging brain: from normal aging to neurodegeneration. *Prog Neurobiol* 83, 375–400.
- Rubio SE, Vega-Flores G, Martínez A, Bosch C, Pérez-Mediavilla A, del Río J, Gruart A, Delgado-García JM, Soriano E, Pascual M. Accelerated aging of the GABAergic septohippocampal pathway and decreased hippocampal rhythms in a mouse model of Alzheimer's disease. *FASEB J*. 2012 Nov;26(11):4458-67.
- Sachdev RN, Gaspard N, Gerrard JL, Hirsch LJ, Spencer DD, Zaveri HP. Delta rhythm in wakefulness: evidence from intracranial recordings in human beings. *J Neurophysiol*. 2015 Jun 17;jn.00249.2015
- Sanchez A, Tripathy D, Yin X, Desobry K, Martinez J, Riley J, Gay D, Luo J, Grammas P. p38 MAPK: a mediator of hypoxia-induced cerebrovascular inflammation. *J Alzheimers Dis*. 2012;32(3):587-97.
- Sarro L, Senjem ML, Lundt ES, Przybelski SA, Lesnick TG, Graff-Radford J, Boeve BF, Lowe VJ, Ferman TJ, Knopman DS, Comi G, Filippi M, Petersen RC, Jack Jr. CR, Kantarci K (2016) Amyloid-beta deposition and regional grey matter atrophy rates in dementia with Lewy bodies. *Brain* 139, 2740–2750.

References

- Schneider F, Baldauf K, Wetzel W, Reymann KG. Behavioral and EEG changes in male 5xFAD mice. *Physiol Behav.* 2014 Aug; 135:25-33.
- Schroeter ML, Stein T, Maslowski N, Neumann J. Neural correlates of Alzheimer's disease and mild cognitive impairment: A systematic and quantitative meta-analysis involving 1351 patients. *Neuroimage.* 1;47(4):1196-206 (2009).
- Sergeant J, Geuze R, van Winsum W. Event-related desynchronization and P300. *Psychophysiology.* 1987 May;24(3):272-7.
- Serra L, Cercignani M, Mastropasqua C, Torso M, Spano B, Makovac E, Viola V, Giulietti G, Marra C, Caltagirone C, Bozzali M (2016) Longitudinal Changes in Functional Brain Connectivity Predicts Conversion to Alzheimer's Disease. *J Alzheimers Dis* 51, 377–389.
- Serrano-Pozo A, Qian J, Monsell SE, Blacker D, Gomez-Isla T, Betensky RA, et al. Mild to moderate Alzheimer dementia with insufficient neuropathological changes. *Ann Neurol.* 2014;75:597–601.[PMC free article] [PubMed]
- Shimamura AP (2011) Episodic retrieval and the cortical binding of relational activity. *Cogn Affect Behav Neurosci* 11, 277–291.
- Shin J, Talnov A. A single trial analysis of hippocampal theta frequency during nonsteady wheel running in rats. *Brain Res.* 897(1-2):217-21 (2001).
- Simon CW, Emmons WH. EEG, consciousness, and sleep. *Science.* 1956 Nov 30;124(3231):1066-9.
- Sinnamon HM. Hippocampal theta activity related to elicitation and inhibition of approach locomotion. *Behav Brain Res.* 160(2):236-49 (2005).
- Soininen H, Partanen J, Laulumaa V, Helkala EL, Laakso M, Riekkinen PJ (1989) Longitudinal EEG spectral analysis in early stage of Alzheimer's disease. *Electroencephalogr Clin Neurophysiol* 72, 290–297.
- Song J, Qin W, Liu Y, Duan Y, Liu J, He X, Li K, Zhang X, Jiang T, Yu C (2013) Aberrant functional organization within and between resting-state networks in AD. *PLoS One* 8, e63727.
- Sperling RA, Aisen PS, Beckett LA, Bennett DA, Craft S, Fagan AM, Iwatsubo T, Jack CR Jr, Kaye J, Montine TJ, Park DC, Reiman EM, Rowe CC, Siemers E, Stern Y, Yaffe K, Carrillo MC, Thies B, Morrison-Bogorad M, Wagster MV, Phelps CH. Toward defining the preclinical stages of Alzheimer's disease: recommendations from the National Institute on Aging-Alzheimer's Association workgroups on diagnostic guidelines for Alzheimer's disease. *Alzheimers Dement.* 2011 May;7(3):280-92.
- Stam CJ, Jelles B, Achtereekte HA, van Birgelen JH, Slaets JP. Diagnostic usefulness of linear and nonlinear quantitative EEG analysis in Alzheimer's disease. *Clin Electroencephalogr.* 1996 Apr;27(2):69-77.
- Steriade M (1994) Sleep oscillations and their blockage by activating systems. *J Psychiatry Neurosci* 19, 354–358.
- Steriade M, Amzica F. Coalescence of sleep rhythms and their chronology in corticothalamic networks. *Sleep Res Online.* 1998;1(1):1-10.
- Steriade M, Llinas RR (1988) The functional states of the thalamus and the associated neuronal interplay. *Physiol Rev* 68, 649–742.
- Steriade M, Nuñez A, Amzica F. Intracellular analysis of relations between the slow (<1 Hz) neocortical oscillation and other sleep rhythms of the electroencephalogram. *J Neurosci* 1993;13:3266–83.
- Steriade M. Cholinergic blockage of network- and intrinsically generated slow oscillations promotes waking and REM sleep activity patterns in thalamic and cortical neurons. *Prog Brain Res* 1993;98:345–55.
- Steriade M. Corticothalamic resonance, states of vigilance and mentation. *Neuroscience.* 2000;101(2):243-76. Review.
- Steriade, M. Cerebello-cerebral interactions during states of vigilance. *Cerebellum.* 2003;2(2):82-3.
- Stevens A, Kircher T. Cognitive decline unlike normal aging is associated with alterations of EEG temporo-spatial characteristics. *Eur Arch Psychiatry Clin Neurosci.* 1998;248(5):259-66.
- Stigsby B, Johannesson G, Ingvar DH (1981) Regional EEG analysis and regional cerebral blood flow in Alzheimer's and Pick's diseases. *Electroencephalogr Clin Neurophysiol* 51, 537–547.
- Sturchler-Pierrat C, Abramowski D, Duke M, Wiederhold KH, Mistl C, Rothacher S, et al. Two amyloid precursor protein transgenic mouse models with Alzheimer disease-like pathology. *Proc Natl Acad Sci U S A.* 25;94(24):13287-92 (1997).
- Supekar K, Uddin LQ, Prater K, Amin H, Greicius MD, Menon V (2010) Development of functional and structural connectivity within the default mode network in young children. *Neuroimage* 52, 290–301.
- Sviderskaia NE, Prudnikov VN, Antonov AG. Characteristics of EEG signs of anxiety in human. *Zh Vyssh Nerv Deiat Im I P Pavlova* 2001; 51:158–65.

References

- Tan AY, Chen Y, Scholl B, Seidemann E, Priebe NJ. Sensory stimulation shifts visual cortex from synchronous to asynchronous states. *Nature* 509: 226–229, 2014.
- Teipel S, Grothe MJ, Zhou J, Sepulcre J, Dyrba M, Sorg C, Babiloni C (2016) Measuring Cortical Connectivity in Alzheimer's Disease as a Brain Neural Network Pathology: Toward Clinical Applications. *J Int Neuropsychol Soc* 22, 138–163.
- Timofeev I, Grenier F, Bazhenov M, Sejnowski TJ, Steriade M. Origin of slow cortical oscillations in deafferented cortical slabs. *Cereb Cortex*. 2000 Dec;10(12):1185-99.
- Tsolaki AC, Kosmidou V, Kompatsiaris IY, Papadaniil C, Hadjileontiadis L, Adam A, Tsolaki M (2017) Brain source localization of MMN and P300 ERPs in mild cognitive impairment and Alzheimer's disease: a high-density EEG approach. *Neurobiol Aging* 55, 190–201.
- Valladares-Neto DC, Buchsbaum MS, Evans WJ, Nguyen D, Nguyen P, Siegel B V, Stanley J, Starr A, Guich S, Rice D (1995) EEG delta, positron emission tomography, and memory deficit in Alzheimer's disease. *Neuropsychobiology* 31, 173–181.
- van der Hiele K, Bollen EL, Vein AA, Reijntjes RH, Westendorp RG, van Buchem MA, Middelkoop HA, van Dijk JG. EEG markers of future cognitive performance in the elderly. *J Clin Neurophysiol*. 2008 Apr;25(2):83-9.
- van der Hiele K, Vein AA, van der Welle A, van der Grond J, Westendorp RG, Bollen EL, van Buchem MA, van Dijk JG, Middelkoop HA. EEG and MRI correlates of mild cognitive impairment and Alzheimer's disease. *Neurobiol Aging*. 2007 Sep;28(9):1322-9.
- van Dinteren R, Arns M, Jongsma MLA, Kessels RPC (2014) P300 development across the lifespan: a systematic review and meta-analysis. *PLoS One* 9, e87347.
- Van Winsum W, Sergeant J, Geuze R. The functional significance of event-related desynchronization of alpha rhythm in attentional and activating tasks. *Electroencephalogr Clin Neurophysiol*. 1984 Dec;58(6):519-24.
- Vanderwolf CH. Hippocampal electrical activity and voluntary movement in the rat. *Electroencephalogr Clin Neurophysiol*. 1969 Apr;26(4):407-18.
- Varma AR, Snowden JS, Lloyd JJ, Talbot PR, Mann DM, Neary D. Evaluation of the NINCDS-ADRDA criteria in the differentiation of Alzheimer's disease and frontotemporal dementia. *J Neurol Neurosurg Psychiatry* 1999; 66: 184–88.
- Vassar R. BACE1 inhibitor drugs in clinical trials for Alzheimer's disease. *Alzheimers Res Ther*. 2014 Dec 24;6(9):89
- Verret L, Krezymon A, Halley H, Trouche S, Zerwas M, Lazouret M, Lassalle JM, Rampon C Transient enriched housing before amyloidosis onset sustains cognitive improvement in Tg2576 mice. *Neurobiol Aging*. 2013 Jan;34(1):211-25.
- Vertes RP. Hippocampal theta rhythm: a tag for short-term memory. *Hippocampus*. 2005;15(7):923-35. Review.
- Vinogradova OS. Expression, control, and probable functional significance of the neuronal theta-rhythm. *Prog Neurobiol*. 45(6):523-83 (1995).
- Vyazovskiy VV, Kopp C, Bösch G, Tobler I. The GABAA receptor agonist THIP alters the EEG in waking and sleep of mice. *Neuropharmacology*. 2005 Apr;48(5):617-26.
- Vyazovskiy VV, Tobler I. Theta activity in the waking EEG is a marker of sleep propensity in the rat. *Brain Res*. 19;1050(1-2):64-71 (2005).
- Vyazovskiy W, Olcese U, Hanlon EC, Nir Y, Cirelli C, Tononi G. Local sleep in awake rats. *Nature*. 2011 Apr 28;472(7344):443-7.
- Wang J, Ikonen S, Gurevicius K, van Groen T, Tanila H. Alteration of cortical EEG in mice carrying mutated human APP transgene. *Brain Res*. 2002 Jul 12;943(2):181-90.
- Watrous AJ, Lee DJ, Izadi A, Gurkoff GG, Shahlaie K, Ekstrom AD. A comparative study of human and rat hippocampal low-frequency oscillations during spatial navigation. *Hippocampus*. 2013 Aug;23(8):656-61.
- Webster SJ, Bachstetter AD, Nelson PT, Schmitt FA, Van Eldik LJ. Using mice to model Alzheimer's dementia: an overview of the clinical disease and the preclinical behavioral changes in 10 mouse models. *Front Genet*. 2014 Apr 23;5:88.
- Weiler M, Northoff G, Damasceno BP, Balthazar MLF (2016) Self, cortical midline structures and the resting state: Implications for Alzheimer's disease. *Neurosci Biobehav Rev* 68, 245–255.
- Westmark CJ, Westmark PR, Beard AM, Hildebrandt SM, Malter JS. Seizure susceptibility and mortality in mice that over-express amyloid precursor protein. *Int J Clin Exp Pathol*. 2008 Jan 1;1(2):157-68.
- Wig GS (2017) Segregated Systems of Human Brain Networks. *Trends Cogn Sci* 21, 981–996.
- Wimmer ME, Rising J, Galante RJ, Wyner A, Pack AI, Abel T. Aging in mice reduces the ability to sustain sleep/wake states. *PLoS One*. 2013;8(12):e81880.

References

- Wolf H, Jelic V, Gertz HJ, Nordberg A, Julin P, Wahlund LO. A critical discussion of the role of neuroimaging in mild cognitive impairment. *Acta Neurol Scand Suppl.* 2003;179:52-76.
- Ye Q, Su F, Shu H, Gong L, Xie CM, Zhou H, Zhang ZJ, Bai F (2017) Shared effects of the clusterin gene on the default mode network among individuals at risk for Alzheimer's disease. *CNS Neurosci Ther* 23, 395–404.
- Yener GG, Basar E (2013) Biomarkers in Alzheimer's disease with a special emphasis on event-related oscillatory responses. *Suppl Clin Neurophysiol* 62, 237–273.
- Zagha E, Casale AE, Sachdev RN, McGinley MJ, McCormick DA. Motor cortex feedback influences sensory processing by modulating network state. *Neuron.* 2013 Aug 7;79(3):567-78.
- Zhang HY, Wang SJ, Liu B, Ma ZL, Yang M, Zhang ZJ, Teng GJ (2010) Resting brain connectivity: changes during the progress of Alzheimer disease. *Radiology* 256, 598–606.
- Zhang W, Savelieva KV, Suwanichkul A, Small DL, Kirkpatrick LL, Xu N, Lanthorn TH, Ye GL. Transmembrane and ubiquitin-like domain containing 1 (Tmub1) regulates locomotor activity and wakefulness in mice and interacts with CAMLG. *PLoS One.* 2010 Jun 22;5(6):e11261.
- Zhou J, Liu S, Ng KK, Wang J (2017) Applications of Resting-State Functional Connectivity to Neurodegenerative Disease. *Neuroimaging Clin N Am* 27, 663–683.
- Zhou M, Liang F, Xiong XR, Li L, Li H, Xiao Z, Tao HW, Zhang LI. Scaling down of balanced excitation and inhibition by active behavioral states in auditory cortex. *Nat Neurosci.* 2014 Jun;17(6):841-50.
- Ziyatdinova S, Gurevicius K, Kutchiashvili N, Bolkvadze T, Nissinen J, Tanila H, Pitkänen A. Spontaneous epileptiform discharges in a mouse model of Alzheimer's disease are suppressed by antiepileptic drugs that block sodium channels. *Epilepsy Res.* 2011 Mar;94(1-2):75-85.
- Ziyatdinova S, Rönnbäck A, Gurevicius K, Miszczuk D, Graff C, Winblad B, et al. Increased Epileptiform EEG Activity and Decreased Seizure Threshold in Arctic APP Transgenic Mouse Model of Alzheimer's Disease. *Curr Alzheimer Res.*13(7):817-30 (2016).